STORM FP7

Solar system plasma turbulence, intermittency and multifractals
International Workshop and School
06-13 September 2015
Mamaia, ROMANIA

Observing MHD turbulence phenomenology in 3D heliosphere

Roberto Bruno
INAF-IAPS, Roma, Italy
roberto.bruno@iaps.inaf.it


Roman-Greek ruins at Tomis-Constanta

Solar wind large scale structure

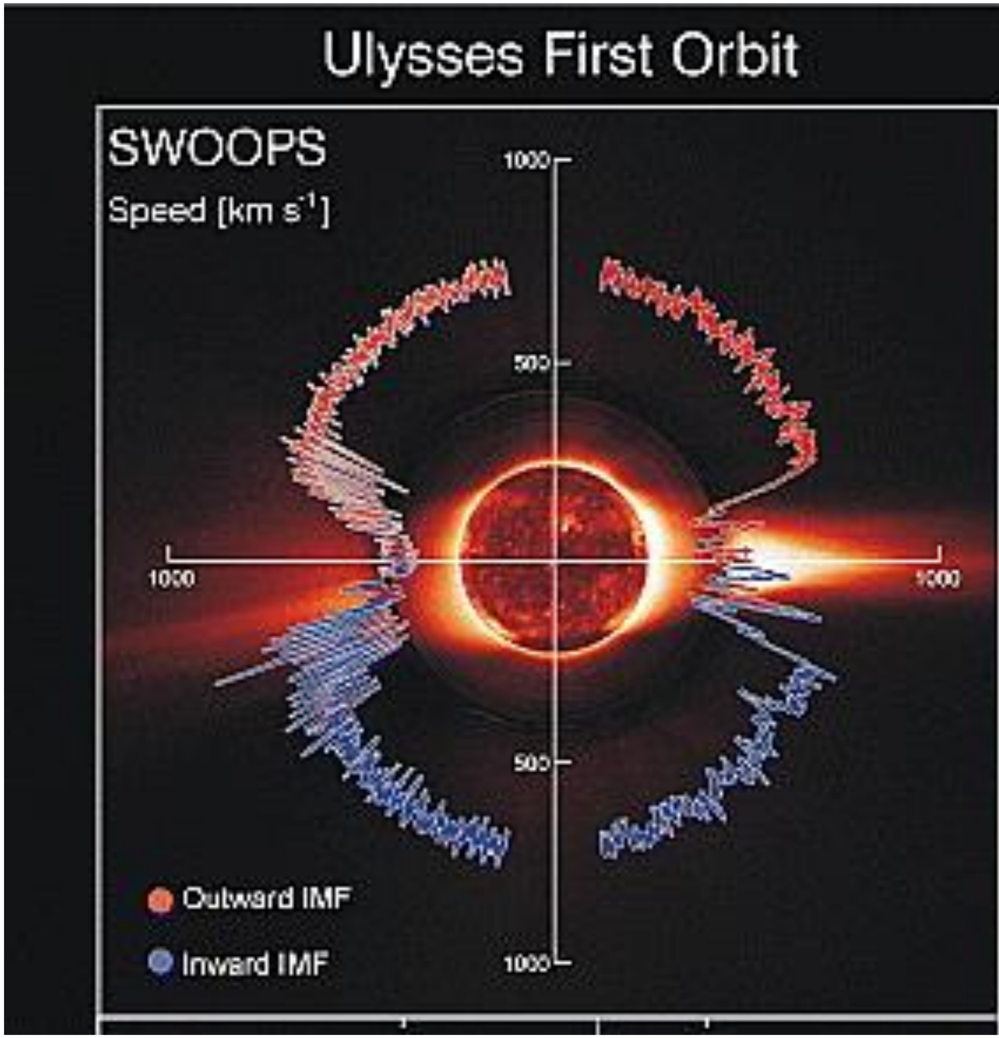

McComas et al, GRL, 2003

Solar minimum:

- fast steady wind at high latitudes
- Fast and slow streams in the ecliptic.

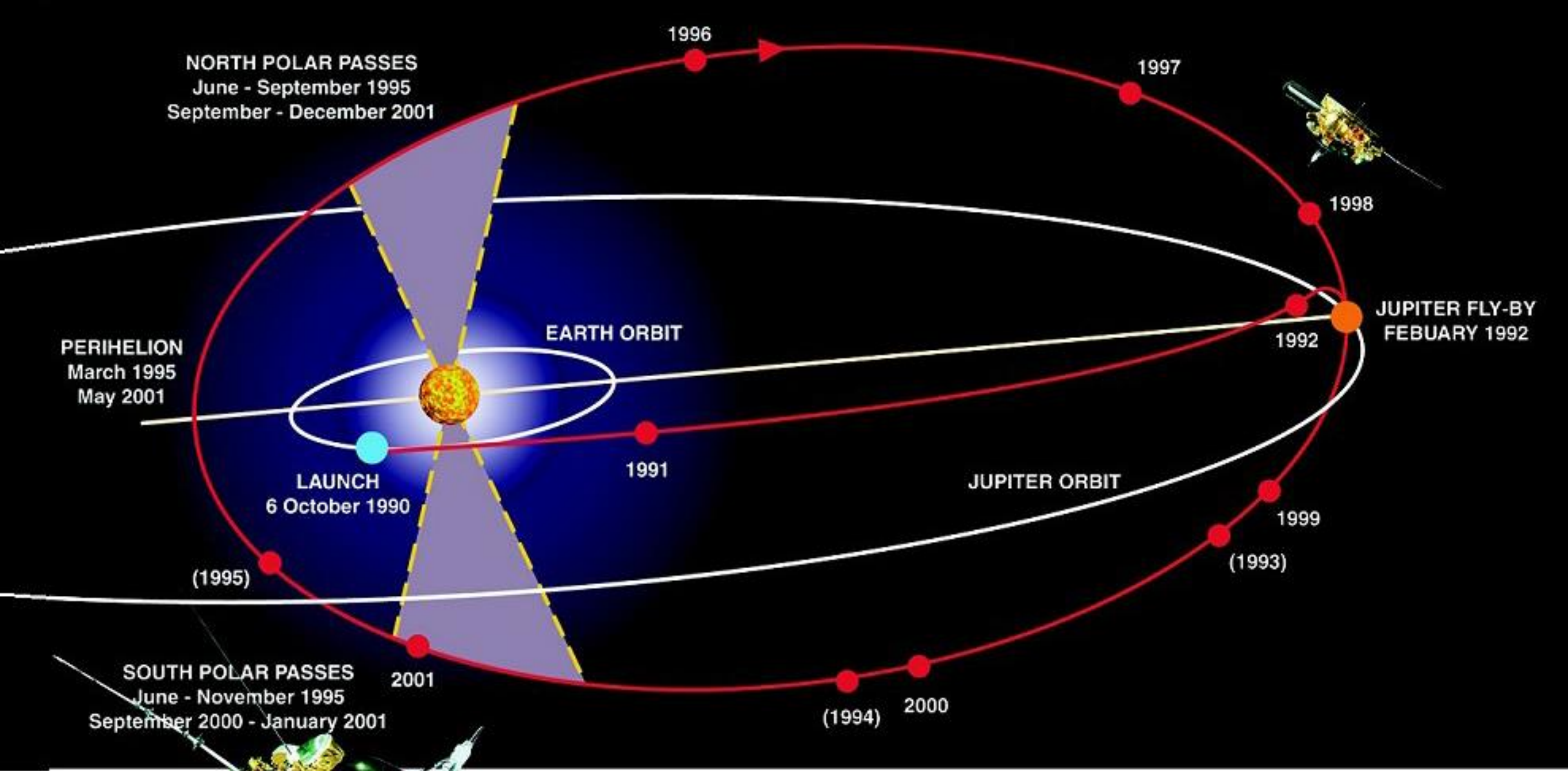

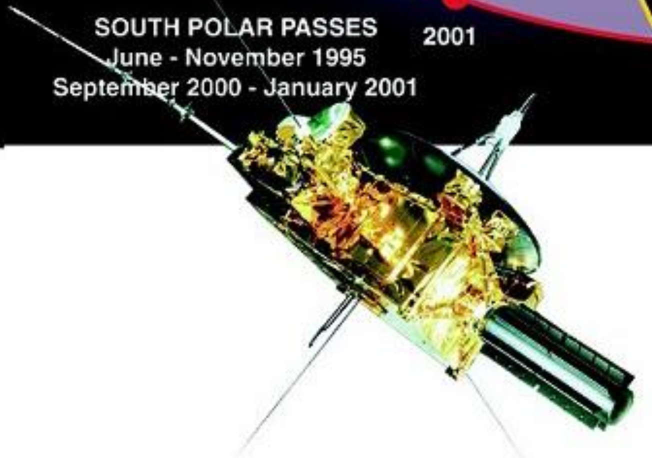

- Latitudinal excursion: ±82°

Most of our knowledge about solar wind plasma and magnetic field in the inner heliosphere is due to Helios 1-2 s/c developed by the Federal Republic of Germany (FRG) in a cooperative program with NASA

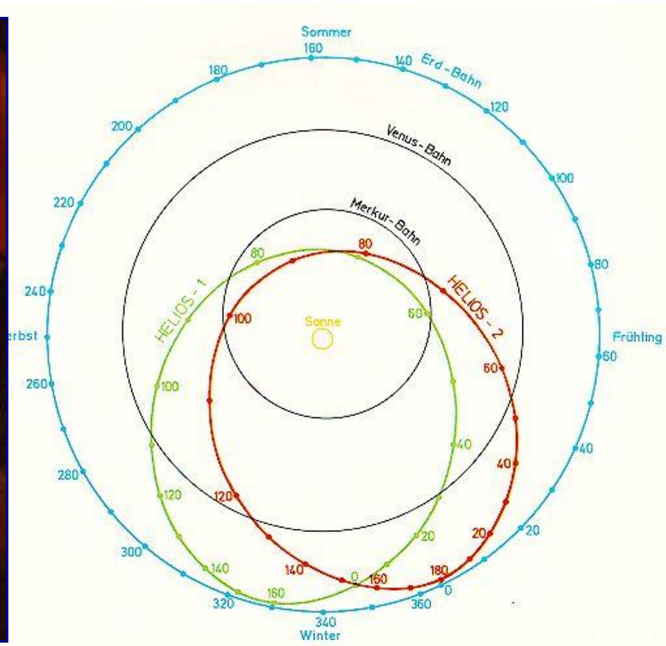

- Two spacecraft, launched in <u>1974(10 Dec) & 1976(15 Jan)</u>
- ecliptic orbit, perihelium @ 0.29AU
- Plasma measurements: protons(+alphas) and electrons
- <u>No composition</u>
- Slow plasma sampling, VDF in 40.5 sec
- Low phase space resolution
- <u>NO imaging</u>

Programme realized in only 5 years!

1969: contract between FRG and NASA approved

10 December 1974: Helios 1 launched

A sample of interplanetary data observed in the ecliptic

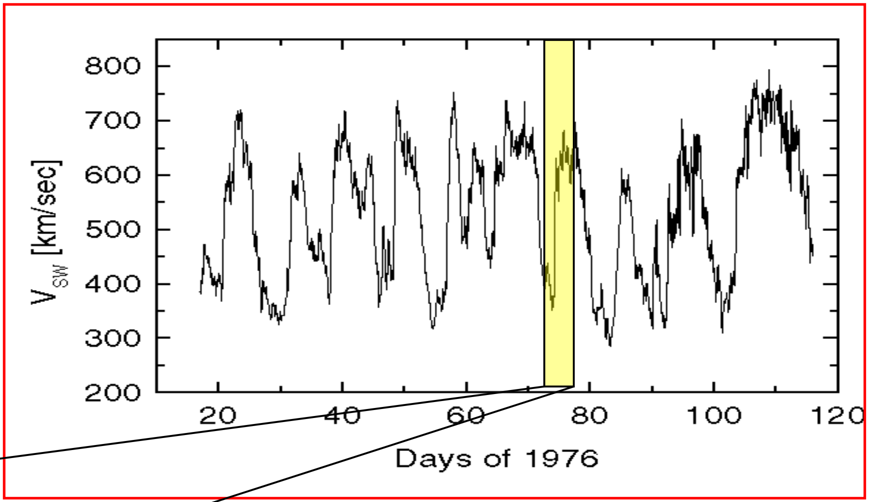

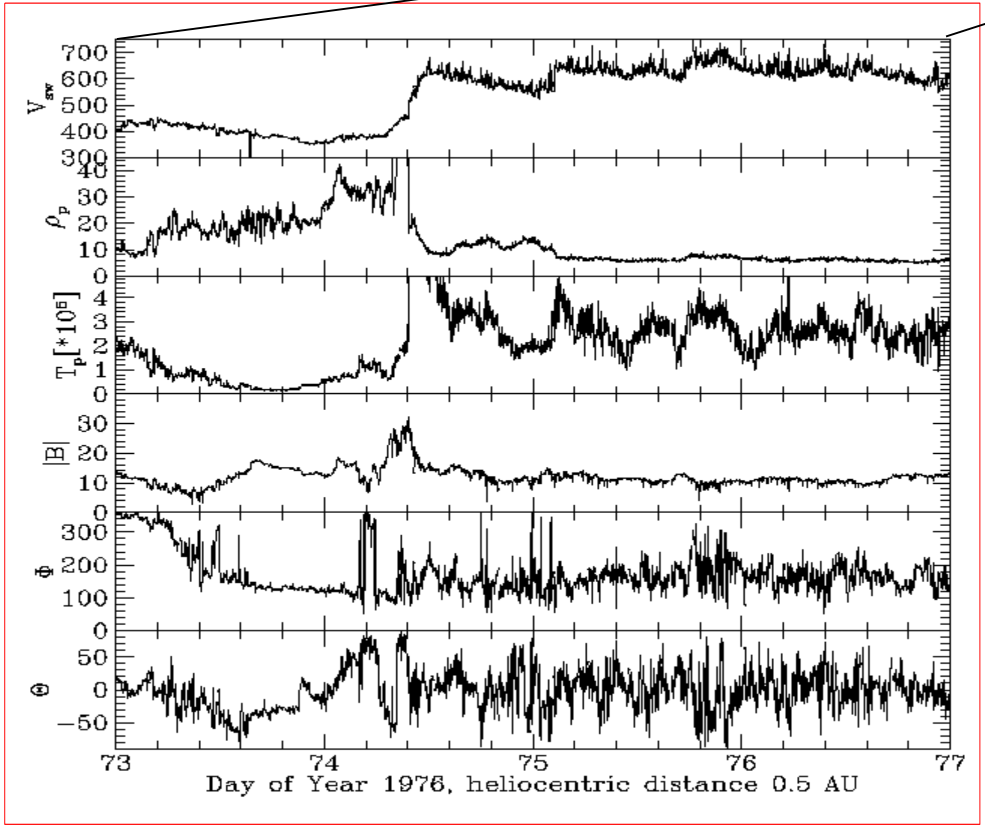

A sample of interplanetary data observed in the ecliptic

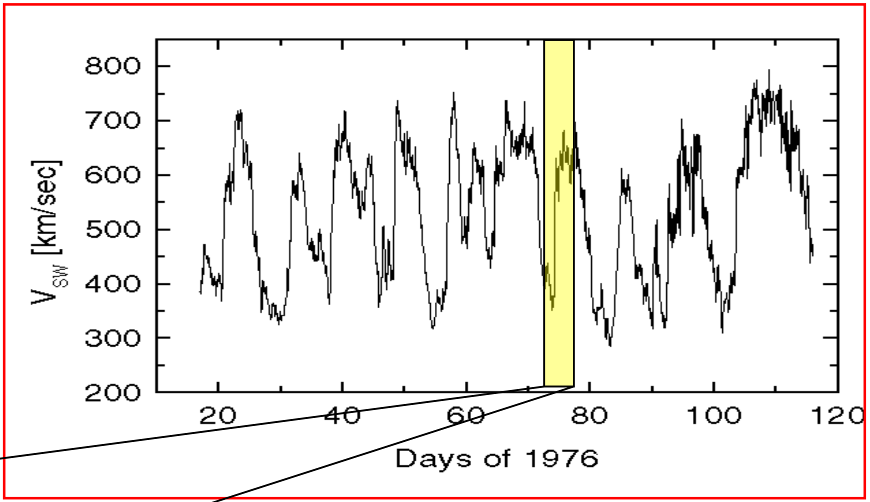

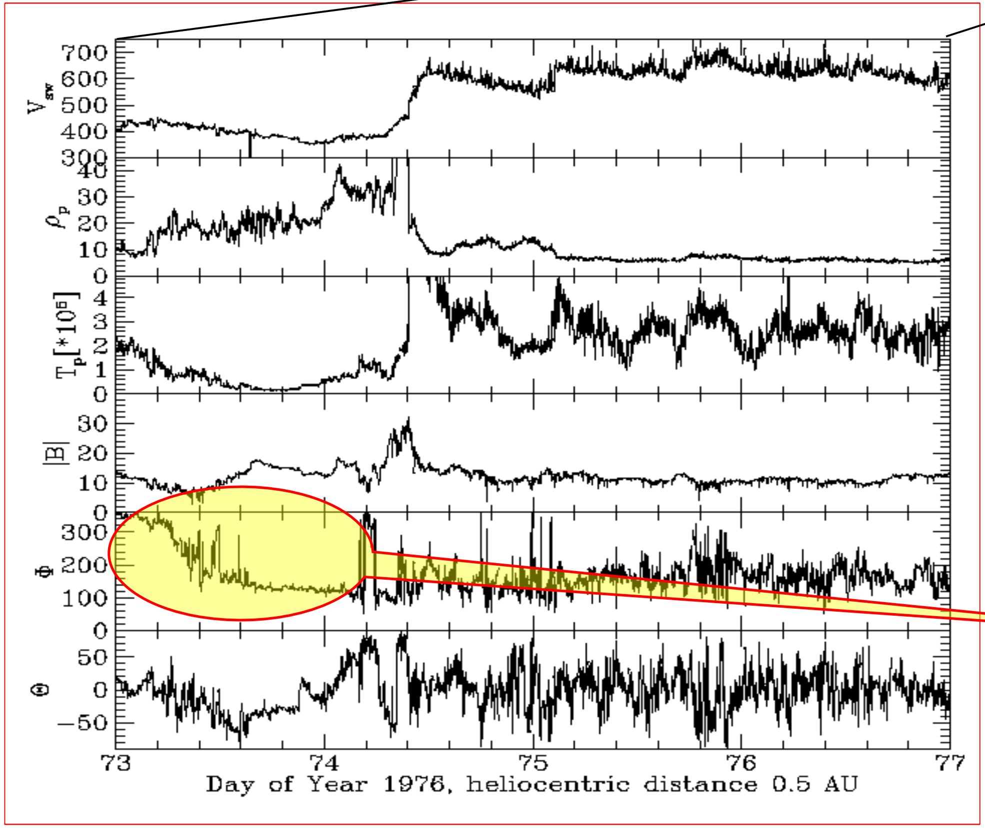

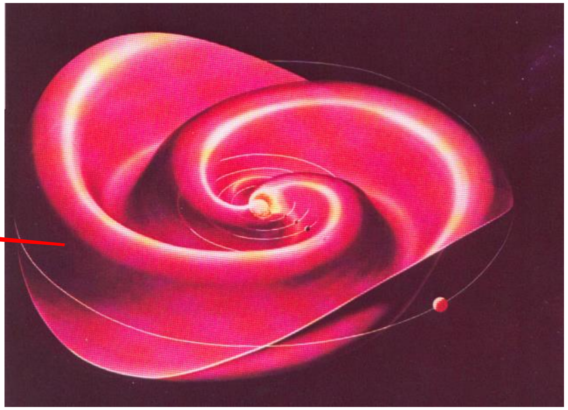

A sample of interplanetary data observed in the ecliptic

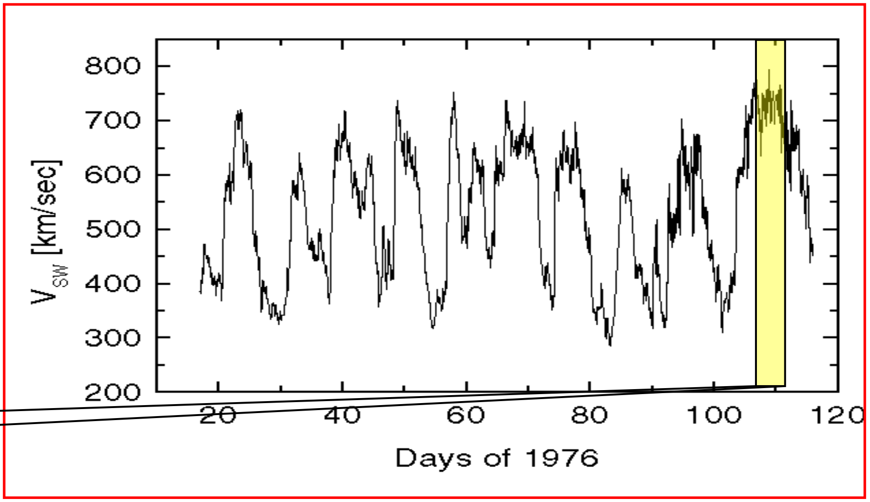

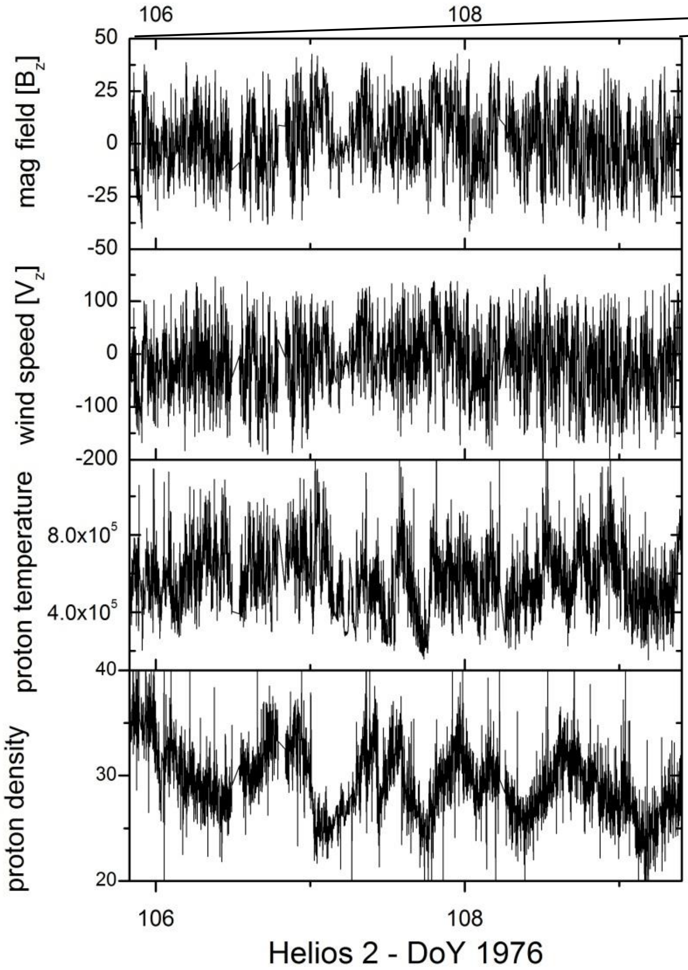

As we will see in the following,
<u>the Solar Wind is a turbulent medium</u>

Turbulence is an old problem…

Arno river in Florence

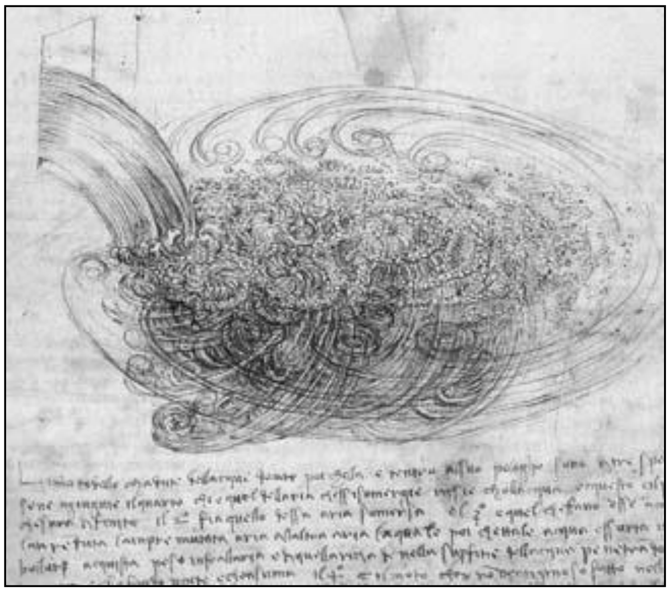

Study by Leonardo da Vinci (1452-1519)
Related to the problem of reducing the rapids in the river Arno

Turbulence is an old problem…

Arno river in Florence

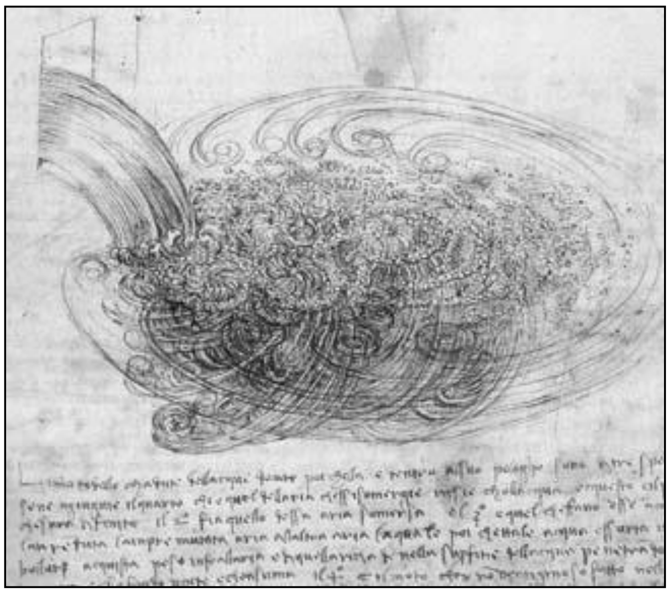

Study by Leonardo da Vinci
(1452-1519)
Related to the problem of reducing the rapids in the river Arno

“*Turbulence still remains the last major unsolved problem in classical physics*.” *Feynman et al. (1977)*

TURBULENCE

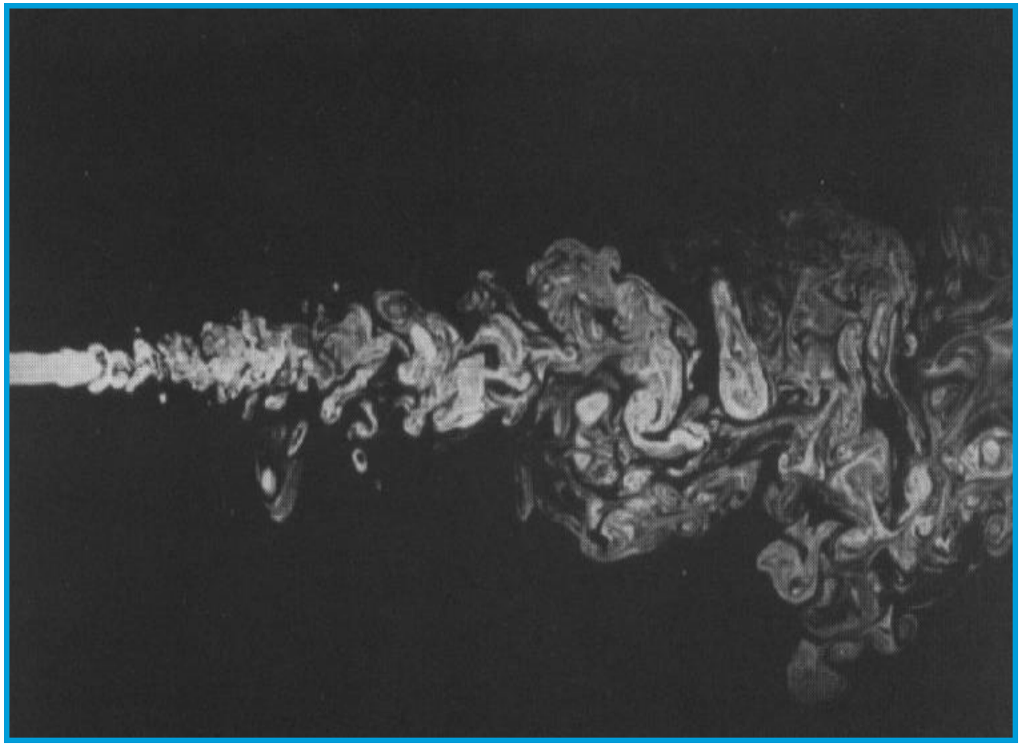

The study of the chaotic behavior
of a fluid flow in space and time

TURBULENCE

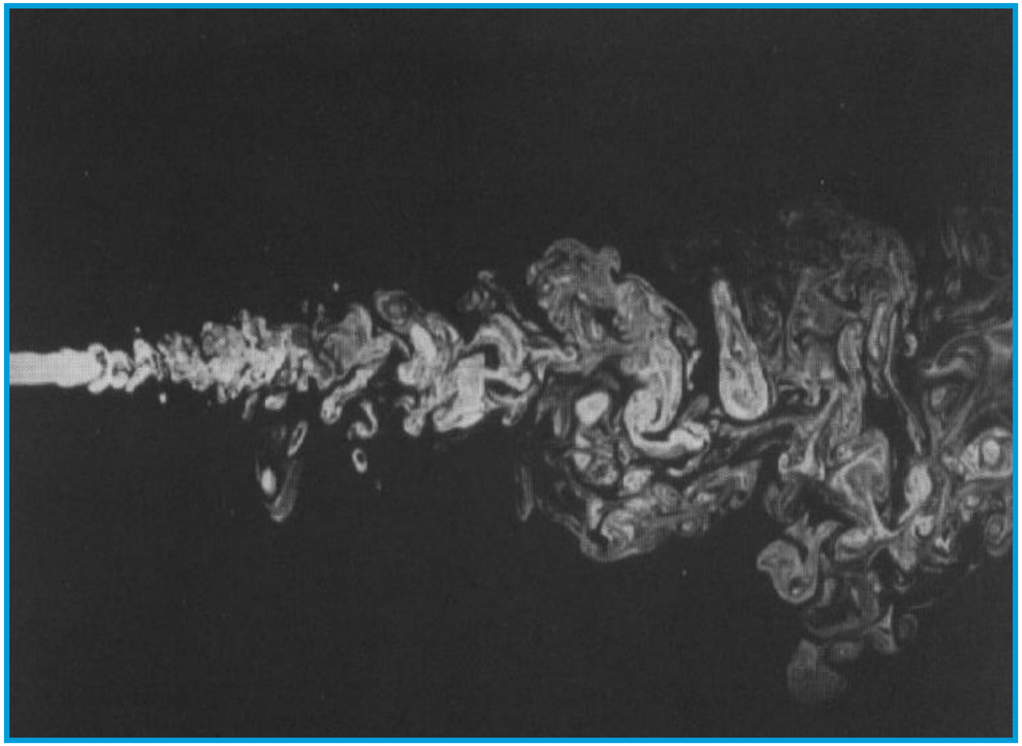

The legacy of Kolmogorov, Andrei Nikolaevich (1903-1987)

The study of the chaotic behavior of a fluid flow in space and time

The first feature we notice in interplanetary fluctuations is an approximate self-similarity when we look at different scales

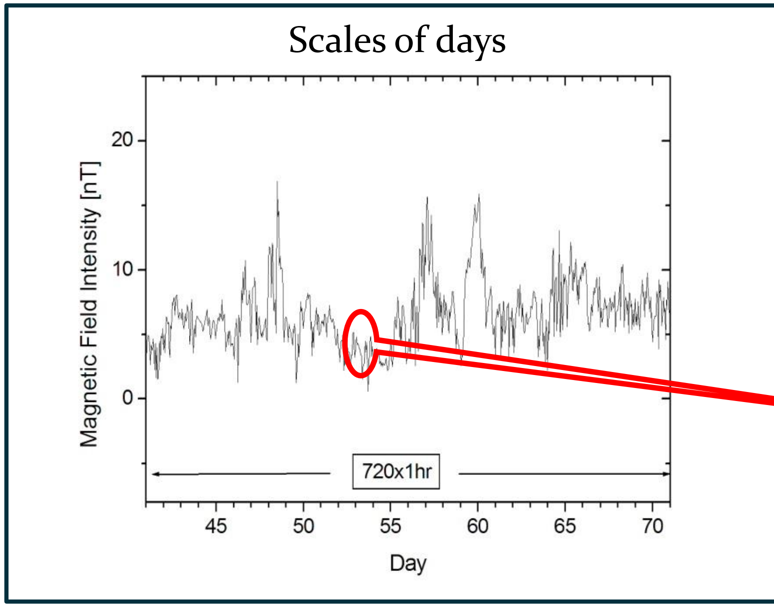

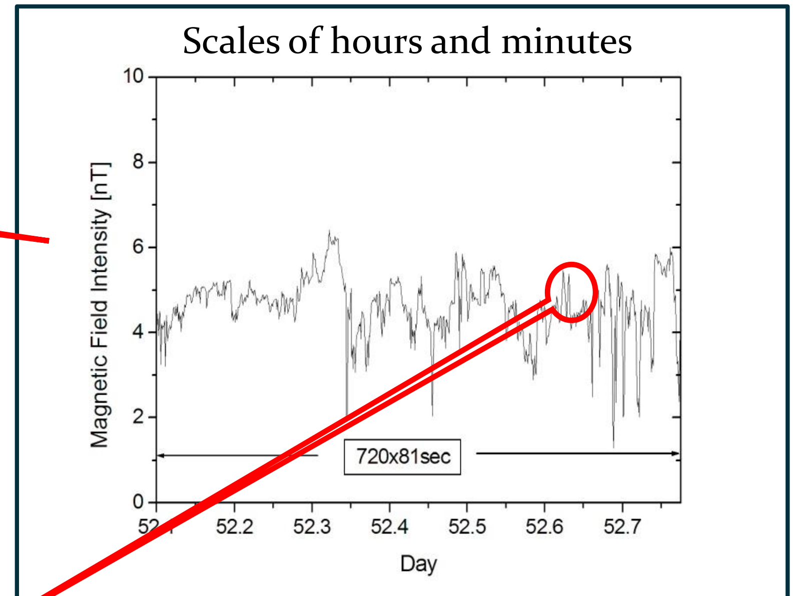

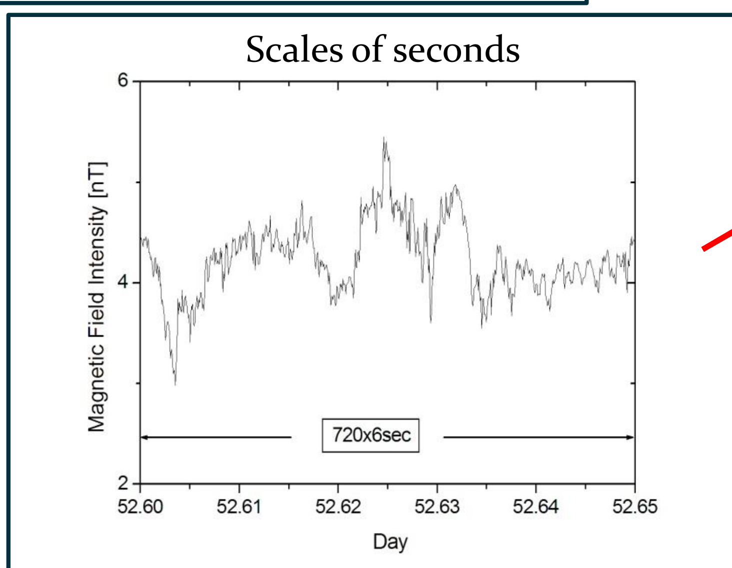

- ❑ Three panels with the same amount of datapoints
- ❑ Similar profiles

self-similarity implies *power-laws*

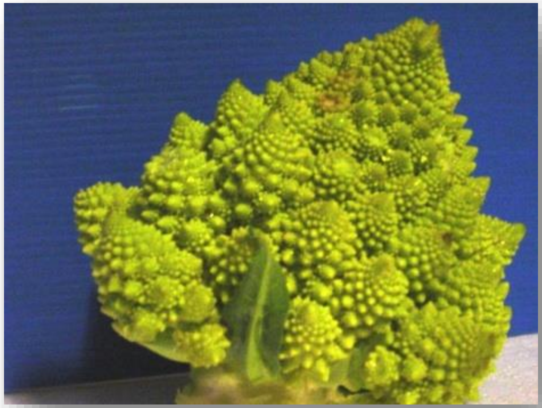

Romanesco broccoli

The field $v(\lambda)$ is said to be "invariant for scale transformation" $\lambda \rightarrow r\lambda$ or "self-similar" if there exists a parameter $\mu(r)$ such that:

$$\boxed{v(\lambda) = \mu(r) v(r\lambda)}$$

The solution of this relation is a power law: $v(\lambda)=C\lambda^h$ where $h=-\log_r \mu(r)$

As a matter of fact, interplanetary fluctuations do show power laws

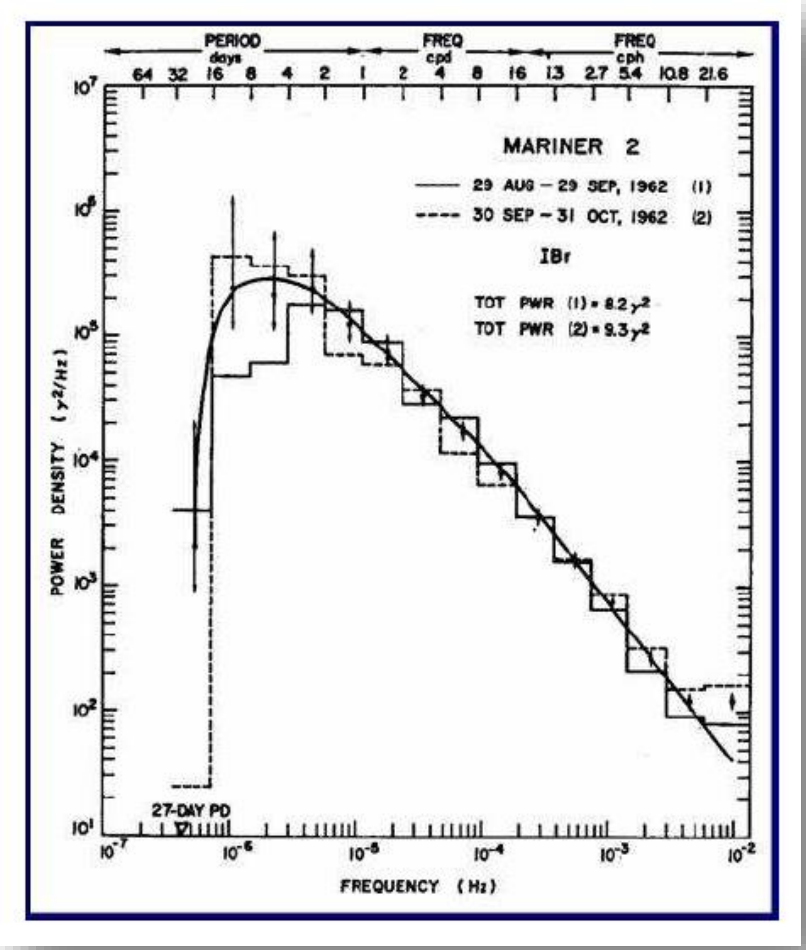

First magnetic energy spectrum
(Coleman, 1968)

The first evidence of the existence of a power law in solar wind fluctuations

MARINER 2
Launch: 1962
Destination: Venus

As a matter of fact, interplanetary fluctuations do show power laws

Scales of fractions of AUs

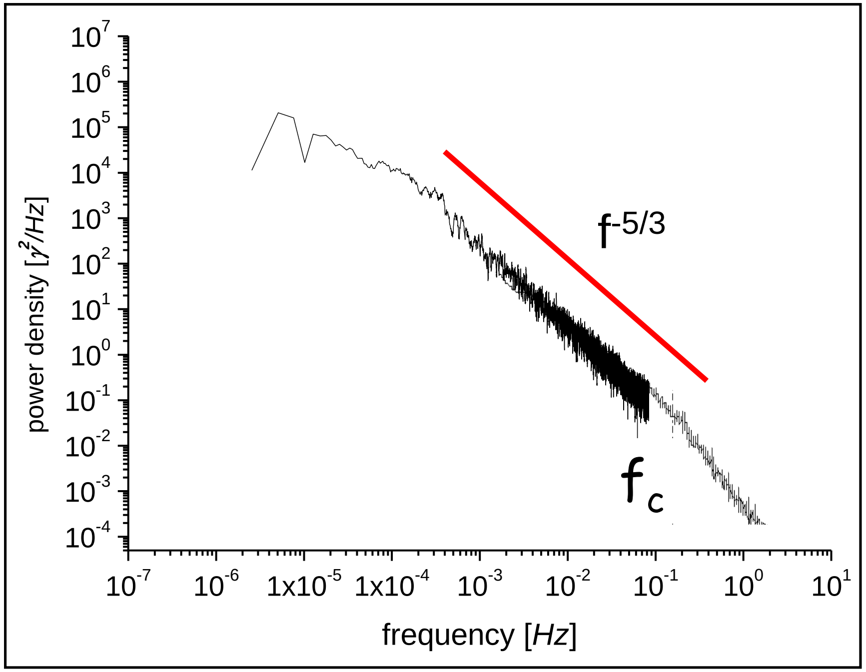

A typical IMF power spectrum in interplanetary space at 1 AU

[Low frequency from Bruno et al., 1985, high freq. tail from Leamon et al, 1999]

Spectral index of turbulent phenomena is universal

Scales of fractions of AUs

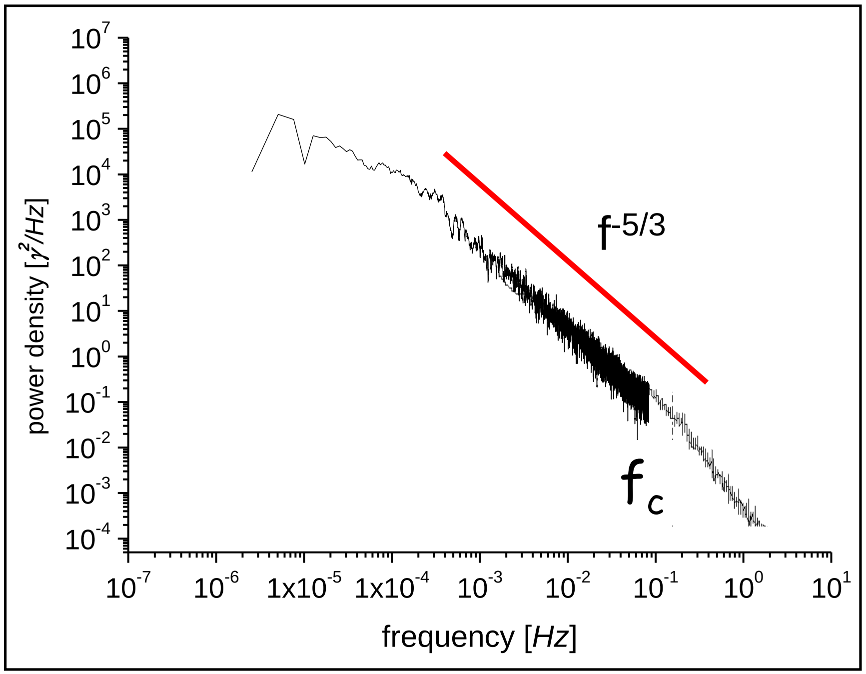

A typical IMF power spectrum in <u>interplanetary space</u> at 1 AU

[Low frequency from Bruno et al., 1985, high freq. tail from Leamon et al, 1999]

Scales of cms

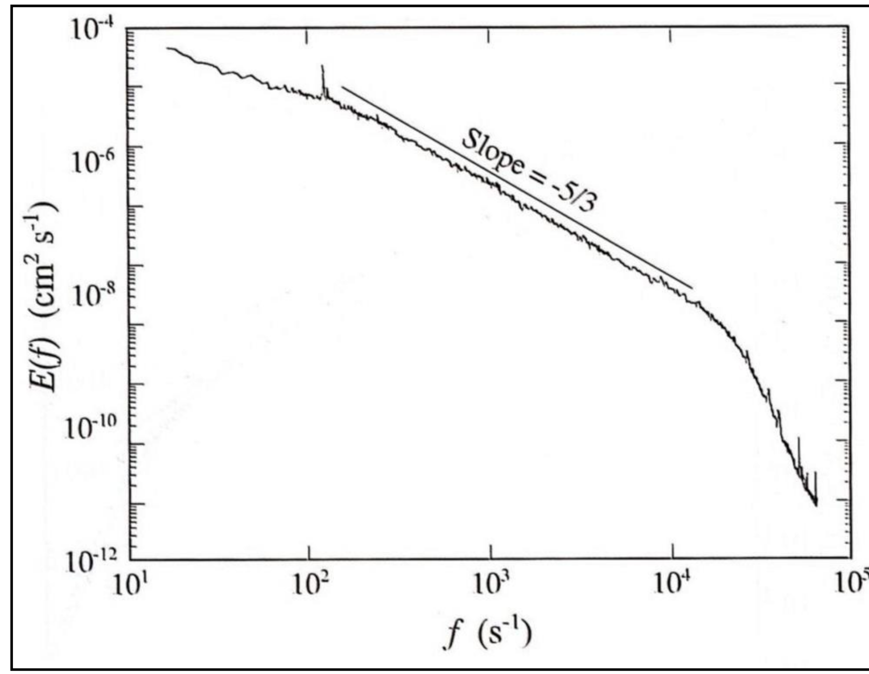

<u>Laboratory experiment on turbulence</u> with low temperature helium gas flow [Maurer et al., 1994]

The phenomenology at the basis of these observations follows the energy cascade *á la* Richardson in the hypothesis of homogeneous and isotropic turbulence

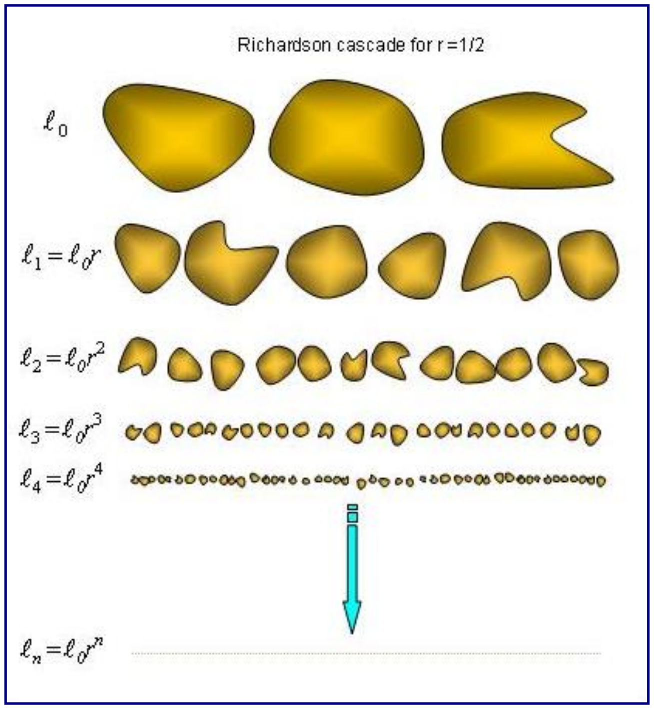

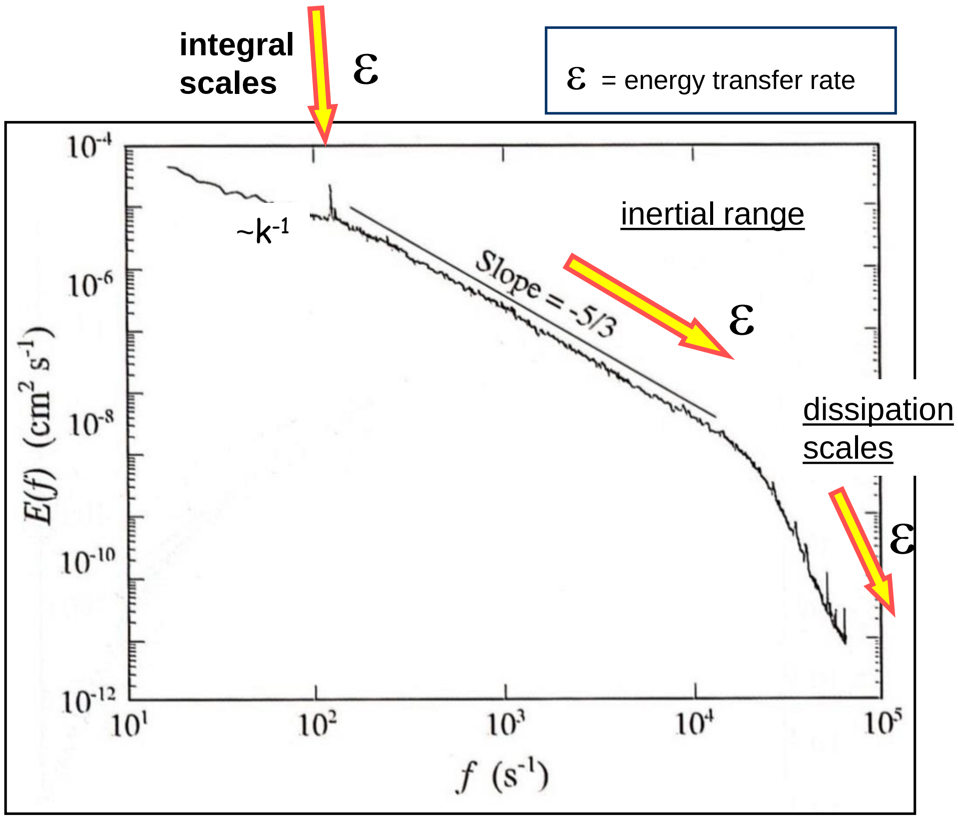

homogeneous=statistically invariant under space translation
isotropic=statistically invariant under simultaneous rotation of δv and ℓ

K41 theory and $k^{-5/3}$ scaling (A.N. Kolmogorov,1941) based on dimensional analysis

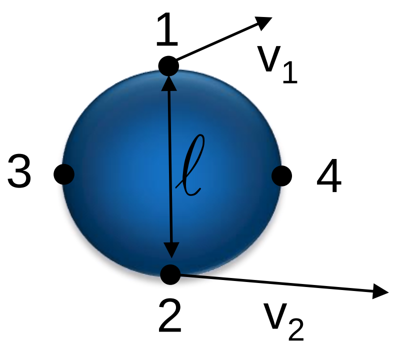

$$\boxed{t_\ell \sim \frac{\ell}{v_2 - v_1} = \frac{\ell}{\delta v_\ell} \rightarrow \frac{\ell}{v_\ell}}$$

eddy turnover time
(generation of new scales)

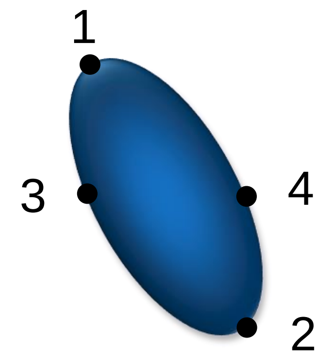

$$\varepsilon_\ell \sim \frac{E_\ell}{t_\ell} \sim \frac{v_\ell^2}{t_\ell} \sim \frac{v_\ell^2 v_\ell}{\ell}$$

$$v_\ell \sim \varepsilon_\ell^{1/3}\, \ell^{1/3}$$

Scaling of power density spectrum

if ε doesn't depend on scale

$$\boxed{\varepsilon_\ell \rightarrow \varepsilon \Rightarrow v_\ell \sim \ell^{1/3}}$$

$$W(k) \sim \delta v_k^2 / k$$

$$k \sim 1/\ell$$

$$\delta v_\ell^2 \sim \ell^{\frac{2}{3}}$$

$$W(k) \sim k^{-1} k^{-\frac{2}{3}} \sim k^{-\frac{5}{3}}$$

Turbulence is the result of nonlinear dynamics and is described by the NS eq.

$$\frac{\partial \vec{u}}{\partial t} + (\vec{u} \cdot \nabla)\vec{u} = -\nabla P + \nu \nabla^2 \vec{u}$$

non-linear

dissipative

$$\vec{\nabla} \cdot \vec{u} = 0$$

Incompressible Navier-Stokes equation
u $\rightarrow$ velocity field
P $\rightarrow$ pressure
$\nu \rightarrow$ kinematic viscosity

$$R_e = \frac{non-linear}{dissipative} = \frac{vL}{\nu}$$

for large $R_e \rightarrow$ non-linear regime

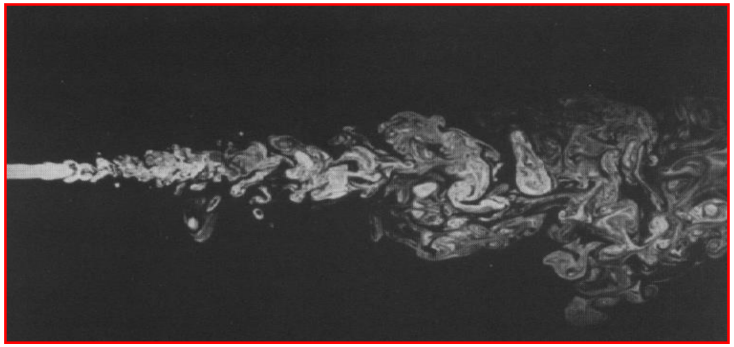

Characteristic scales in turbulence

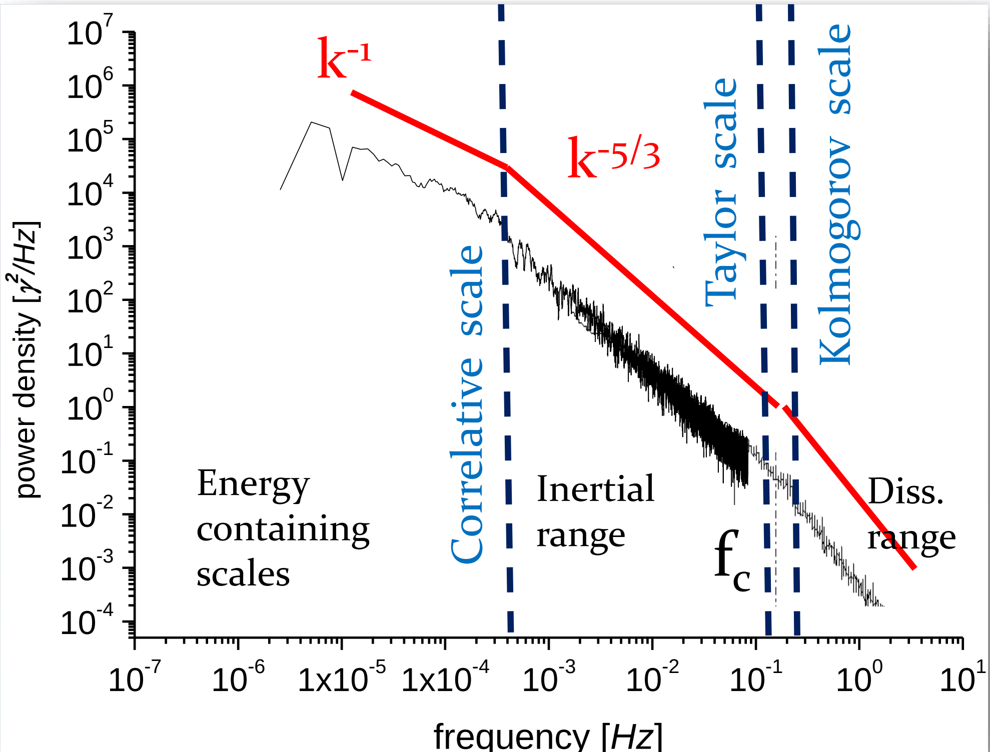

typical IMF power spectrum in at 1 AU

[Low frequency from Bruno et al., 1985, high freq. tail from Leamon et al, 1999]

$$\boxed{R_m^{eff} = \left(\frac{\lambda_C}{\lambda_T}\right)^2}$$

(Batchelor, 1970)

- Correlative Scale/Integral Scale:
  - the largest separation distance over which eddies are still correlated. i.e. the largest turb. eddy size.
- Taylor scale:
  - The scale size at which viscous dissipation begins to affect the eddies.
  - Several times larger than Kolmogorov scale
  - it marks the transition from the inertial range to the dissipation range.
- Kolmogorov scale:
  - The scale size that characterizes the smallest dissipation-scale eddies

The *Taylor Scale* and *Correlative Scale* can be obtained from the two point correlation function

$$\boxed{R(r) = \langle V(x+r)V(x) \rangle_x / \langle (V(x))^2 \rangle}$$

- Taylor scale:
  - Radius of curvature of the Correlation function at the origin.
- Correlative/Integral scale:
  - Scale at which turbulent fluctuation are no longer correlated.

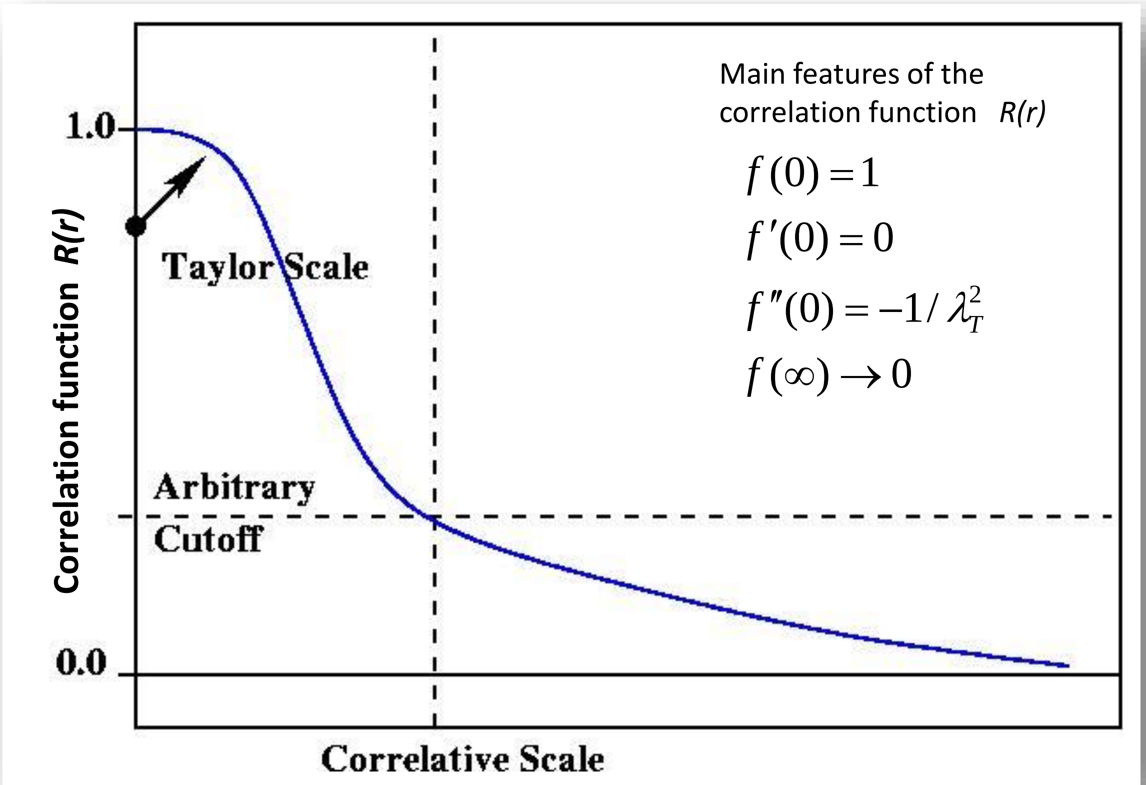

(adapted from Weygand et al., 2007)

We can determine:

- the *Taylor Scale* from Taylor expansion of the two-point correlation function for r→0:

$$\boxed{R(r) \approx 1 - \frac{r^2}{2\lambda_T^{\,2}} + \dots}$$

(Tennekes, and Lumley , 1972)

where *r* is the spacecraft separation and *R(r)* is the two-point correlation function.

- the *Correlative Scale* from:

$$\boxed{R(r) = R_0 \exp(-r/\lambda_C)}$$

(Batchelor, 1970)

- the *effective* magnetic Reynolds number from:

$$\boxed{R_m^{eff} = \left(\frac{\lambda_C}{\lambda_T}\right)^2}$$

(Batchelor, 1970)

- First experimental estimate of the effective Reynolds number in the solar wind (previous estimates obtained only from single spacecraft observations using theTaylor hypothesis)
- First evaluation the two-point correlation functions using simultaneous measurements from Wind, ACE, Geotail, IMP8 and Cluster spacecraft (Matthaeus et al., 2005).

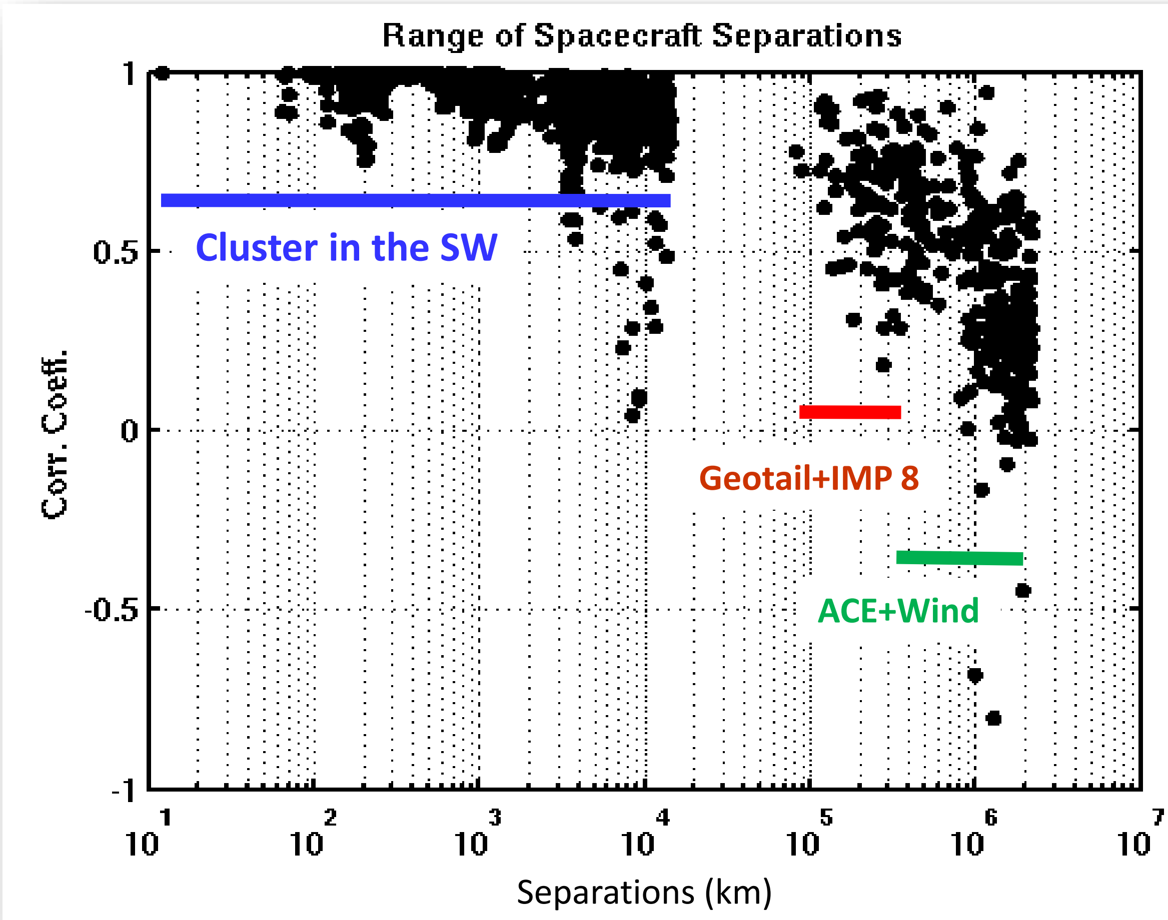

(Matthaeus et al., 2005, Weygand et al., 2007)

Experimental evaluation of λ_C and λ_T in the solar wind at 1 AU

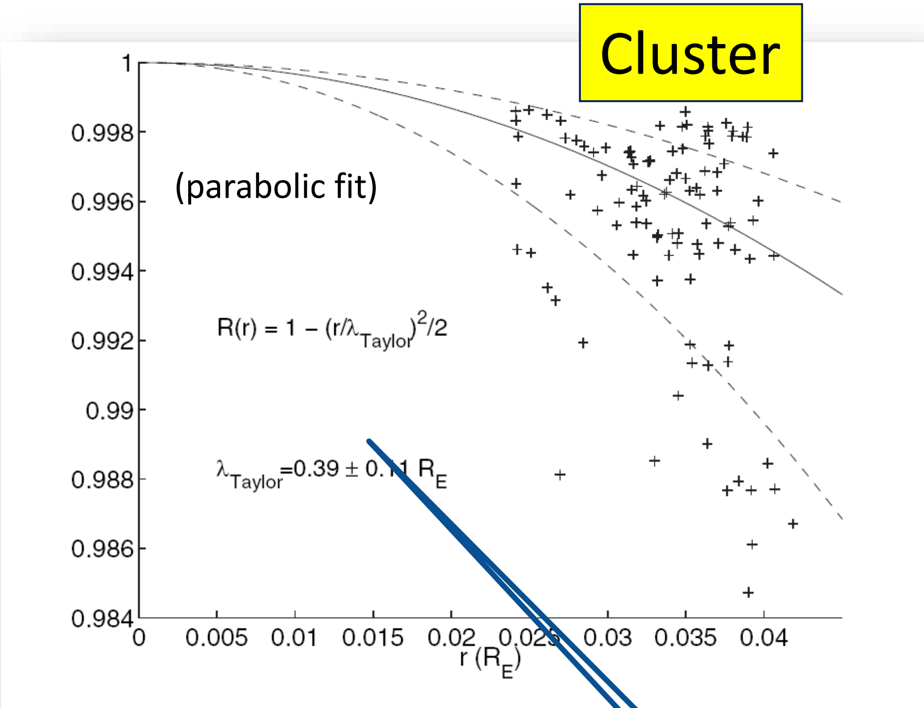

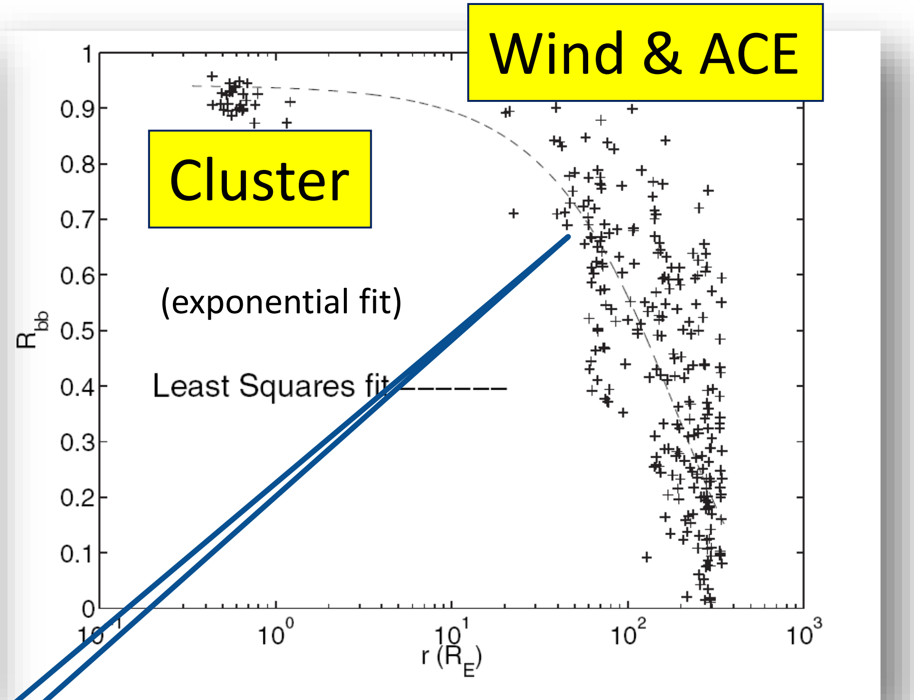

(Matthaeus et al., 2005
Weygand et al., 2007)

$\lambda_T \sim 2.4 \cdot 10^3$ km
$\lambda_C \sim 1.3 \cdot 10^6$ km

$$R_m^{eff} = \left(\frac{\lambda_C}{\lambda_T}\right)^2 \approx 2.3 \cdot 10^5$$

high Reynolds number → turbulent fluid → non-linear interactions expected

Solar wind turbulence: first experimental evidence for the existence of a spectral radial evolution

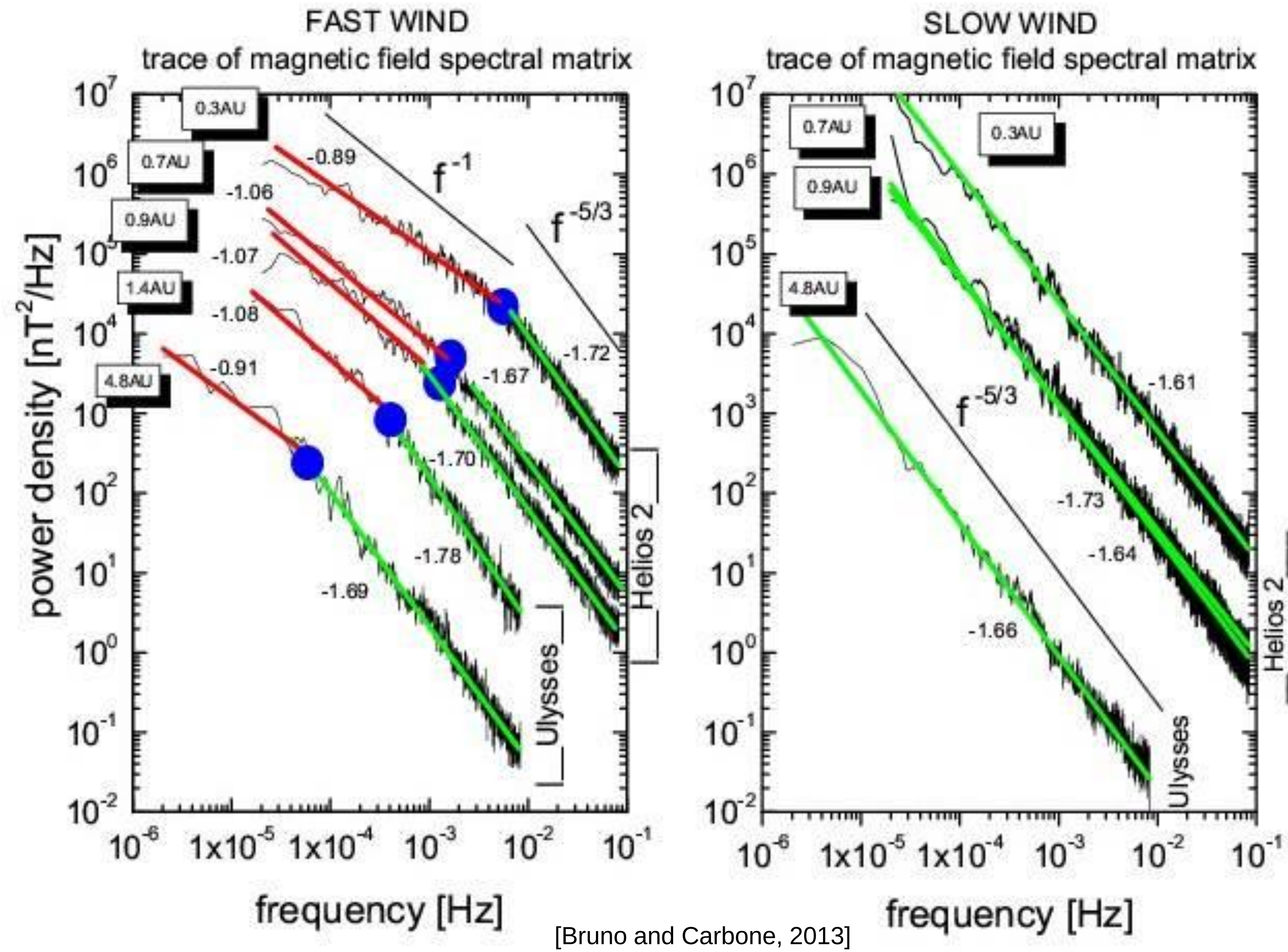

[Bruno and Carbone, 2013]

Solar wind turbulence: first experimental evidence for the existence of a spectral radial evolution

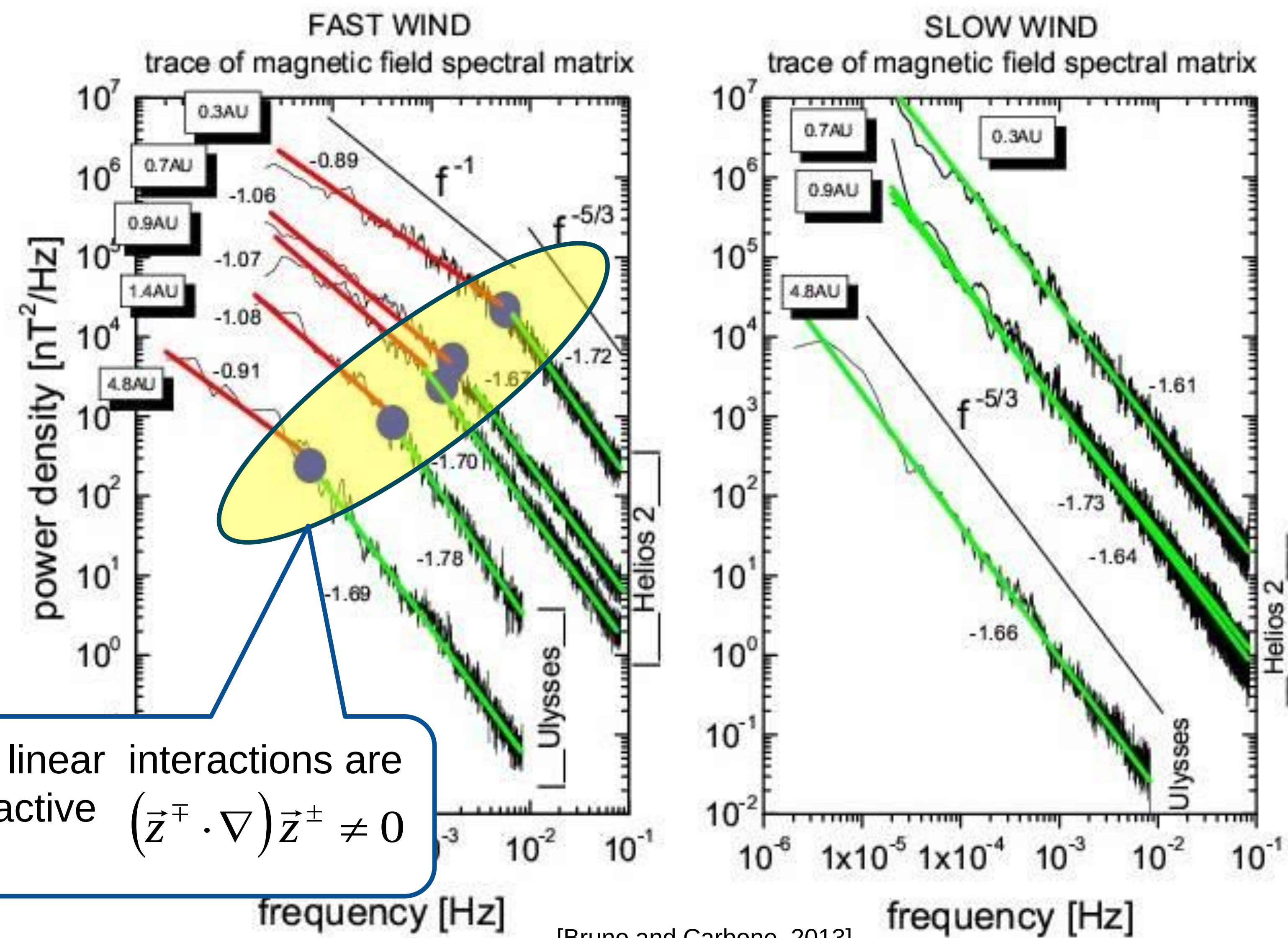

Non linear interactions are still active $\left(\vec{z}^{\mp}\cdot\nabla\right)\vec{z}^{\pm}\neq 0$

[Bruno and Carbone, 2013]

NS equations for the hydromagnetic case

$$\frac{\partial \vec{u}}{\partial t} + (\vec{u} \cdot \nabla)\vec{u} = -\nabla P + \nu \nabla^2 \vec{u}$$

$$\vec{\nabla} \cdot \vec{u} = 0$$

Incompressible
Navier-Stokes equation
u $\rightarrow$ velocity field
P $\rightarrow$ pressure
$\nu \rightarrow$ kinematic viscosity

non-linear

dissipative

$$\frac{\partial \vec{z}^{\pm}}{\partial t} + (\vec{z}^{\mp} \cdot \nabla)\vec{z}^{\pm} = -\nabla P + \frac{\nu + \mu}{2} \nabla^2 \vec{z}^{\pm}$$

$$\vec{z}^{\pm} = \vec{u} \pm \vec{b} = \vec{u} \pm \vec{B} / \sqrt{4\pi\rho}$$

Hydromagnetic flows: same "structure" of NS equations

Elsässer variables

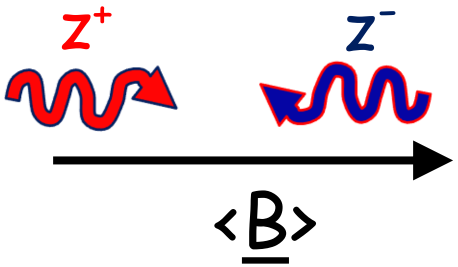

NS equations for the hydromagnetic case

$$\frac{\partial \vec{u}}{\partial t} + (\vec{u} \cdot \nabla)\vec{u} = -\nabla P + \nu \nabla^2 \vec{u}$$

$$\vec{\nabla} \cdot \vec{u} = 0$$

Incompressible
Navier-Stokes equation
u $\rightarrow$ velocity field
P $\rightarrow$ pressure
ν $\rightarrow$ kinematic viscosity

non-linear

dissipative

$$\frac{\partial \vec{z}^{\pm}}{\partial t} + (\vec{z}^{\mp} \cdot \nabla)\vec{z}^{\pm} = -\nabla P + \frac{\nu + \mu}{2} \nabla^2 \vec{z}^{\pm}$$

$$\vec{z}^{\pm} = \vec{u} \pm \vec{b} = \vec{u} \pm \vec{B} / \sqrt{4\pi\rho}$$

Hydromagnetic flows: same "structure" of NS equations

Nonlinear interactions and the consequent energy cascade need both Z^+ and Z^-

Definition of the Elsässer variables

$$\boxed{\delta\vec{z}^{\pm} = \delta\vec{v} \pm \frac{\delta\vec{b}}{\sqrt{4\pi\rho}}}$$

$$\boxed{\mathrm{sign}[-\vec{k}\cdot\vec{B}_0]}$$

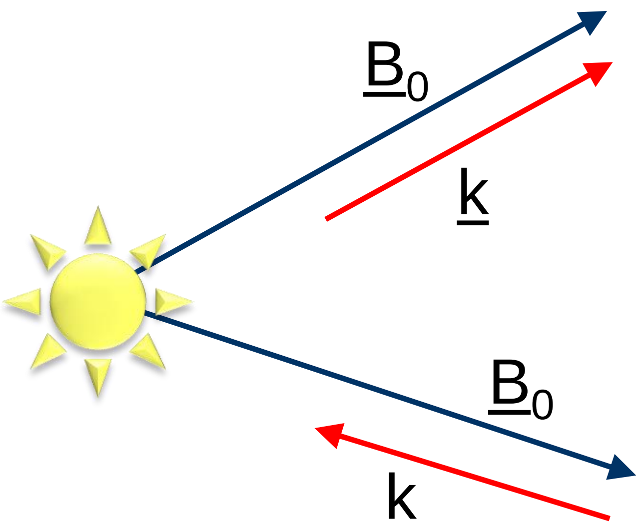

$$\boxed{\delta\vec{z}^{+} = \delta\vec{v} - \frac{\delta\vec{b}}{\sqrt{4\pi\rho}}}$$

outward propagating wave

$$\boxed{\delta\vec{z}^{-} = \delta\vec{v} + \frac{\delta\vec{b}}{\sqrt{4\pi\rho}}}$$

inward propagating wave

Definition of the Elsässer variables

$$\boxed{\delta\vec{z}^{\pm} = \delta\vec{v} \pm \frac{\delta\vec{b}}{\sqrt{4\pi\rho}}}$$

$$\boxed{\mathrm{sign}[-\vec{k}\cdot\vec{B}_0]}$$

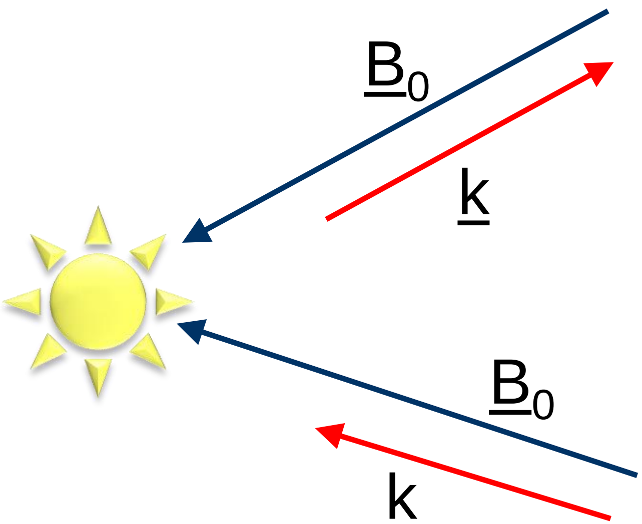

$$\boxed{\delta\vec{z}^{+} = \delta\vec{v} + \frac{\delta\vec{b}}{\sqrt{4\pi\rho}}}$$

outward propagating wave

$$\boxed{\delta\vec{z}^{-} = \delta\vec{v} - \frac{\delta\vec{b}}{\sqrt{4\pi\rho}}}$$

inward propagating wave

Solar wind turbulence is studied by means of the ideal MHD invariants (E, H_c, H_m)

Statistical approach to turbulence

The statistical description of MHD turbulence relies on the evaluation of the three quadratic invariants of the ideal system (no dissipation)

1) total energy per unit density

$$E_t = \frac{1}{2}\left\langle v^2 + b^2 \right\rangle$$

where b is in Alfvén units

$$b \rightarrow \frac{b}{\sqrt{4\pi\rho}}$$

2) cross helicity

$$H_c = \left\langle \vec{v} \cdot \vec{b} \right\rangle$$

3) magnetic helicity

$$H_m = \left\langle \vec{a} \cdot \vec{b} \right\rangle$$

where b is defined via

$$\vec{b} = \vec{\nabla} \times \vec{a}$$

In the following we will use a combination of these invariants to describe the phenomenology of turbulent fluctuations in the solar wind and to understand their nature

Sometimes it is more convenient to use the normalized expressions for cross-helicity and magnetic helicity

$$\boxed{\sigma_c(k) = \frac{2H_c(k)}{E_t(k)}} \quad \boxed{\sigma_m(k) = \frac{kH_m(k)}{E_m(k)}}$$

$$E_m = \left\langle \delta b^2 \right\rangle$$

$$E_t = \left\langle \delta v^2 \right\rangle + \left\langle \delta b^2 \right\rangle$$

σ_c and σ_m can vary between **+1** and **-1**

- the sign of σ_c indicates correlation or anticorrelation between δv and δb
- the sign of σ_m indicates left or right hand polarization

The 2 quadratic invariants E_t and H_c can be expressed in terms of the Elsässer variables

Fields:

$$\boxed{z^{\pm} = v \pm b}$$

Second order moments:

$$e^{\pm} = \frac{1}{2} < \left(z^{\pm}\right)^2 >$$

e^+ and e^- energy

$$e^{v} = \frac{1}{2} < v^2 >$$

Kinetic energy

$$e^{b} = \frac{1}{2} < b^2 >$$

Magnetic energy

$$e^{c} = \frac{1}{2} < v \cdot b >$$

Cross-helicity

The 2 quadratic invariants E_t and H_c can be expressed in terms of the Elsässer variables

Fields:

$$\mathrm{z}^{\pm} = \mathrm{v} \pm \mathrm{b}$$

Normalized parameters:

$$\sigma_c = \frac{2e^c}{e^v + e^b} = \frac{e^+ - e^-}{e^+ + e^-}$$

Normalized cross-helicity

$$\sigma_R = \frac{2e^R}{e^+ + e^-} = \frac{e^v - e^b}{e^v + e^b}$$

Normalized residual energy

$$-1 \le \sigma_c \le 1$$

$$-1 \le \sigma_R \le 1$$

$$r_A = \frac{e^v}{e^b}$$

Alfvén ratio

for an Alfvén wave:

$r_A = e^V/e^B = 1$

$\sigma_C = (e^+ - e^-)/(e^+ + e^-) = \pm 1$

$\sigma_R = (e^V - e^B)/(e^V + e^B) = 0$

observations in the ecliptic

An overview on the main features of solar wind fluctuations at MHD scales in fast and slow wind and their evolution during radial expansion

- Fast and slow wind features should never be averaged together.

«*Asking for the average solar wind might appear as silly as asking for the taste af an average drink. What is the average between wine and beer? Obviously a mere mixing – and averaging means mixing – does not lead to a meaningful result.*
Better taste and judge separately and then compare, if you wish.»

[Rainer Schwenn, Solar Wind 5, 1982]

Differences in the spectral signature of fast and slow wind

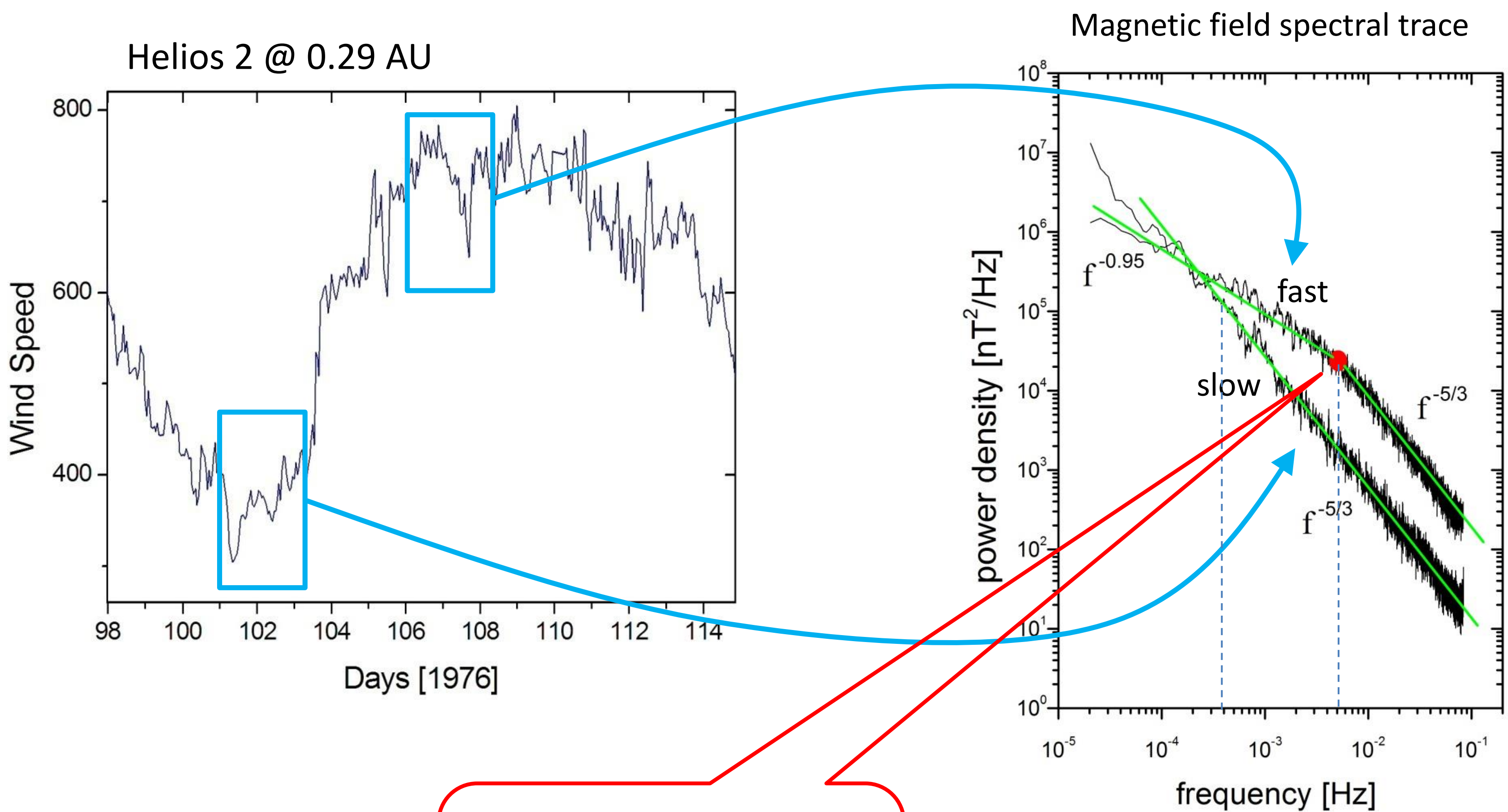

The spectral break in the fast wind spectrum suggests shorter correlation lengths

The spectral break in the fast wind spectrum suggests shorter correlation lengths

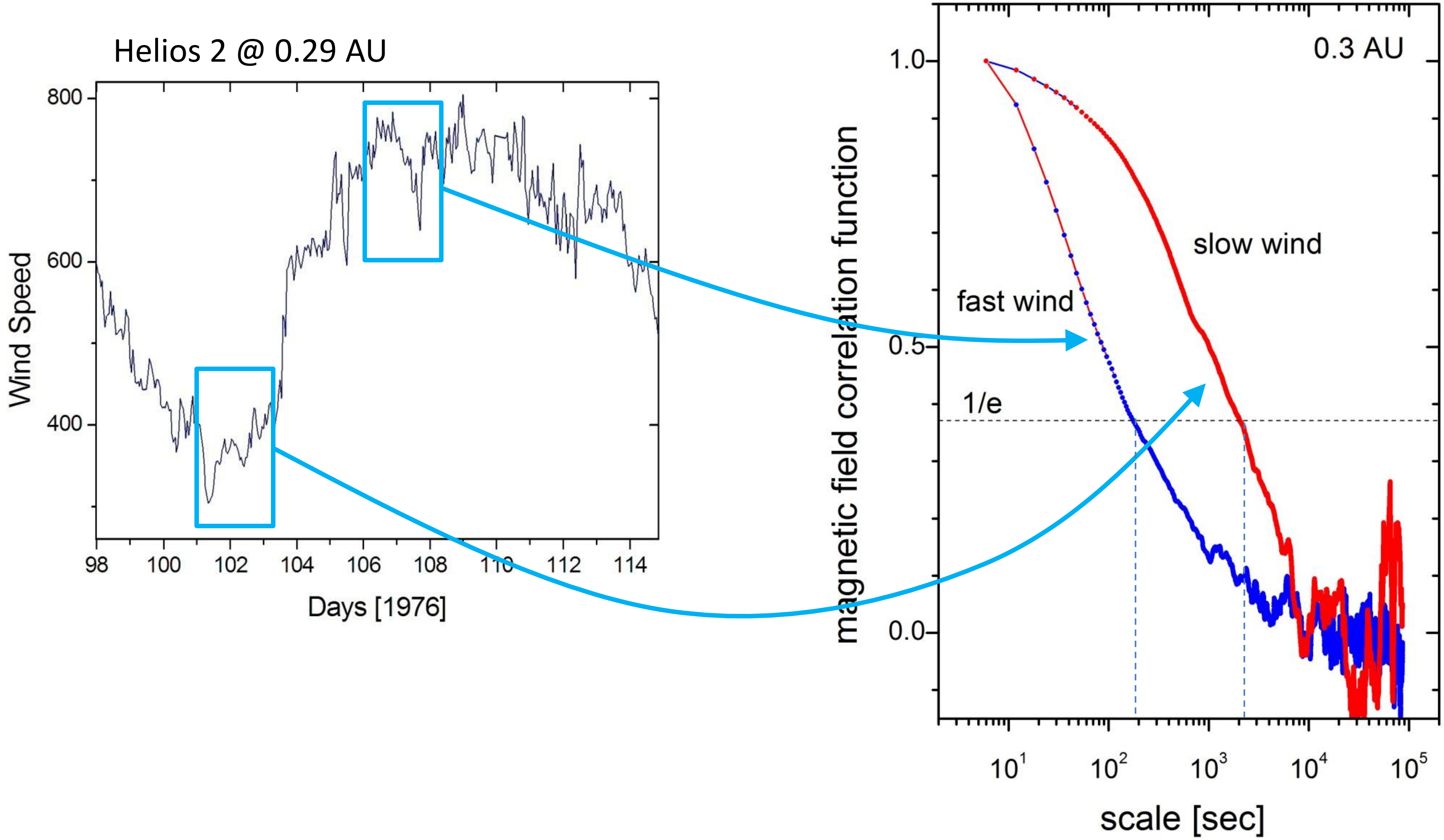

Differences also in the variance anisotropy of the fluctuations wrt Parker's spiral

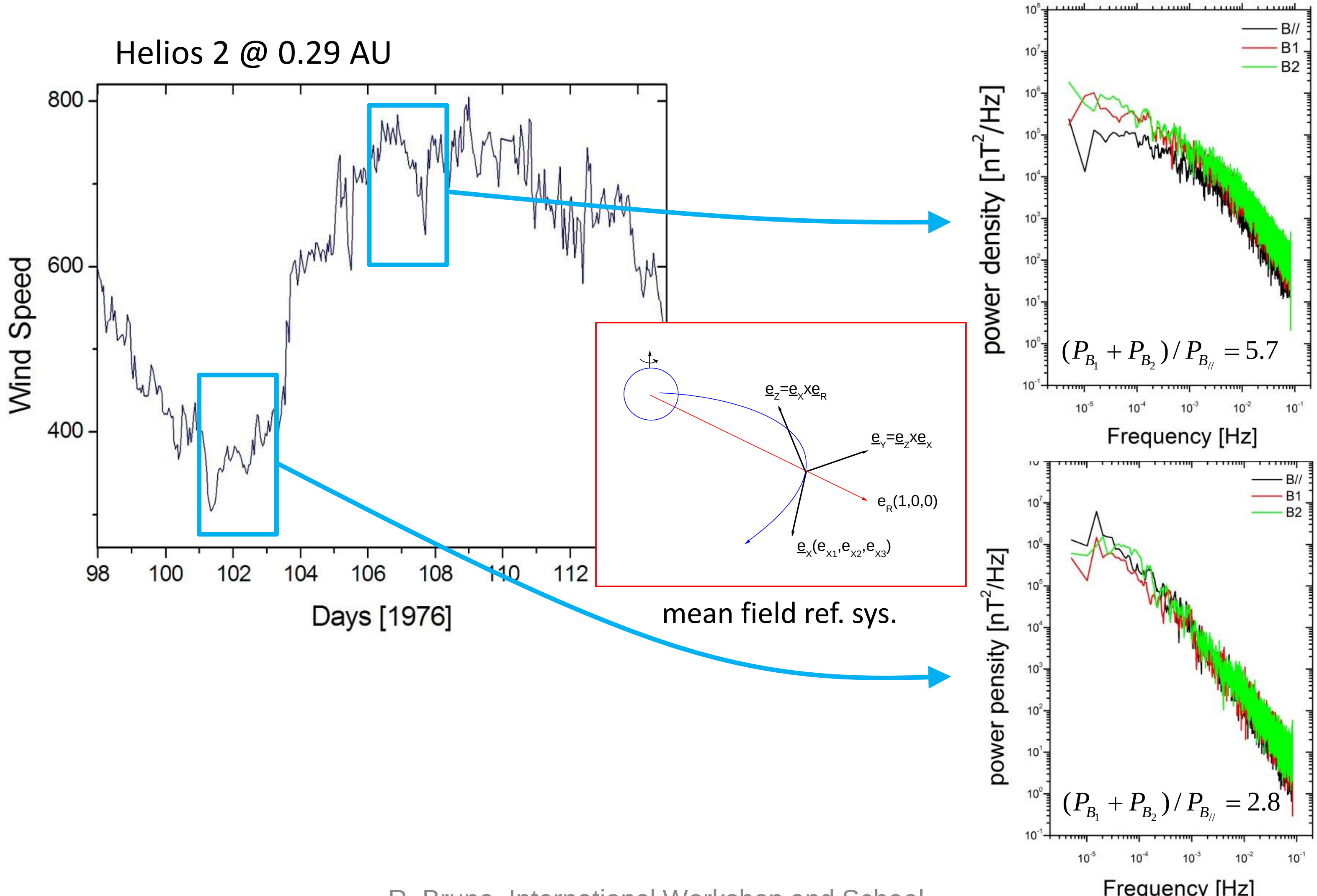

Differences also in the amplitude of directional fluctuations of velocity and magnetic field vectors

Helios 2 @ 0.29 AU

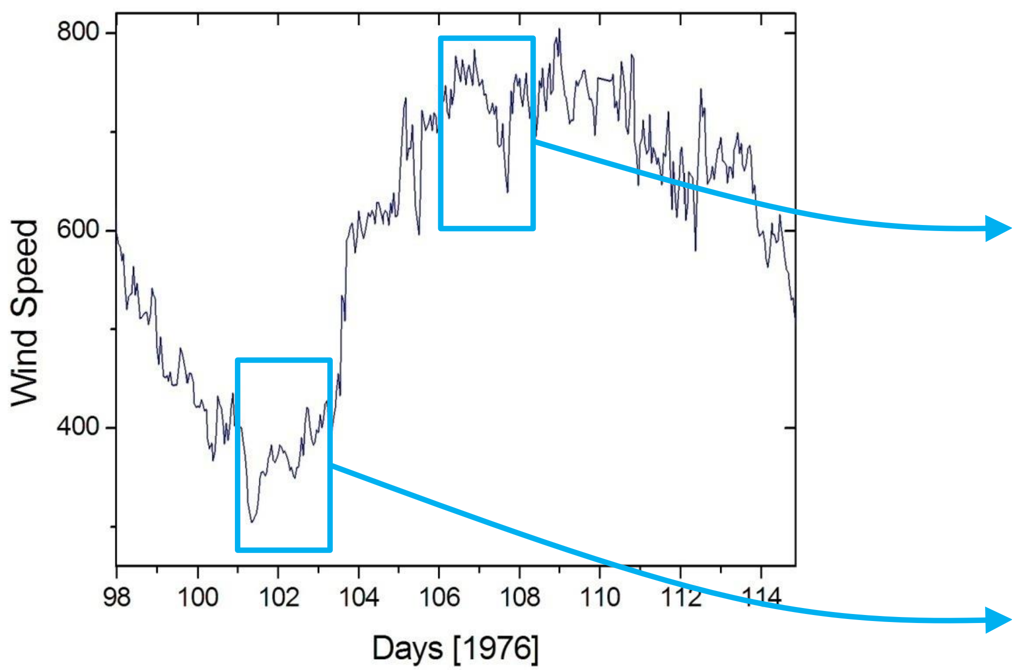

Angular histograms

[scale 81 s]

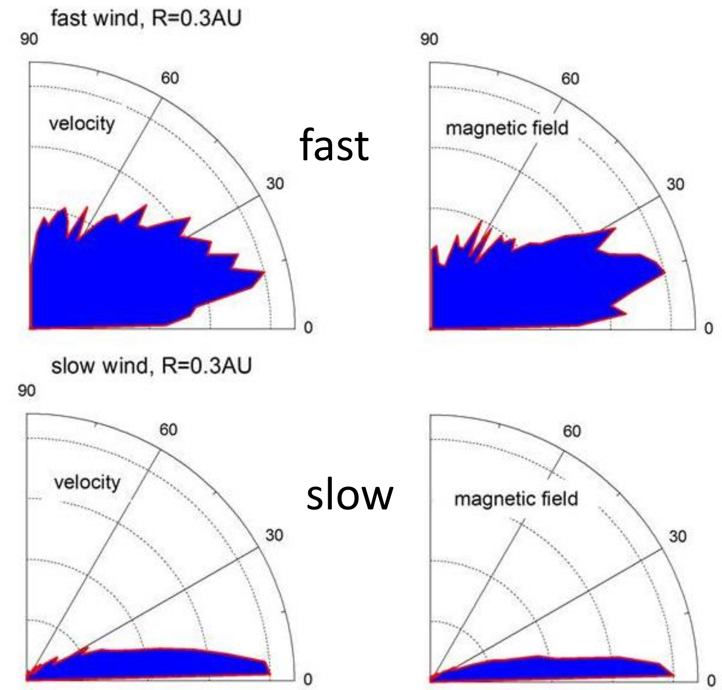

Distributions of the angle formed between two successive vectors time resolution=81sec

Differences also in the spatial distribution of the fluctuations

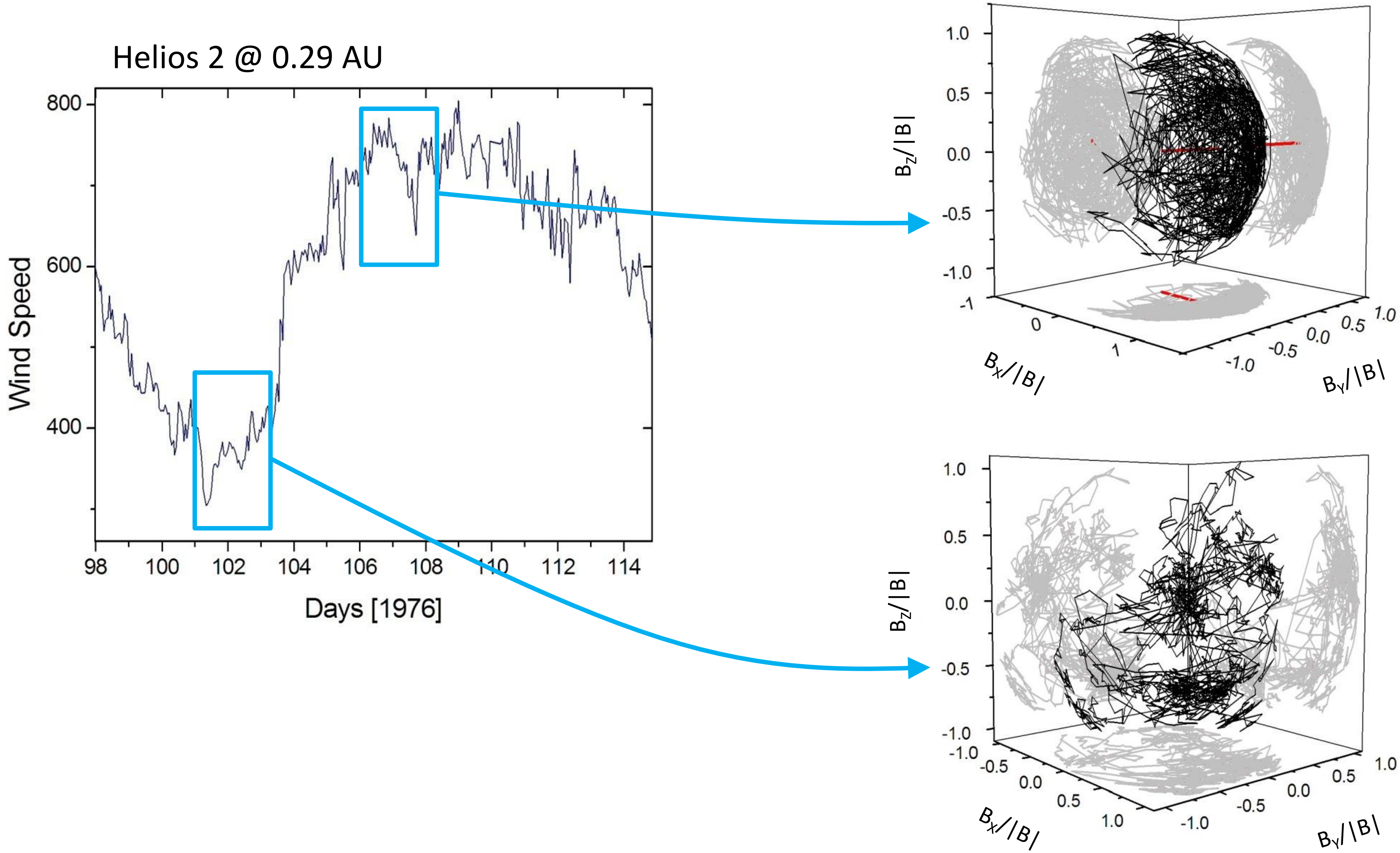

Differences in the orientation of the minimum variance direction

Helios 2 @ 0.29 AU

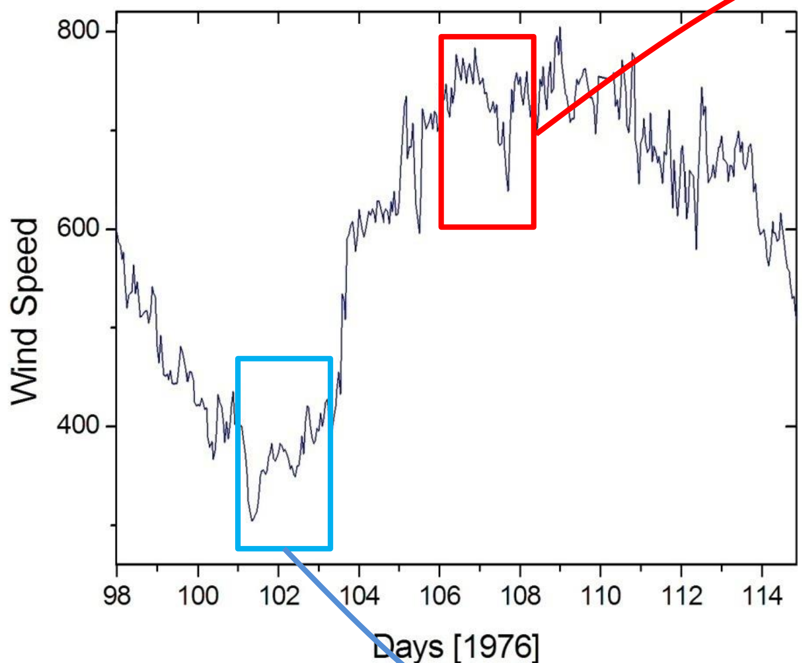

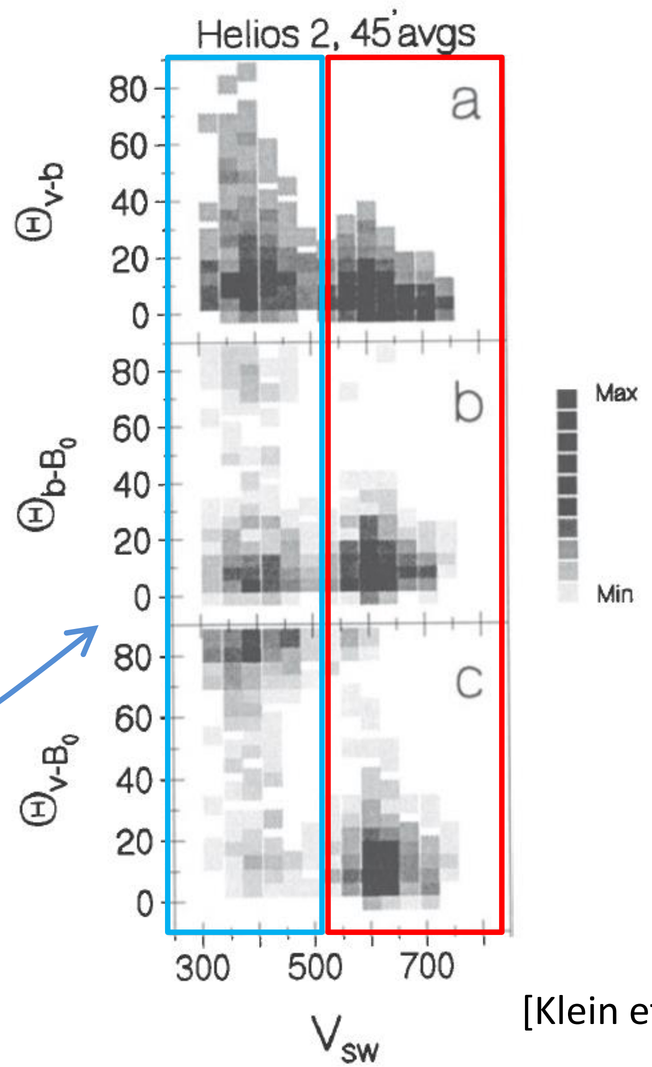

$\boldsymbol{\theta_{v\text{-}b}}$: angle between MVD of $\delta\mathbf{b}$ and $\delta\mathbf{v}$

$\boldsymbol{\theta_{b\text{-}B0}}$: angle between MVD of $\delta\mathbf{b}$ and $\mathbf{B}_0$

$\boldsymbol{\theta_{v\text{-}B0}}$: angle between MVD of $\delta\mathbf{v}$ and $\mathbf{B}_0$

❑ fast wind: the local field orders the behaviour of the fluctuations

[Klein et al., 1993]

Differences in the level of normalized crosshelicity

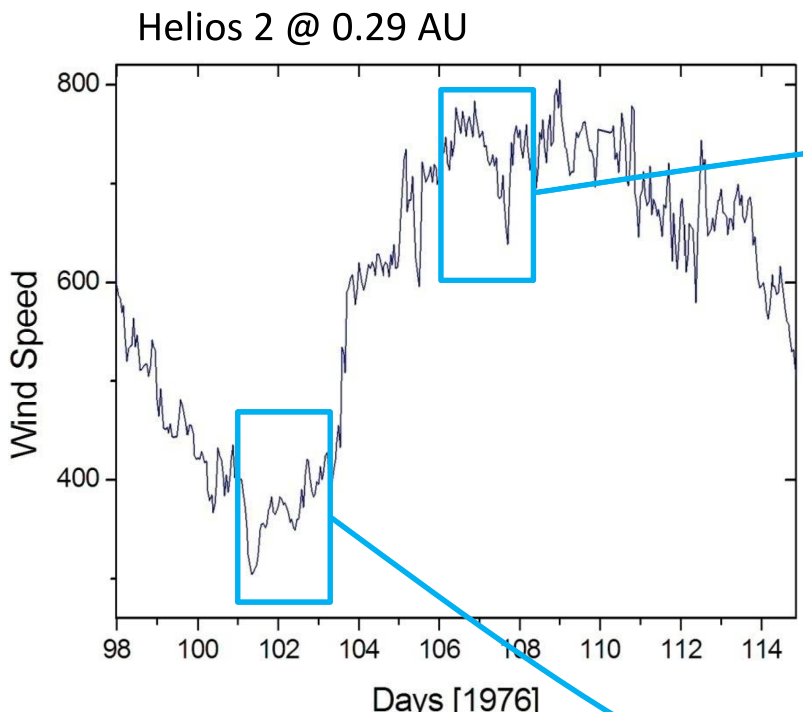

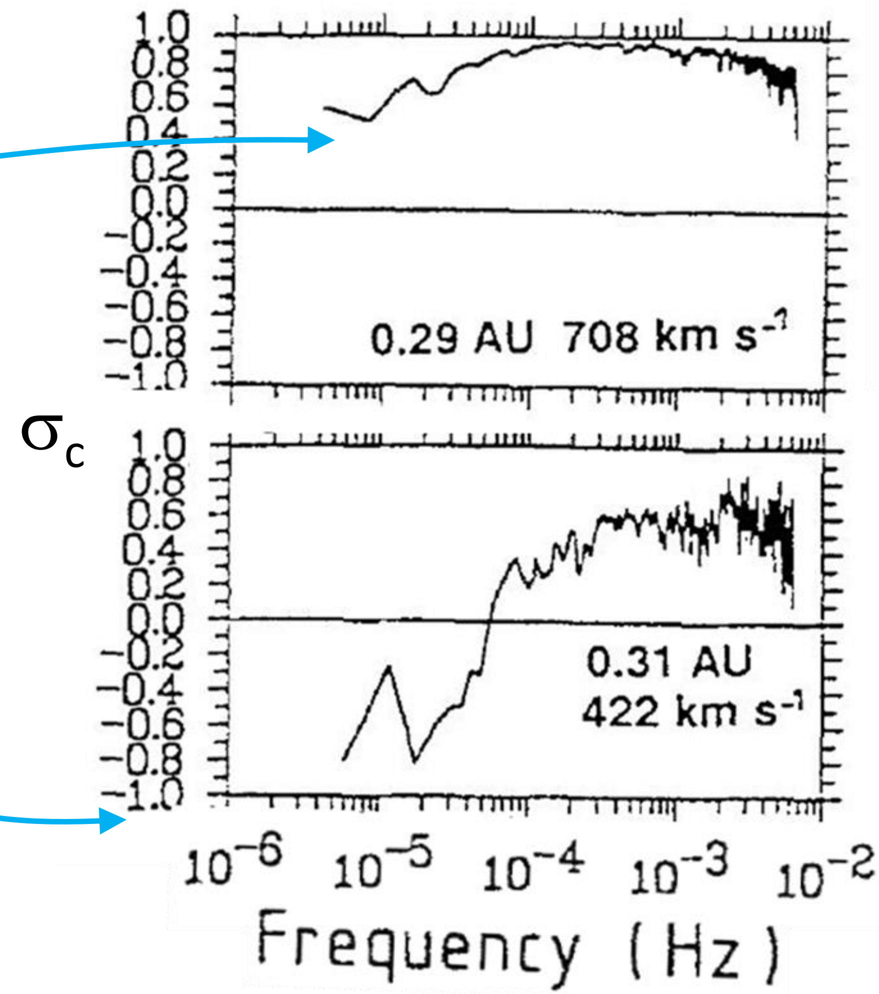

$$e(f_k) = \frac{1}{2}\left(e^{+}(f_k) + e^{-}(f_k)\right)$$

$$e^{c}(f_k) = \frac{1}{2}\left(e^{+}(f_k) - e^{-}(f_k)\right)$$

$$\sigma_c(f_k) = \frac{e^{c}(f_k)}{e(f_k)} \rightarrow \in [-1;+1]$$

[adapted from Marsch and Tu, 1990]

Differences in the level of magnetic and kinetic energy content

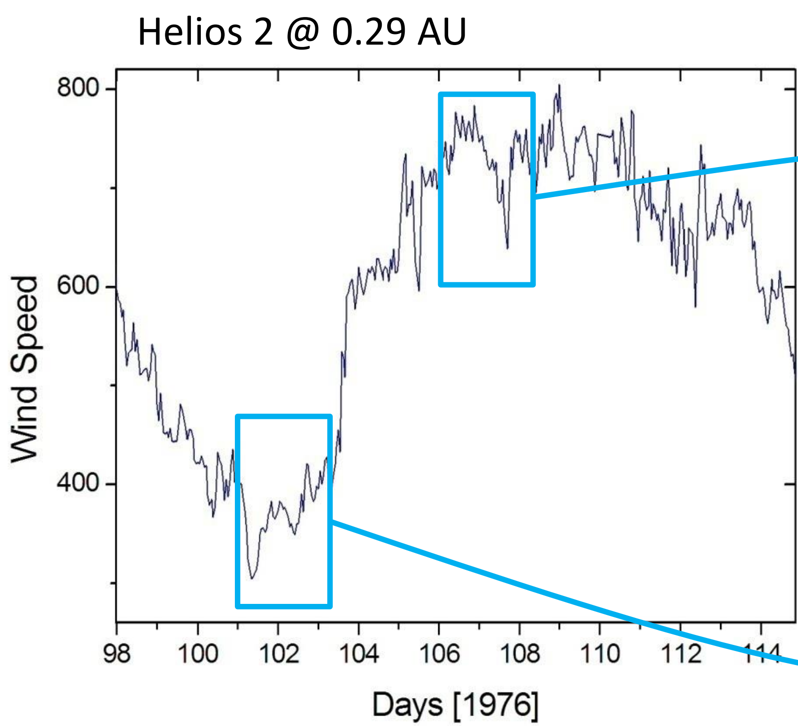

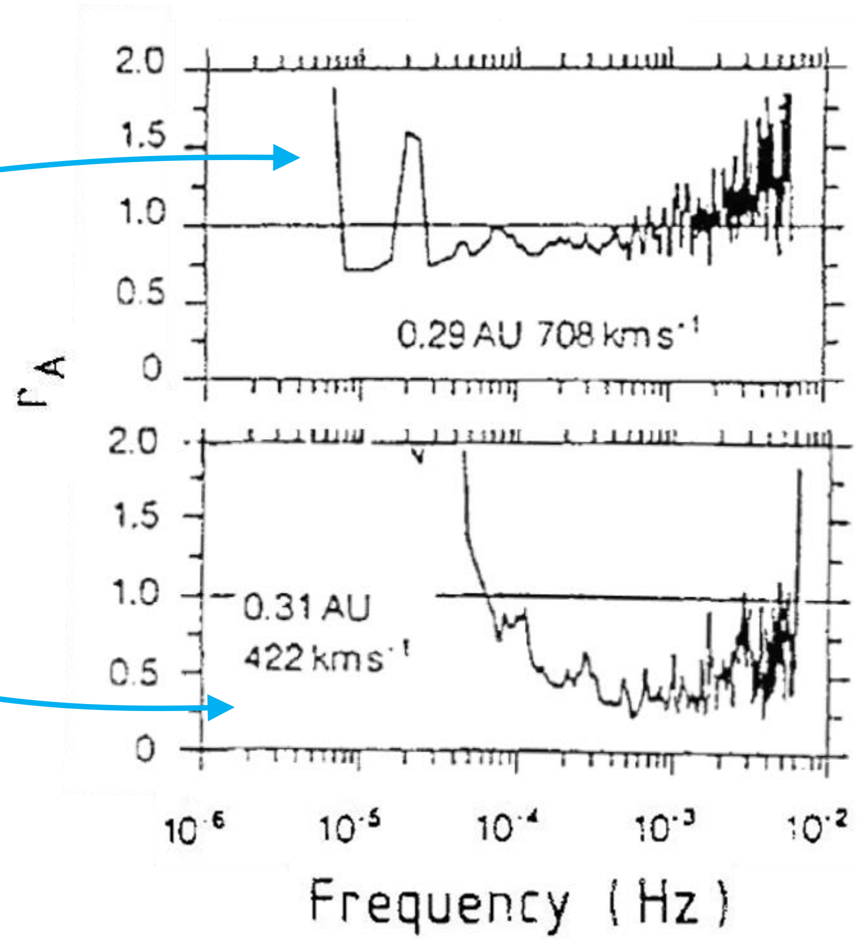

$$r_A(f_k) = e_v(f_k) / e_b(f_k)$$

$$\sigma_r(f_k) = \frac{e_v(f_k) - e_b(f_k)}{e_v(f_k) + e_b(f_k)} \rightarrow \in [-1;+1]$$

[adapted from Marsch and Tu, 1990]

Differences in Intermittency along the velocity profile

a measure of the non-Gaussianity of the fluctuations

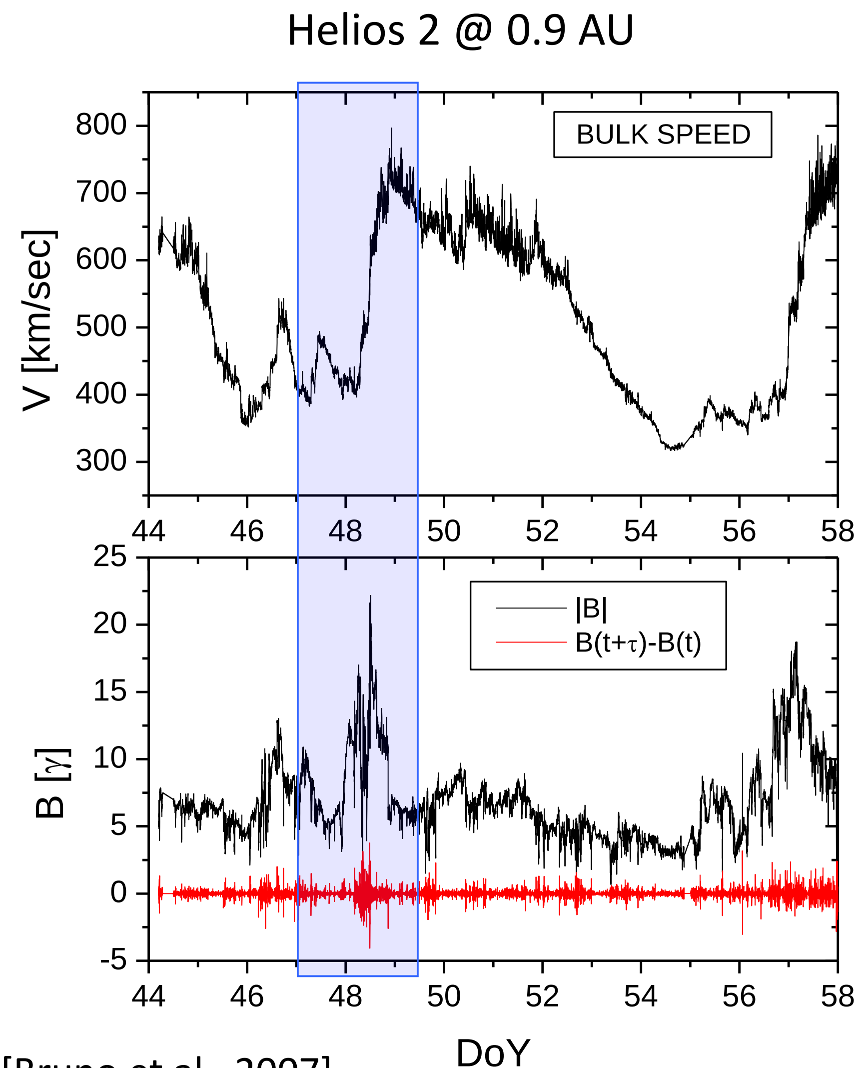

[Bruno et al., 2007]

Intermittency strongly depends on the location within the stream

$$F_\tau = S^4_\tau/(S^2_\tau)^2$$

$$S^p_\tau = <(\xi(t+\tau)-\xi(t))^p>$$

Magnetic field flatness

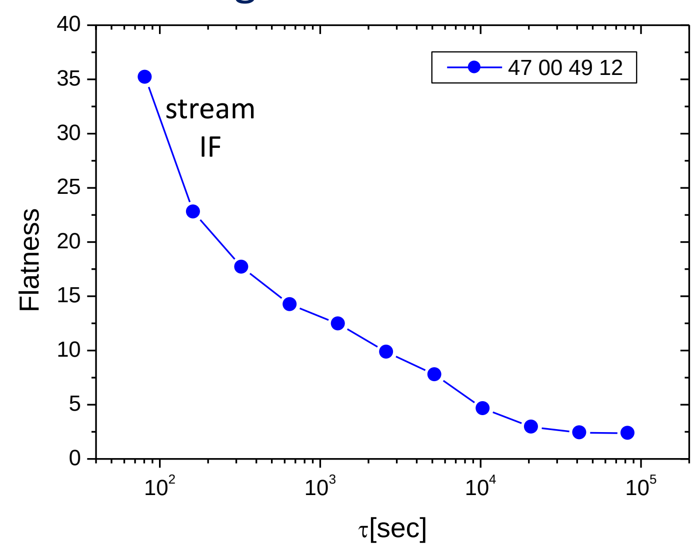

Differences in Intermittency along the velocity profile

a measure of the non-Gaussianity of the fluctuations

Helios 2 @ 0.9 AU

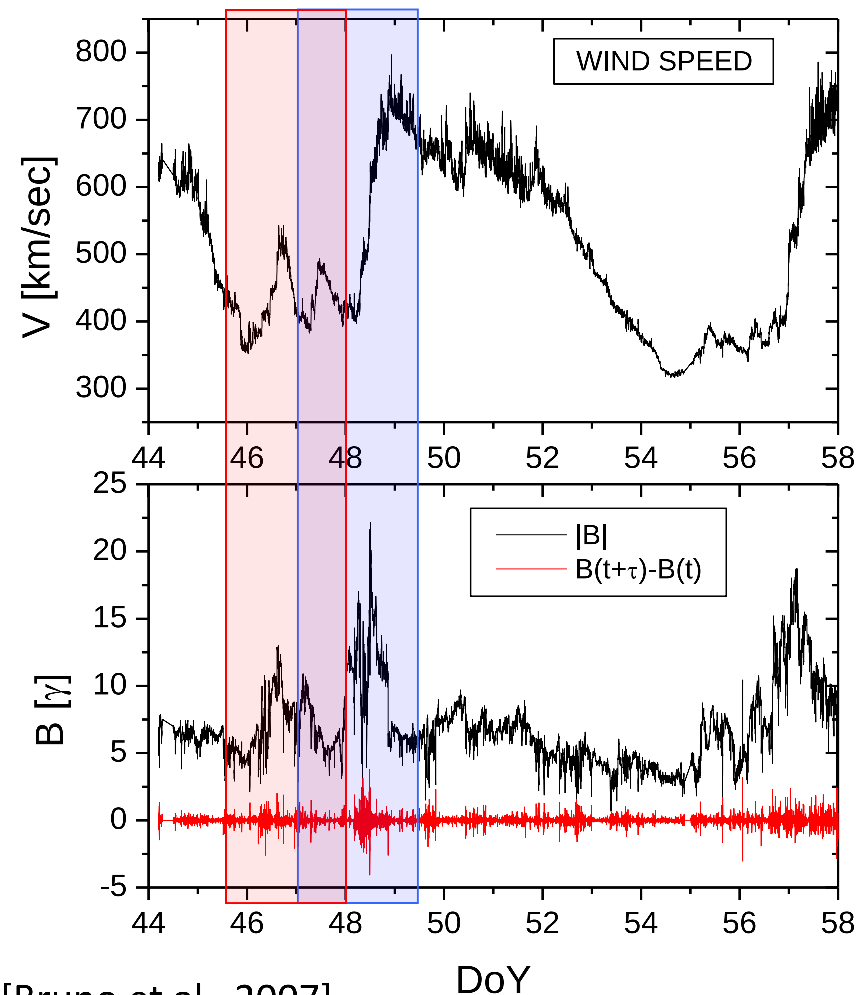

[Bruno et al., 2007]

Intermittency strongly depends on the location within the stream

$$F_\tau = S_\tau^4/(S_\tau^2)^2$$
$$S_\tau^p = <(\xi(t+\tau)-\xi(t))^p>$$

Magnetic field flatness

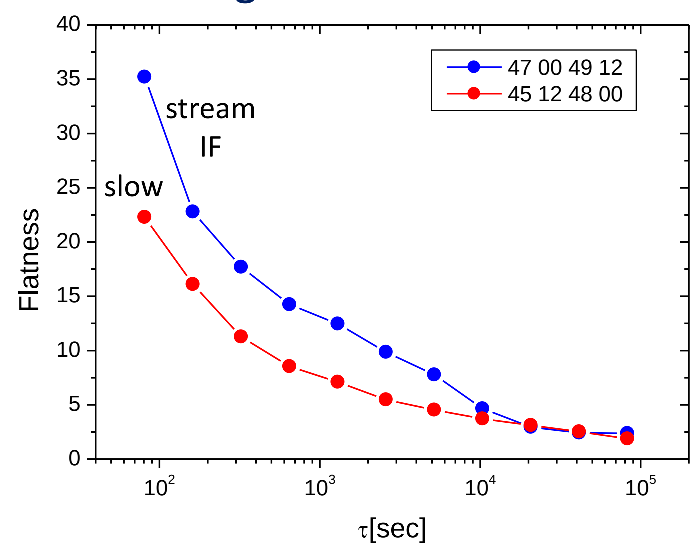

Differences in Intermittency along the velocity profile

$\underbrace{\text{Intermittency}}_{\text{a measure of the non-Gaussianity of the fluctuations}}$

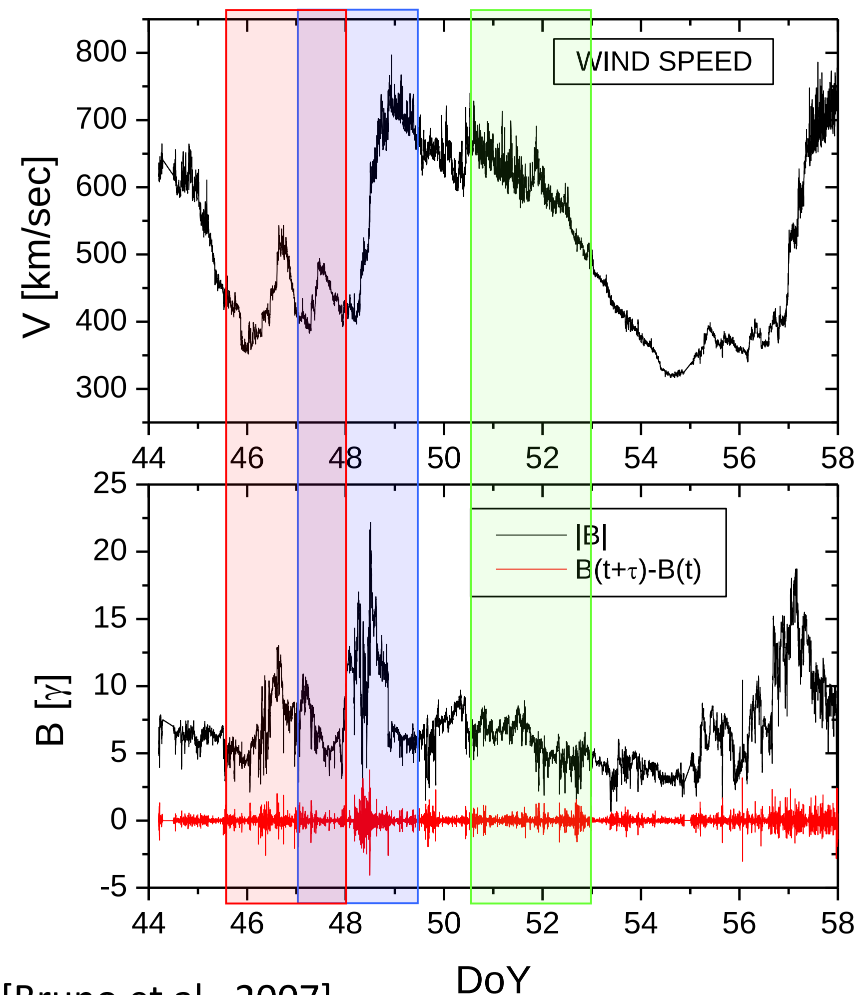

[Bruno et al., 2007]

Intermittency strongly depends on the location within the stream

$$F_\tau = S_\tau^4/(S_\tau^2)^2$$

$$S_\tau^p = \langle (\xi(t+\tau) - \xi(t))^p \rangle$$

Magnetic field flatness

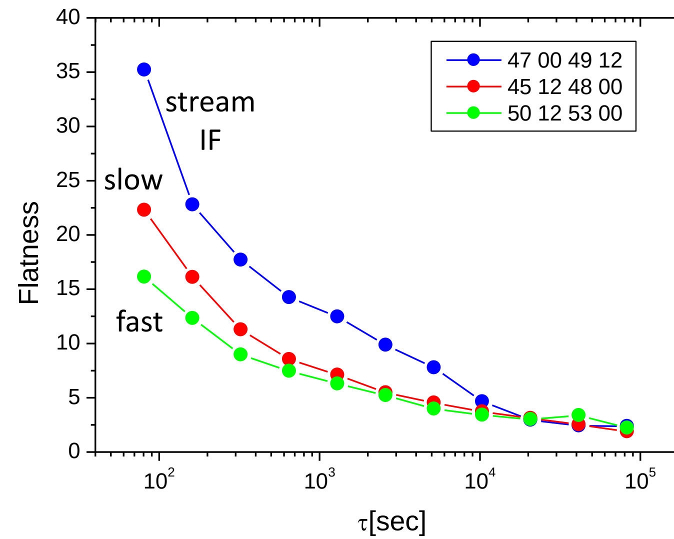

Differences in the Alfvénic character of the fluctuations in fast and slow wind

$$v_{az} = sign[-\vec{k} \cdot \vec{B}_0] \frac{b_z}{\sqrt{4\pi\rho}}$$

Helios 2 @ 0.29 AU

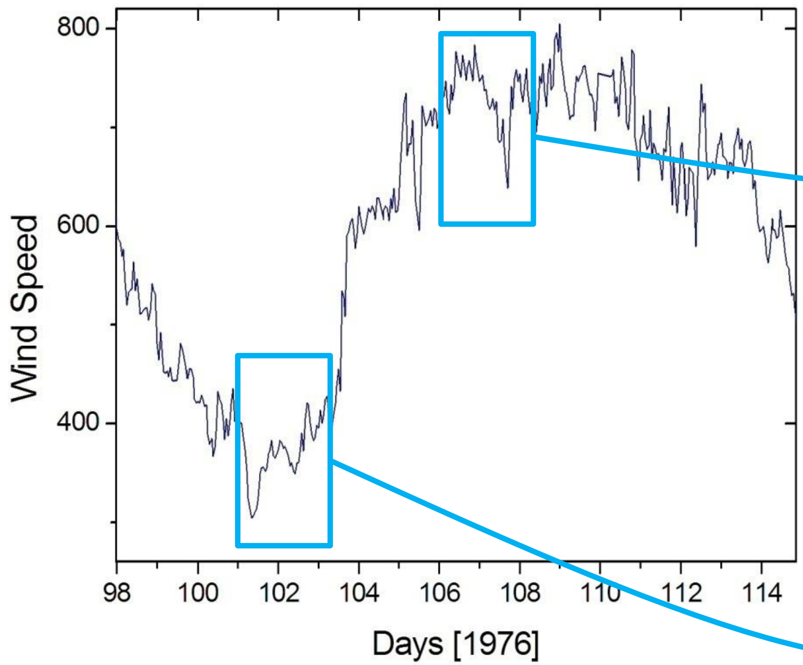

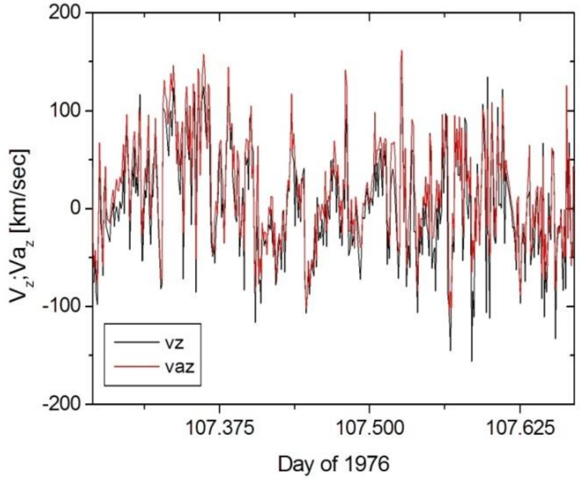

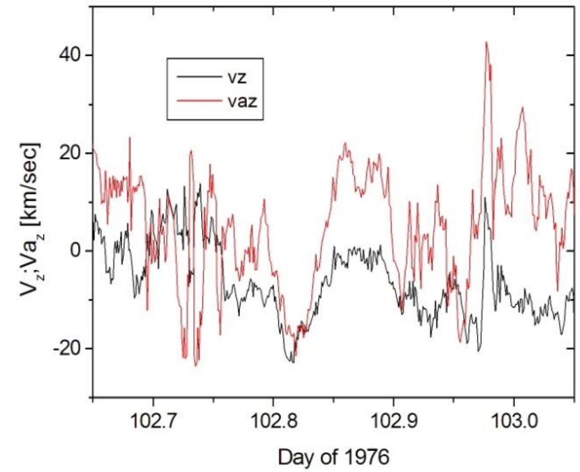

Differences in the $\delta \underline{B}$-$\delta \underline{V}$ alignment

$$\hat{\theta}_{\tau} = \cos^{-1}\left\langle \frac{\Delta\vec{v}_{\tau}(t)\cdot\Delta\vec{b}_{\tau}(t)}{|\Delta\vec{v}_{\tau}(t)||\Delta\vec{b}_{\tau}(t)|} \right\rangle_t$$

Helios 2 @ 0.29 AU

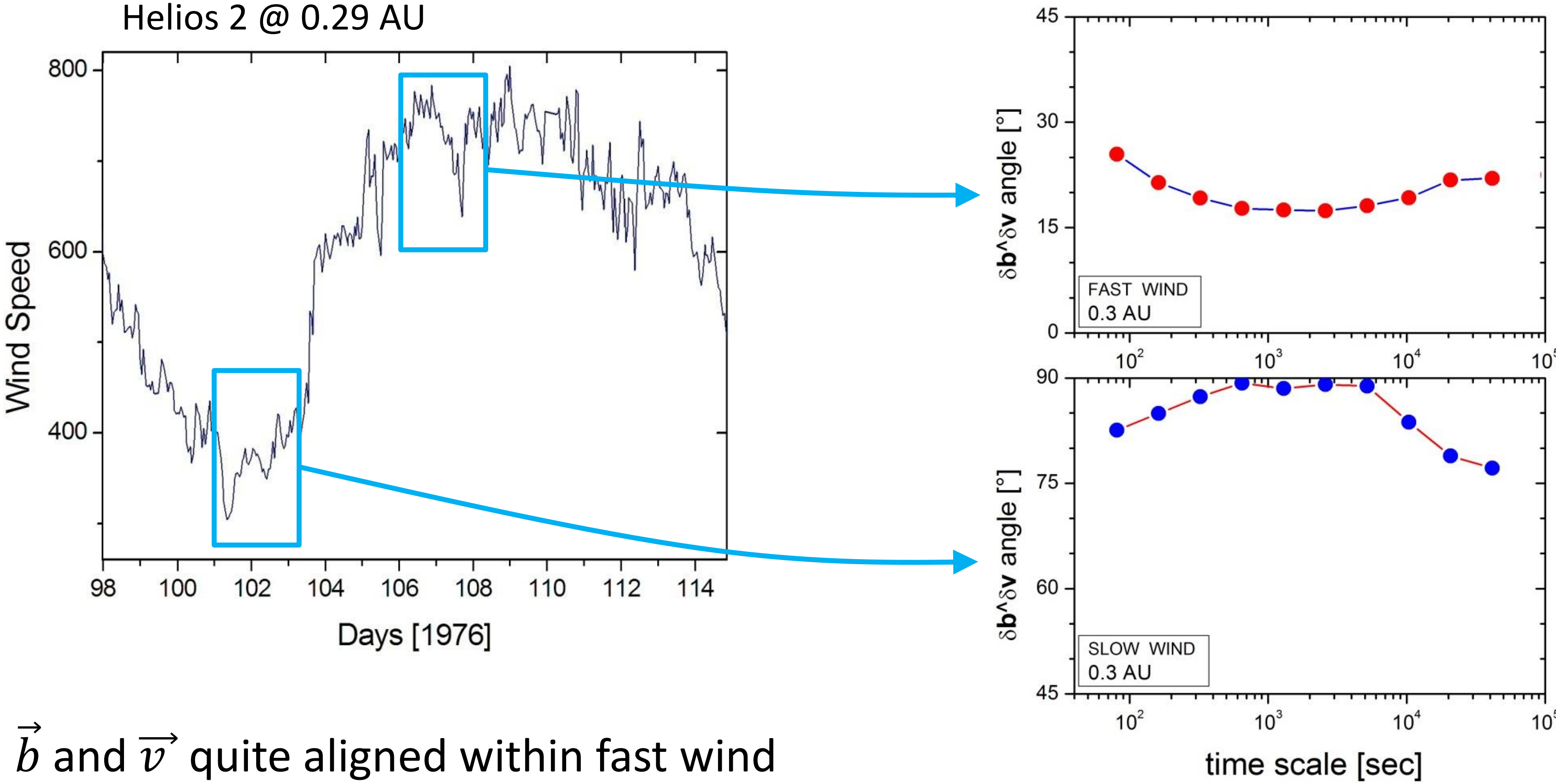

$\vec{b}$ and $\vec{v}$ quite aligned within fast wind

best alignment ~ 20-30 min

Alfvénic correlations: fast vs slow wind

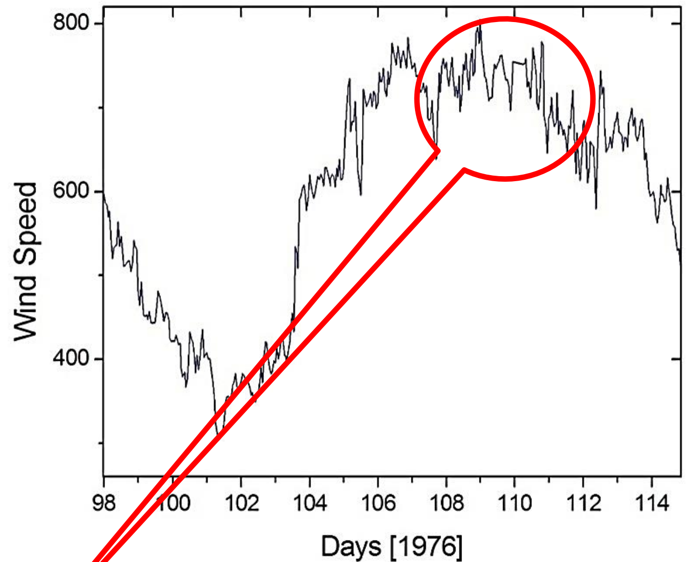

0.3 AU

Fast wind:
fluctuations strongly Alfvénic

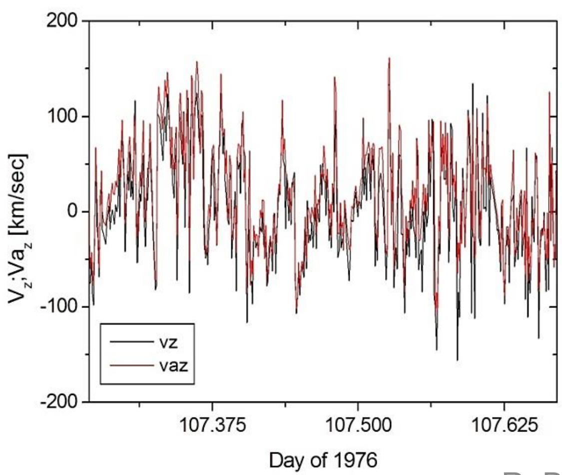

Outward modes largely dominate

FFT($Z^{\pm}$)$\rightarrow e^{\pm}$

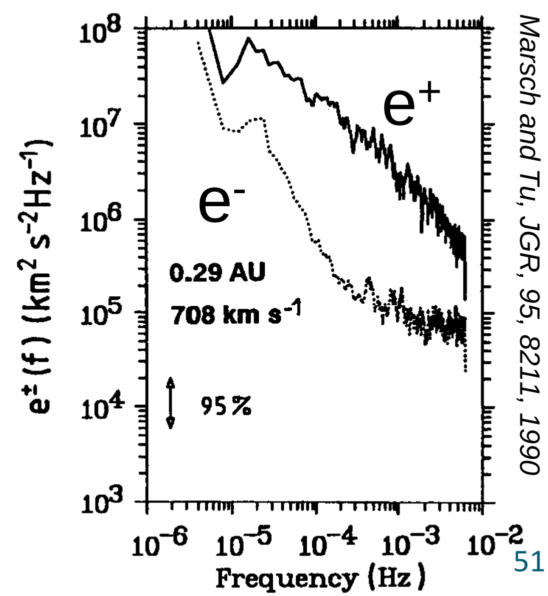

Alfvénic correlations: fast vs slow wind

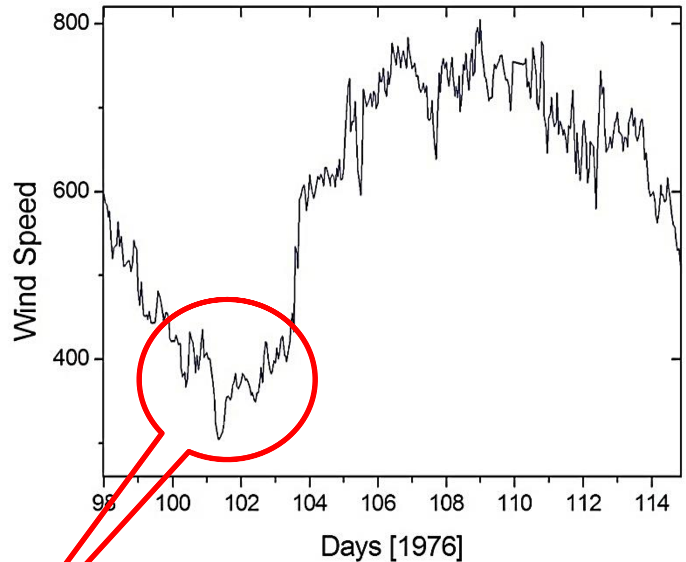

0.3 AU

Slow wind:
fluctuations
scarcely Alfvénic

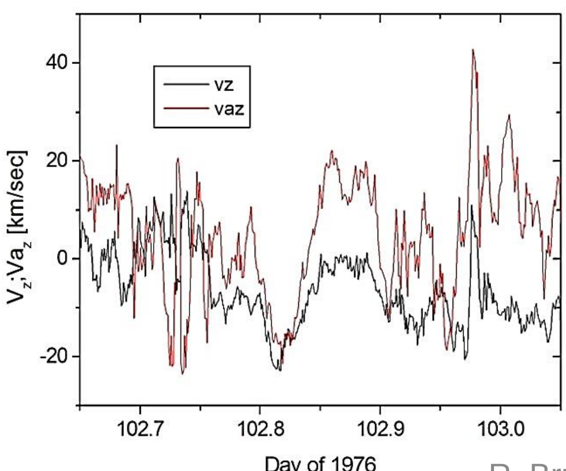

$FFT(Z^{\pm}) \rightarrow e^{\pm}$

outward modes
≅ inward modes

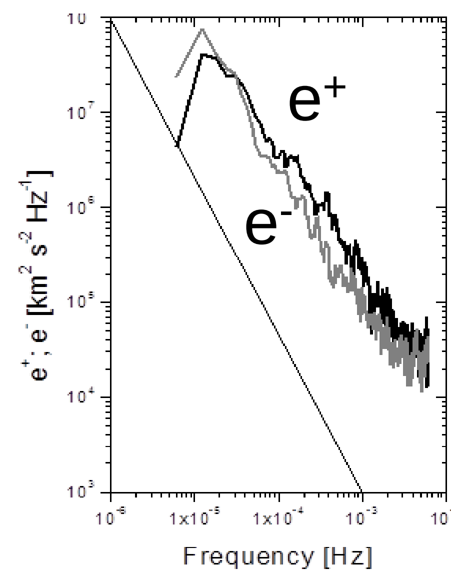

All these features evolve with the radial distance from the Sun

[Fast wind tends to resemble slow wind as the distance increase]

For increasing distance:

- e⁺ decreases towards e⁻
- spectral slope evolves towards -5/3

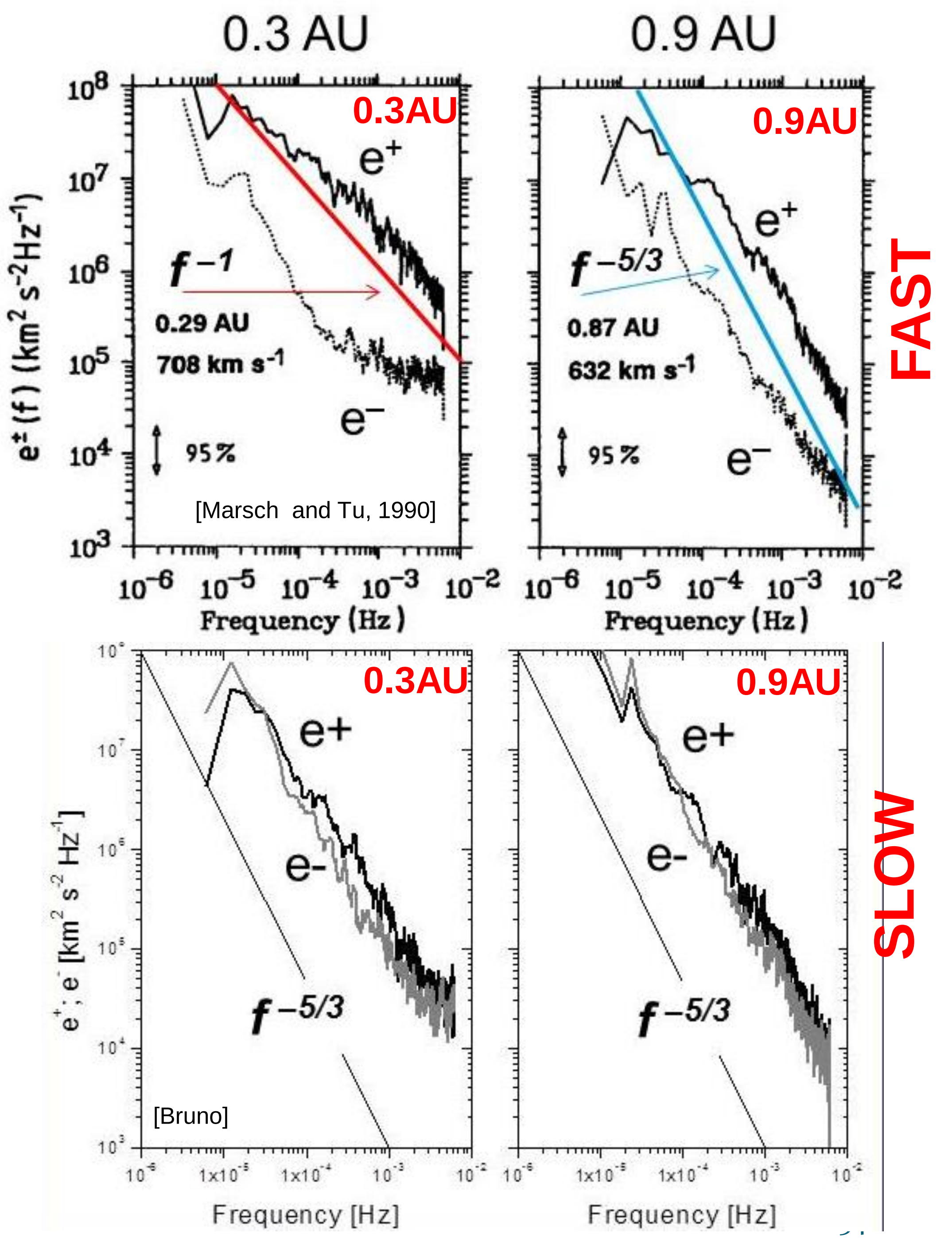

- No much radial evolution
- spectral slopes always close to -5/3

Since $e^+ \rightarrow e^-$, $\delta \underline{B}$-$\delta \underline{V}$ alignment decreases during expansion

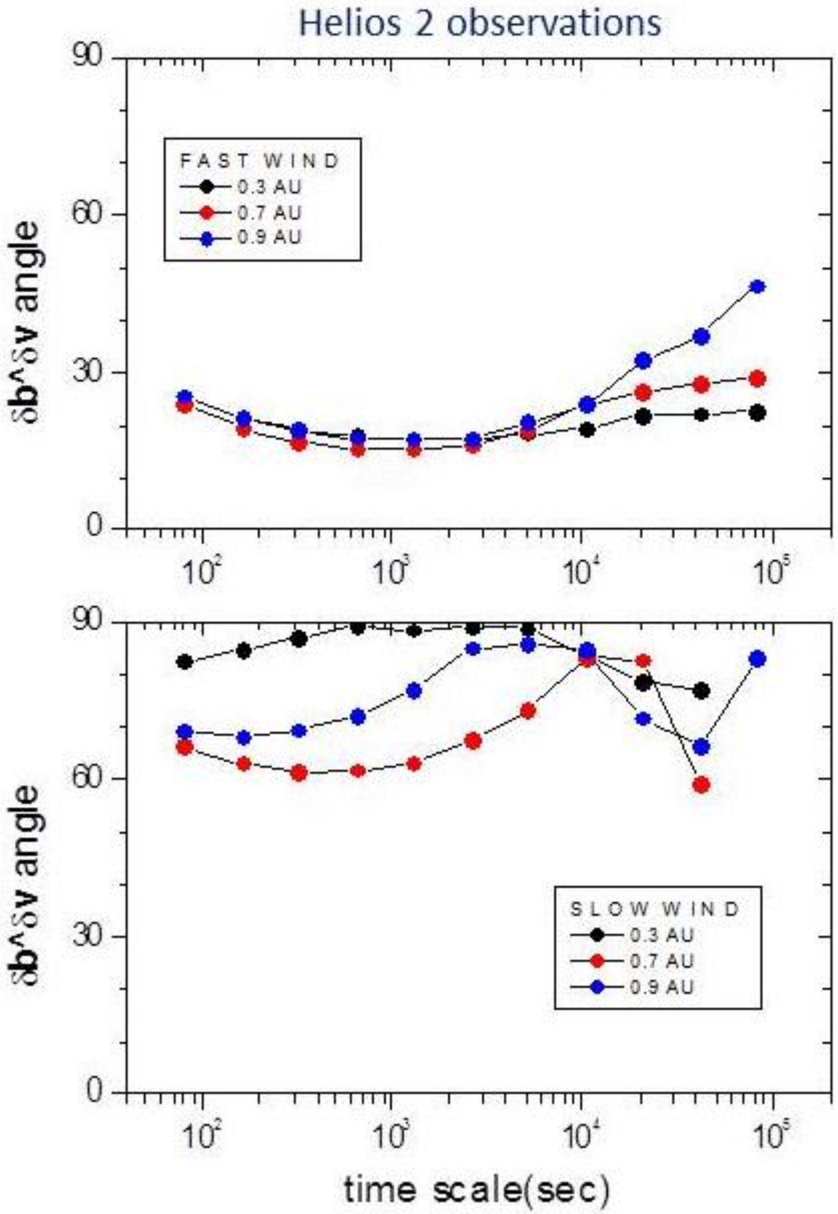

- Best alignment for younger turbulence (0.3AU)

- No alignment for slow wind, as expected from fully developed turbulence ($|\delta Z^+|=|\delta Z^-|$)

Radial evolution of MHD turbulence in terms of σ_R and σ_C (scale of 1hr)

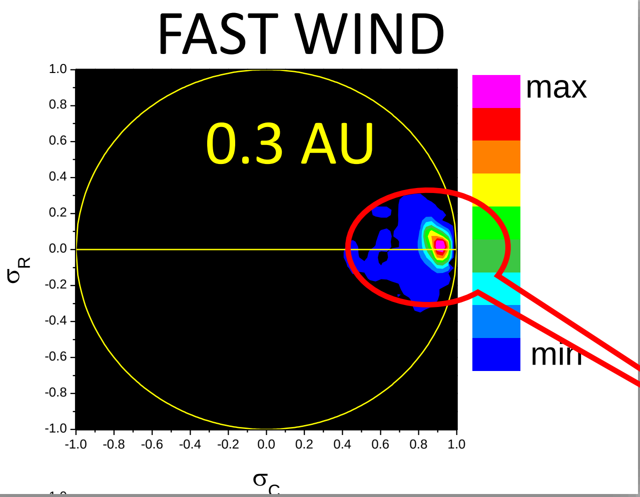

Alfvénic population

$$\sigma_C = \frac{e^+ - e^-}{e^+ + e^-} = \frac{2 < v \cdot b >}{e^v + e^b}$$

$$\sigma_R = \frac{e^v - e^b}{e^v + e^b}$$

$$\sigma_C^2 + \sigma_R^2 \le 1$$

Radial evolution of MHD turbulence in terms of σ_R and σ_C (scale of 1hr)

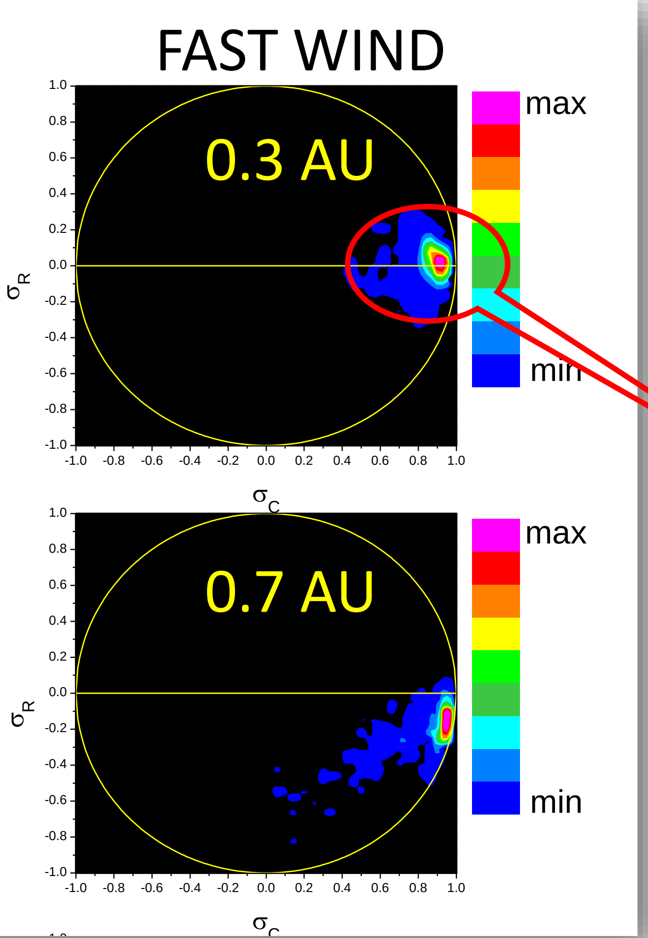

Alfvénic population

$$\sigma_C = \frac{e^+ - e^-}{e^+ + e^-} = \frac{2 < v \cdot b >}{e^v + e^b}$$

$$\sigma_R = \frac{e^v - e^b}{e^v + e^b}$$

$$\sigma_C^2 + \sigma_R^2 \le 1$$

Radial evolution of MHD turbulence in terms of σ_R and σ_C (scale of 1hr)

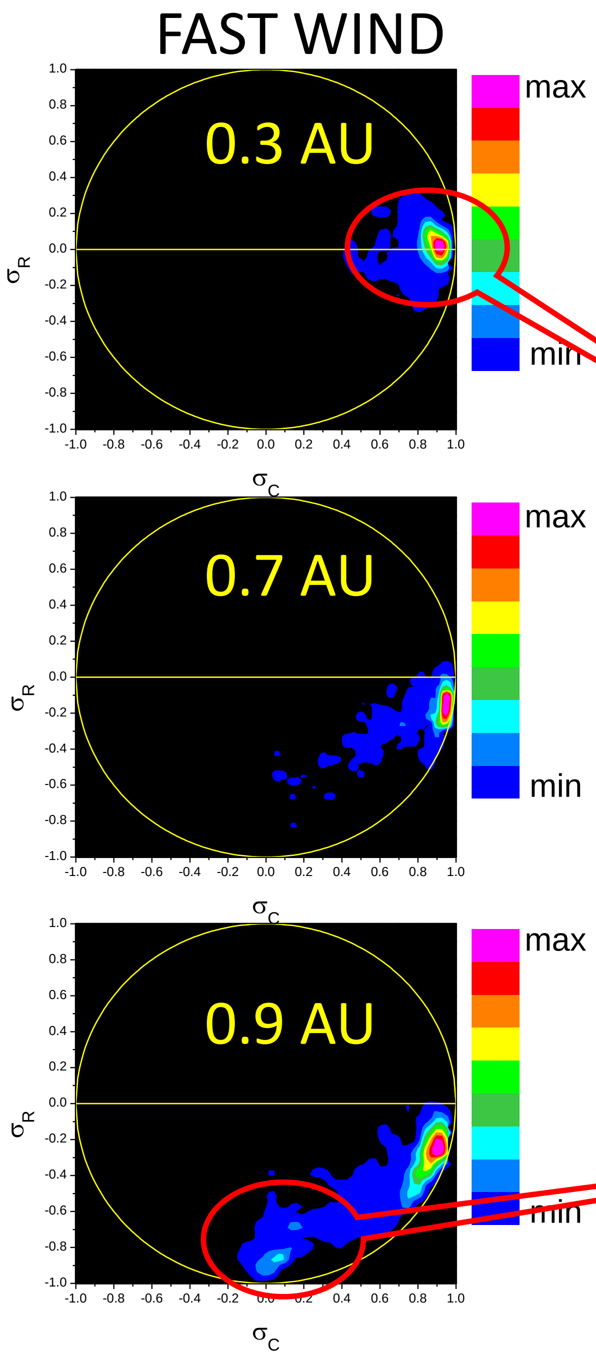

(Bruno et al., 2007)

Alfvénic population

$$\sigma_C = \frac{e^+ - e^-}{e^+ + e^-} = \frac{2 < v \cdot b >}{e^v + e^b}$$

$$\sigma_R = \frac{e^v - e^b}{e^v + e^b}$$

$$\sigma_C^2 + \sigma_R^2 \leq 1$$

A new population appears, characterized by magnetic energy excess and low Alfvénicity

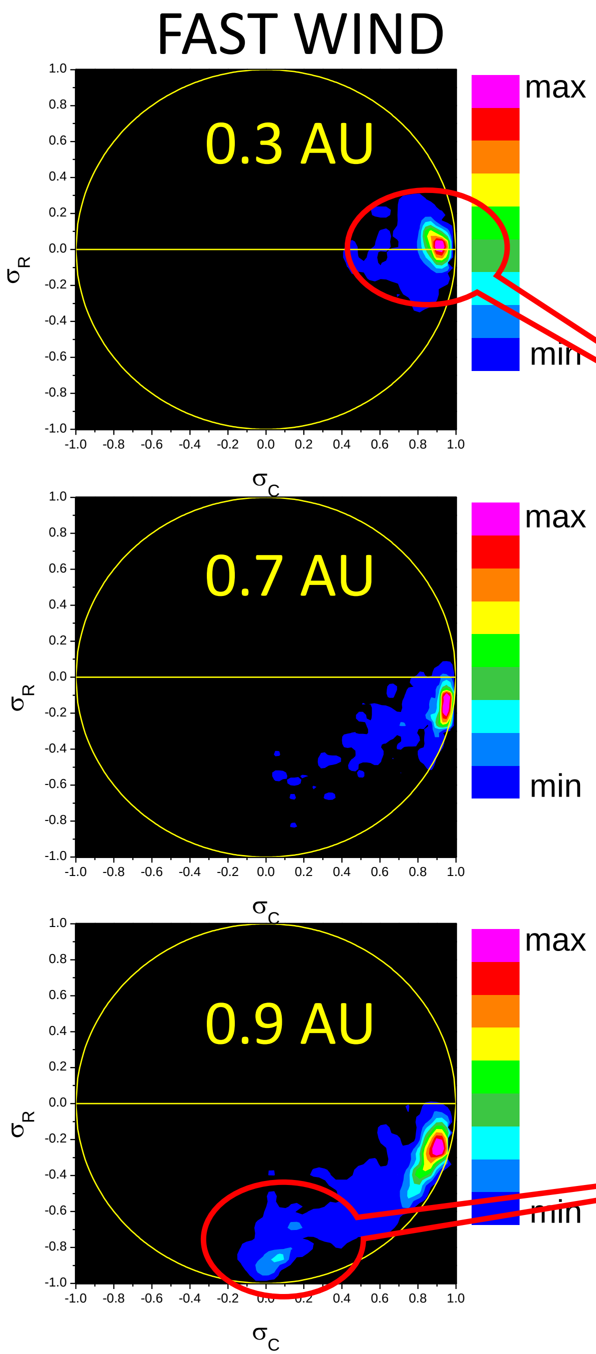

(Bruno et al., 2007)

Radial evolution of MHD turbulence in terms of σ_R and σ_C (scale of 1hr)

Alfvénic population

$$\sigma_C = \frac{e^+ - e^-}{e^+ + e^-} = \frac{2 < v \cdot b >}{e^v + e^b}$$

$$\sigma_R = \frac{e^v - e^b}{e^v + e^b}$$

$$\sigma_C^2 + \sigma_R^2 \leq 1$$

this might be a result of turbulence evolution or the signature of underlying advected structure

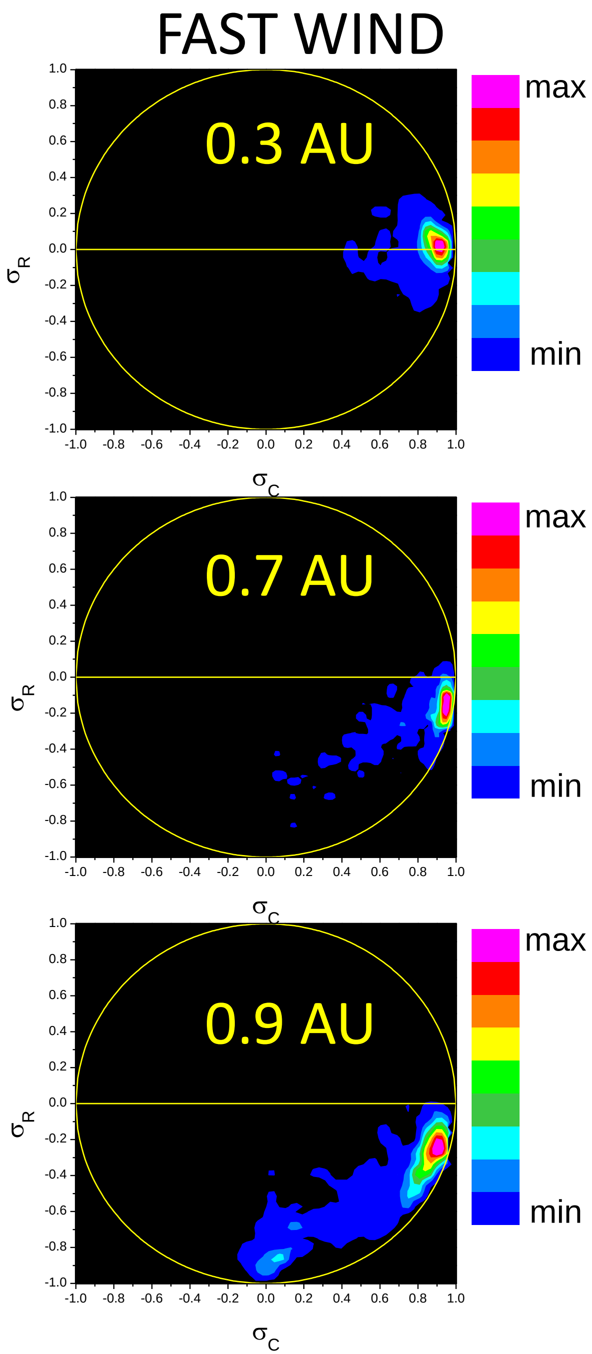

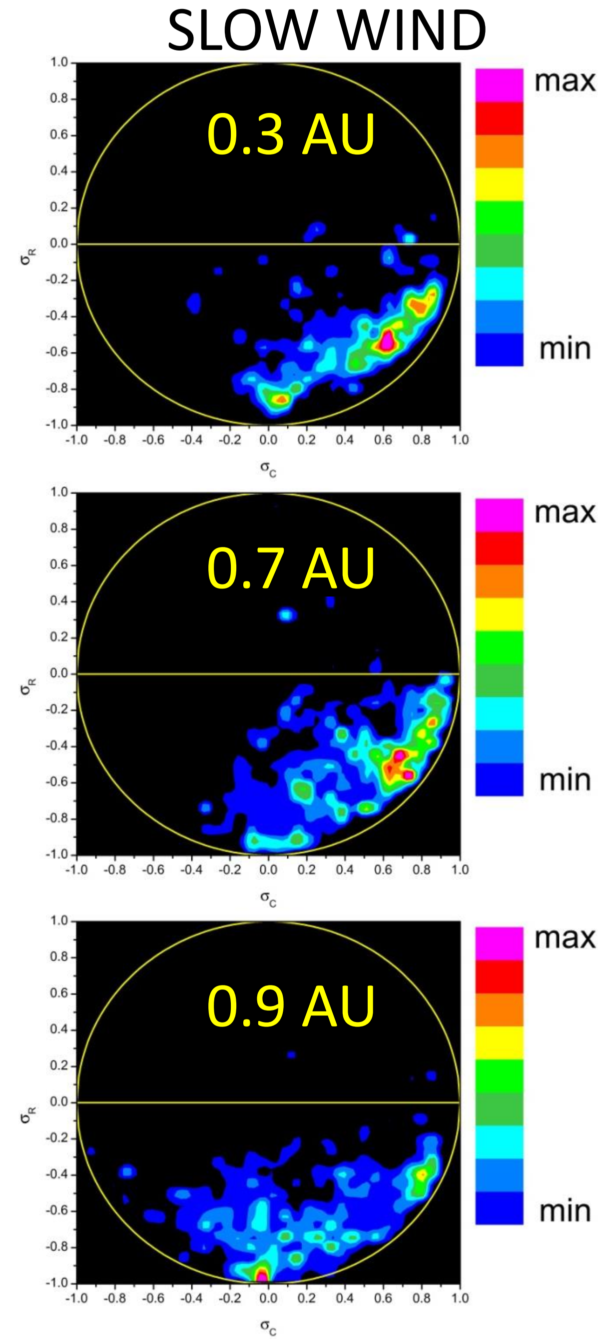

Helios 2 observations

Different situation in Slow-Wind:

- no evolution
- second population already present at 0.3 AU

Several contributions suggested that incompressible turbulence is not purely *slab* (Alfvénic)

(*Thieme et al.*, 1988, 1989; *Tu et al.*, 1989, 1997; *Tu and Marsch,* 1990, 1993; *Bieber and Matthaeus, 1996; Crooker et al.*, 1996; *Bruno et al.*, 2001, 2003, 2004; Chang and Wu, 2002; Chang, 2003; Chang et al., 2004; Tu and Marsch, 1992, Chang et al., 2002, Borovsky, 2006, 2008, 2009, Li, 2007, 2008)

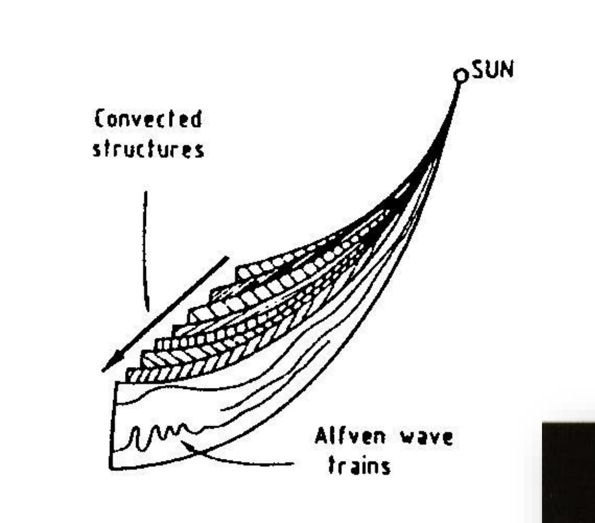

[Tu and Marsch, 1992]

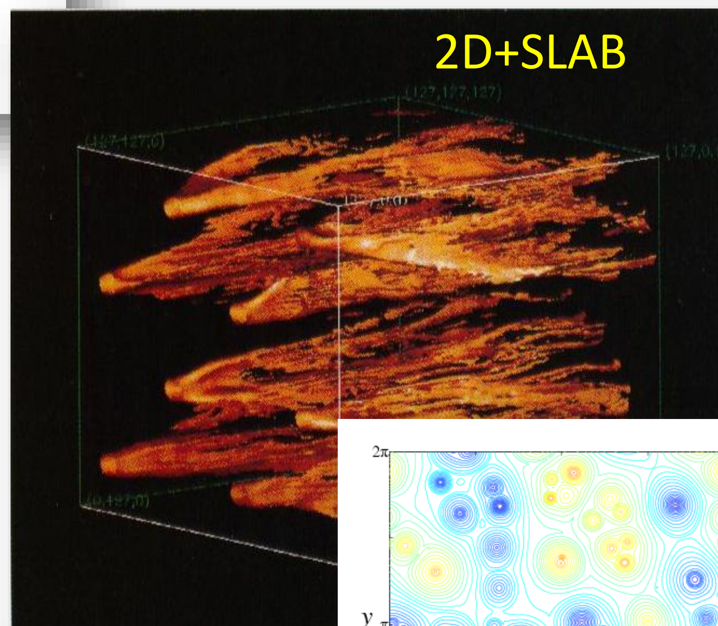

[Bieber et al., 1996]

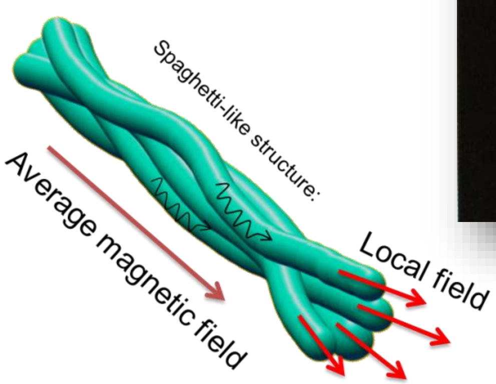

[Bruno et al., 2001]

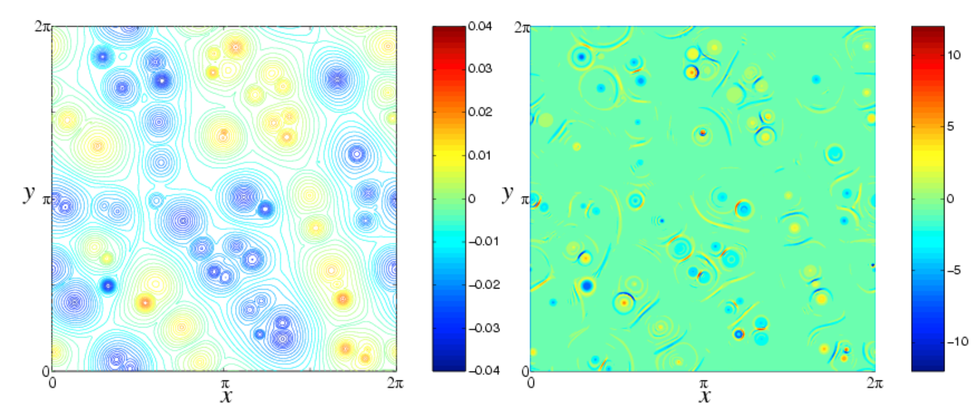

Figure 2.2 2D MHD simulation of coherent structures (left panel) and current sheets (right panel) generated by initially randomly distributed current filaments after an elapsed time of $t = 300$ units. (For reference, the sound wave and Alfvén wave traveling times through a distance of 2π are approximately 4.4 and 60, respectively.)

(Chang et al., 2002)

k// and k⊥ are the ingredients of Slab and 2D turbulence model

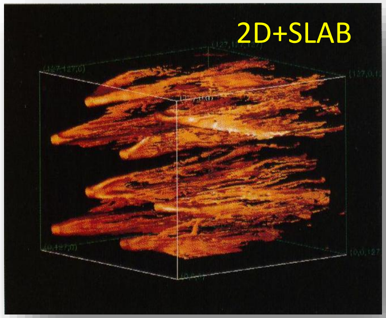

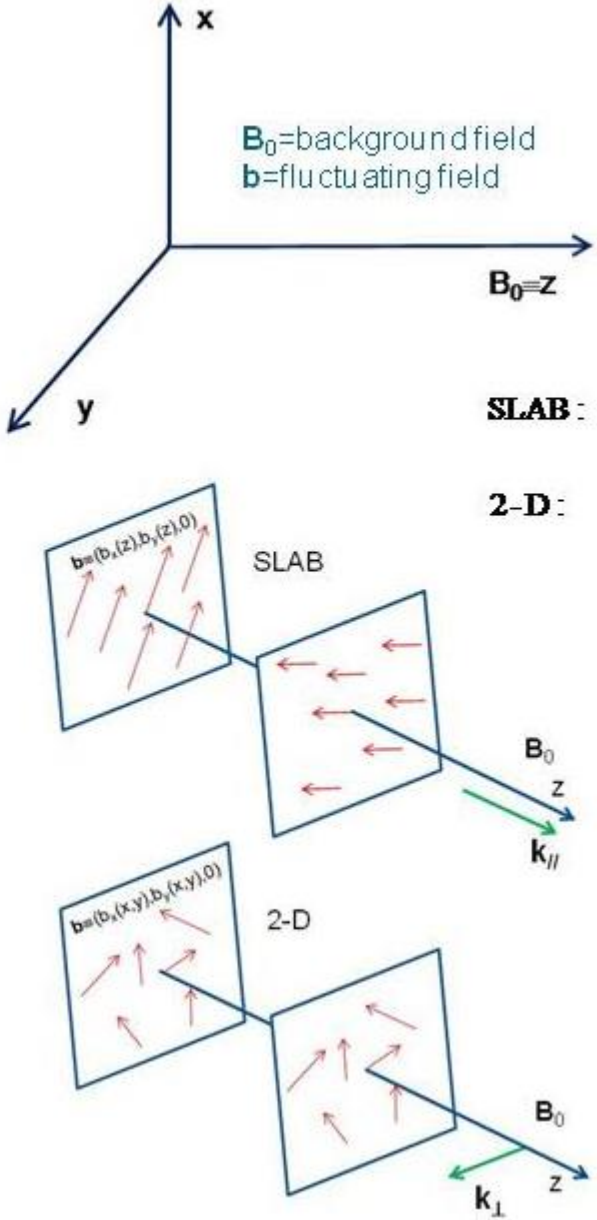

$$e^{-i(\omega t-\vec{k}\cdot\vec{r})} \Rightarrow k_x \sim \frac{\partial}{\partial x};\ k_y \sim \frac{\partial}{\partial y};\ k_z \sim \frac{\partial}{\partial z}$$

SLAB: $$b\equiv(b_x(z),b_y(z),0)\Rightarrow \frac{\partial}{\partial x}=\frac{\partial}{\partial y}=0\Rightarrow k_x=k_y=0\Rightarrow k\equiv(0,0,k_z)\Rightarrow k_{//}$$

2-D: $$b\equiv(b_x(x,y),b_y(x,y),0)\Rightarrow \frac{\partial}{\partial x}\neq 0,\ \frac{\partial}{\partial y}\neq 0,\ \frac{\partial}{\partial z}=0\Rightarrow k\equiv(k_x,k_y,0)\Rightarrow k_\perp$$

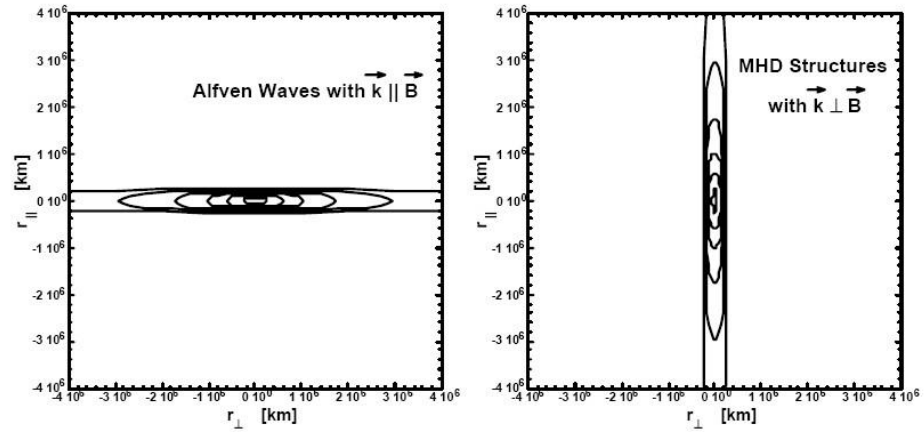

[Bieber et al., 1996]

- ❑ Axisimmetry assumed

Dominance of $k_\perp$ or $k_{//}$ has implications in the correlation lengths anisotropy

observations at 1AU [ISEE3 data]

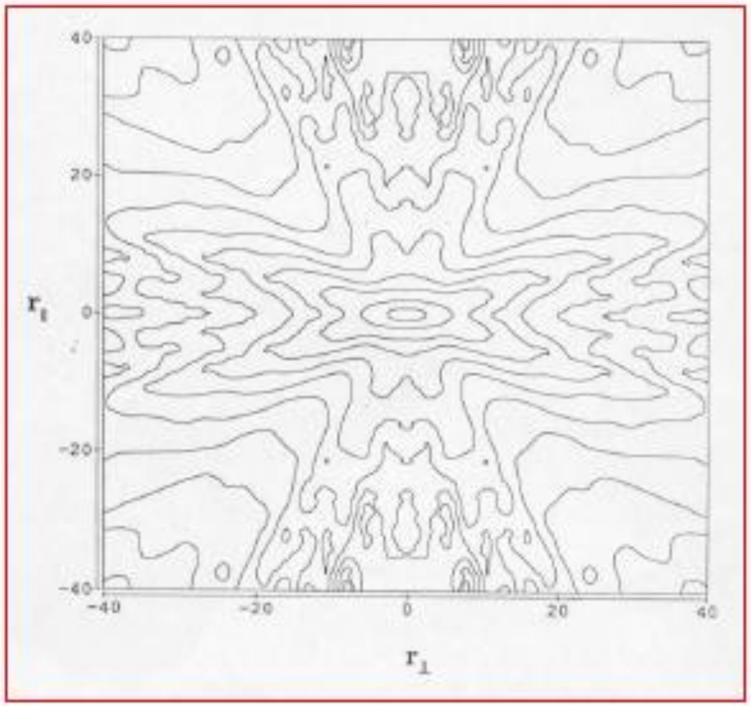

Numerical model

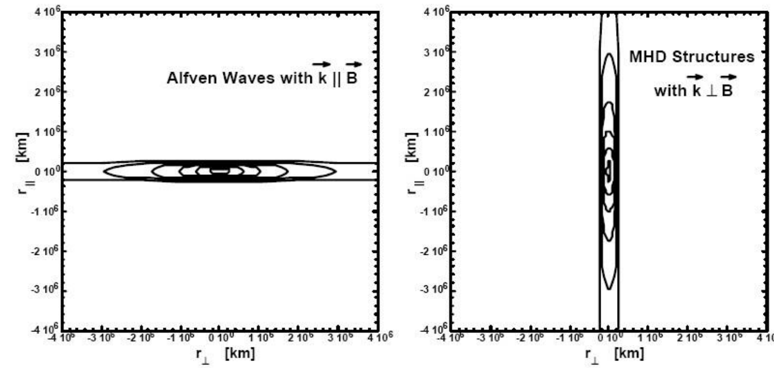

[Bieber et al., 1996]

Figure 26: Contour plot of the 2D correlation function of interplanetary magnetic field fluctuations as a function of parallel and perpendicular distance with respect to the mean magnetic field. The separation in $r_\parallel$ and $r_\perp$ is in units of 10^{10} cm (adopted from Matthaeus *et al.*, 1990, © 1990 American Geophysical Union, reproduced by permission of American Geophysical Union).

Shebalin et al., (1983) proposed the anisotropy development due to 3-wave resonant interaction

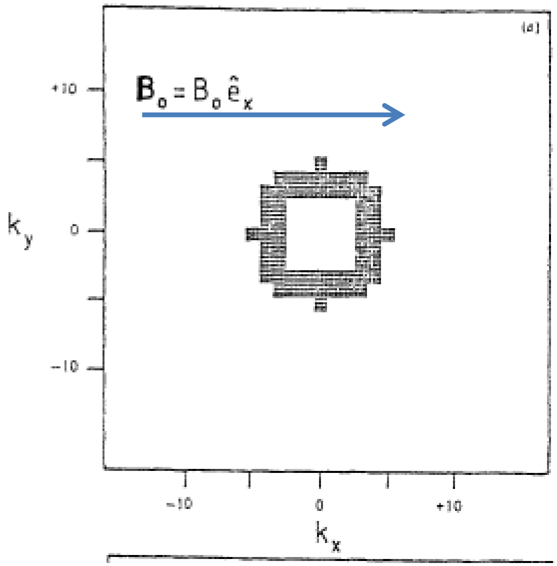

- 2D incompressible MHD simulation
- Initial isotropic spectrum
- magnetic field:
  - $\mathbf{B}_0 = B_0 \mathbf{e}_x$ mean field
  - $\mathbf{B} = (B_x, B_y, 0)$ turbulent field
- non-zero couplings between right and left travelling waves

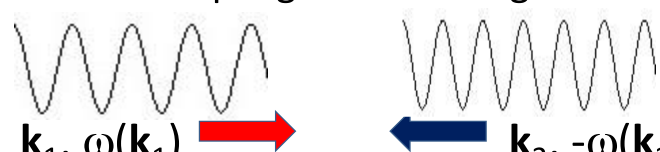

$\mathbf{k}_1, \omega(\mathbf{k}_1)$ $\quad$ $\mathbf{k}_2, -\omega(\mathbf{k}_2)$

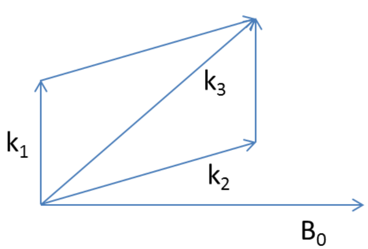

Condition for 3-wave resonant interaction:

$$\begin{cases} \mathbf{k}_3 = \mathbf{k}_1 + \mathbf{k}_2 \\ \pm\omega(\mathbf{k}_3) = \omega(\mathbf{k}_1) - \omega(\mathbf{k}_2) \end{cases}$$

Since $\omega(\mathbf{k}) = \mathbf{k} \cdot \mathbf{B}_0$ possible solutions: $\omega(\mathbf{k}_1) = 0$ or $\omega(\mathbf{k}_2) = 0$

$\Rightarrow$ either $\mathbf{k}_1$ or $\mathbf{k}_2 \perp \mathbf{B}_0$

Result: excitation of a wave with larger $k_\perp$ but never with larger $k_{//}$. Turbulence evolves towards a dominance of $k_\perp$

Shebalin et al., (1983) proposed the anisotropy development due to 3-wave resonant interaction

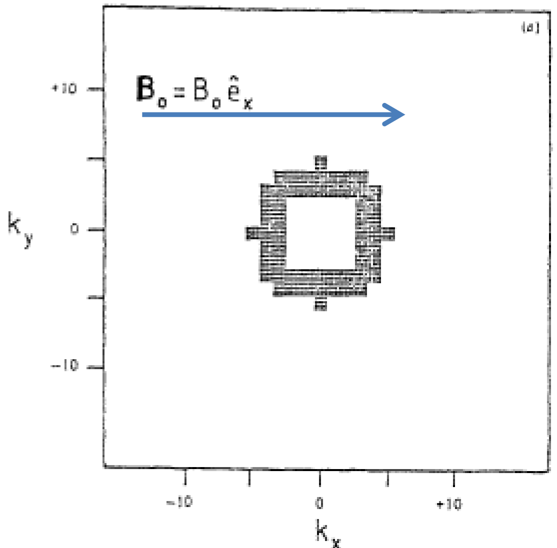

- 2D incompressible MHD simulation
- Initial isotropic spectrum
- magnetic field:
  - $\mathbf{B}_0 = B_0 \mathbf{e}_x$ mean field
  - $\mathbf{B} = (B_x, B_y, 0)$ turbulent field
- non-zero couplings between right and left travelling waves

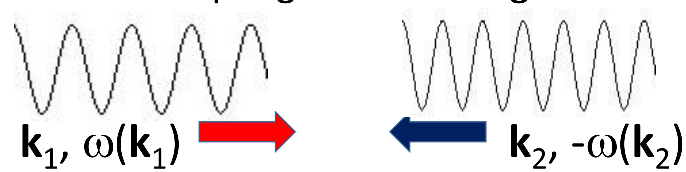

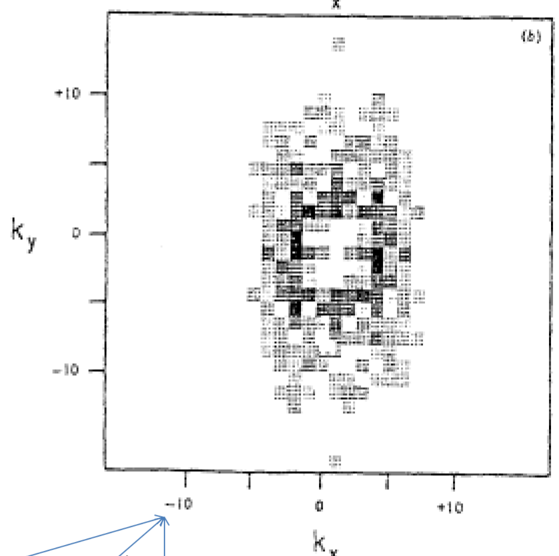

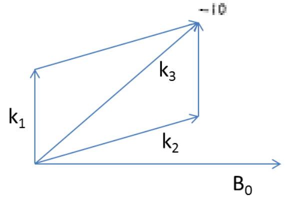

Condition for 3-wave resonant interaction:

$$\begin{cases} \mathbf{k}_3 = \mathbf{k}_1 + \mathbf{k}_2 \\ \pm\omega(\mathbf{k}_3) = \omega(\mathbf{k}_1) - \omega(\mathbf{k}_2) \end{cases}$$

Since $\omega(\mathbf{k}) = \mathbf{k} \cdot \mathbf{B}_0$ possible solutions: $\omega(\mathbf{k}_1) = 0$ or $\omega(\mathbf{k}_2) = 0$

$\Rightarrow$ either $\mathbf{k}_1$ or $\mathbf{k}_2 \perp \mathbf{B}_0$

Result: excitation of a wave with larger $k_\perp$ but never with larger $k_{//}$. Turbulence evolves towards a dominance of $k_\perp$

Goldreich and Sridhar [1995] (GS95) proposed a new mechanism characterized by the so called "*Critical Balance*" conjecture

Alfvénic turbulence reaches a state for which there is a balance between non-linear time and Alfvén time:

$$\tau_S \approx \tau_A \quad \Longrightarrow \quad \boxed{k_\perp / k_{//} \approx \left(k_\perp L\right)^{1/3}}$$

["L" is the initial scale of excitation]

- ❑ Parallel and perpendicular spatial scales of eddies are correlated
- ❑ As the cascade proceeds to larger $k_\perp$, the eddies become more elongated along $\mathbf{B}_0$

3D spectrum

$$\boxed{P(k_\perp, k_{//}) \propto \frac{V_A^2}{k_\perp^{10/3} L^{1/3}} f\left(\frac{k_{//} L^{1/3}}{k_\perp^{2/3}}\right)}$$

- ❑ If only slab and 2D turbulence are present $\rightarrow$

$$\boxed{\begin{aligned} &P_\perp(f;\theta_B = 90°) \propto f^{-5/3} \\ &P_{//}(f;\theta_B = 0°) \propto f^{-2} \\ &P_{//}(f_i) < P_\perp(f_i) \end{aligned}}$$

[Horbury et al., 2008]

$$\boxed{\begin{array}{l} P_{\perp}(f;\theta_B = 90°) \propto f^{-5/3} \\ P_{//}(f;\theta_B = 0°) \propto f^{-2} \\ P_{//}(f_i) < P_{\perp}(f_i) \end{array}}$$

θ_B is the angle between sampling direction and mean field direction

The possibility to observe a different scaling Introduces the problem of defining what the *"mean field"* is

About the problem of defining the "*mean field*"

Fluctuations at a given scale are sensitive to the local magnetic field, but the definition of "*local*" varies with the spatial scales of interest.

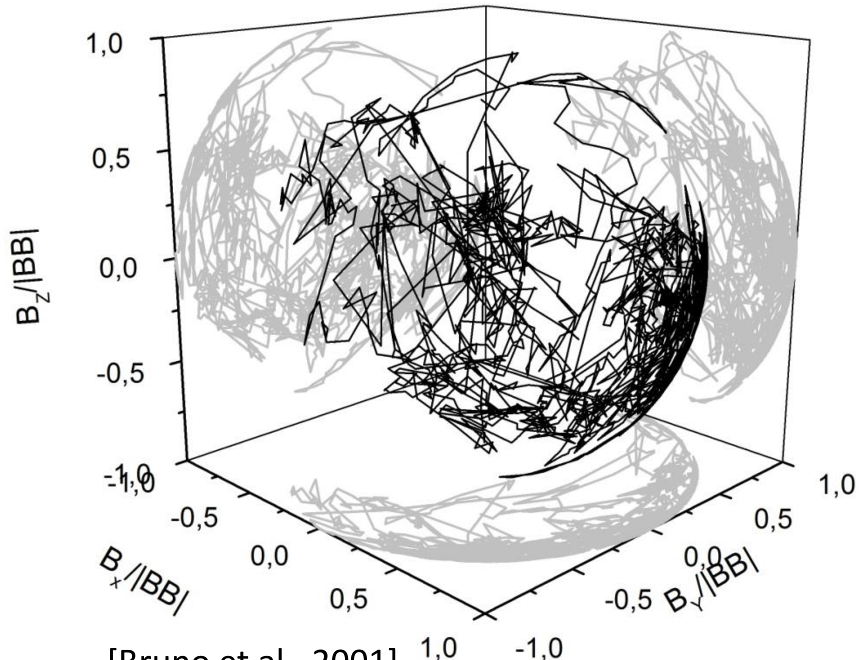

[Bruno et al., 2001]

About 3 hrs of 6s averages of Helios 2, fast wind at 0.9AU

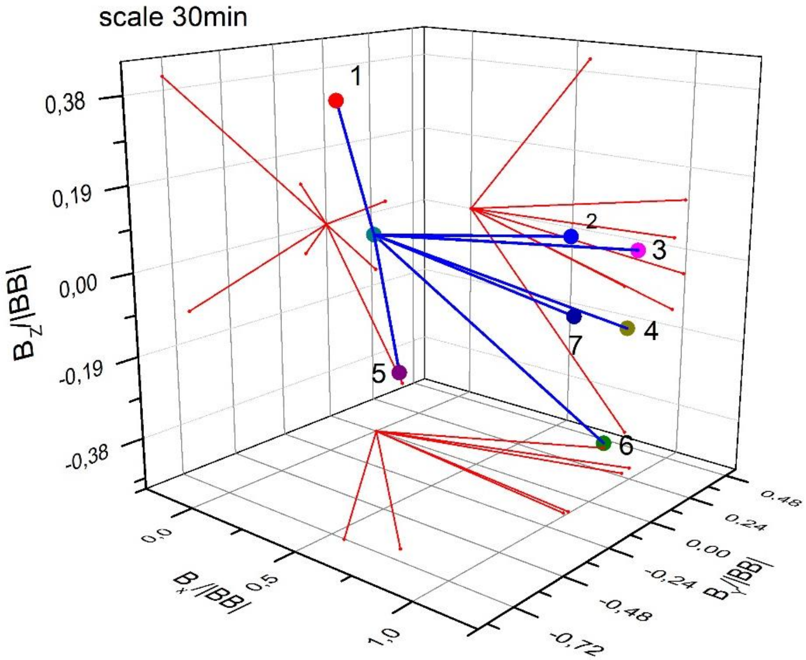

Anisotropy test by Bieber et al. [1996] in the solar wind

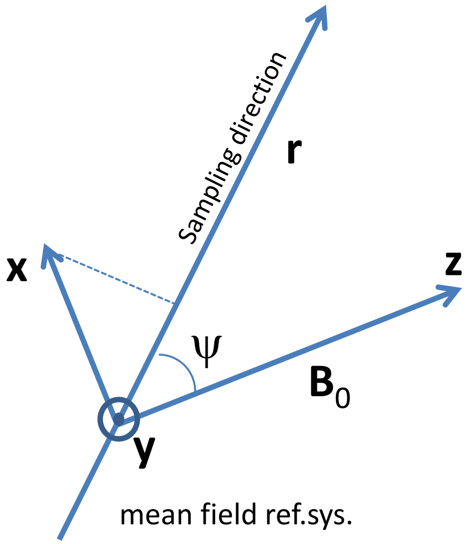

Data rotated into the mean field ref.sys.

$P_{yy} \equiv P_{\perp}$ [perpendicular spectrum]
$P_{xx} \equiv P_{(//)}$ [quasi parallel spectrum]

$P_{\perp}$ [fluctuations $\perp$ to the sampling direction]
$P_{(//)}$ [fluctuations with one component // to the sampling direction]

$$fP_{\perp}(f) = C_S\left(\frac{2\pi f}{V_w \cos\psi}\right)^{1-q} + C_2\frac{2q}{(1+q)}\left(\frac{2\pi f}{V_w \sin\psi}\right)^{1-q}$$

$$fP_{(\|)}(f) = C_S\left(\frac{2\pi f}{V_w \cos\psi}\right)^{1-q} + C_2\frac{2}{(1+q)}\left(\frac{2\pi f}{V_w \sin\psi}\right)^{1-q}$$

- ❑C_S and C_2 are the amplitude of slab and 2D components
- ❑q is the spectral index around a certain frequency within inertial range
- ❑2D gives a different contribution to $P_{\perp}$ and $P_{(//)}$

Helios data for the anisotropy test by Bieber et al. [1996]

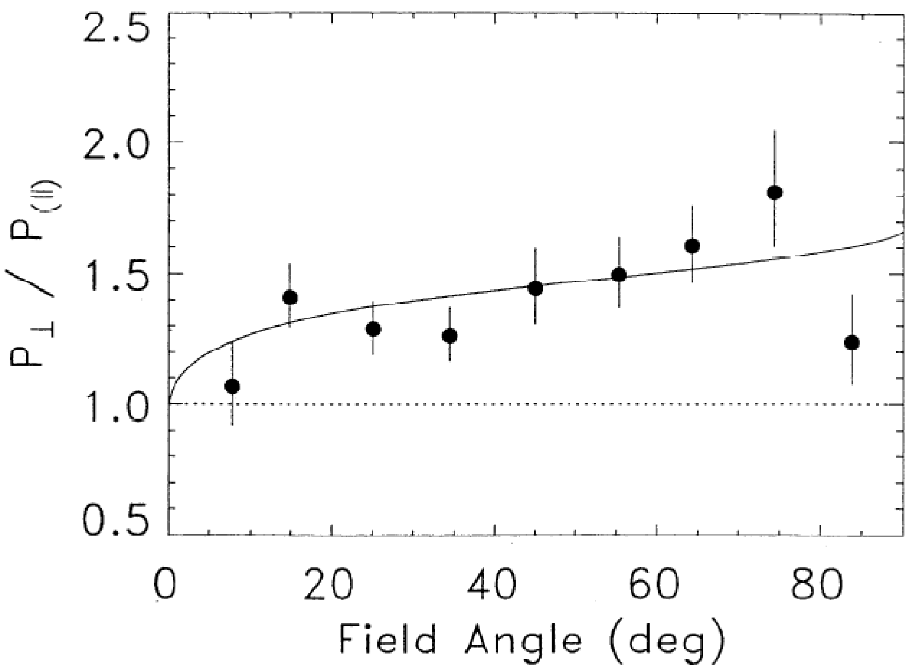

- ❑ fast and slow(dominating) wind mixed together
- ❑ Ratio of perpendicular to parallel power fitted by a composite geometry with <u>**74% 2D and 26% slab**</u>
- ❑ Dataset: Helios 1&2 between <u>0.3 and 1AU</u>, 454 spectra of 34 min each taken during SEP events

➢ Dramatically different results are expected selecting only Alfvénic high velocity streams (time res. in Helios data not sufficient)

- ❑ $P_\perp$ [fluctuations $\perp$ to the sampling direction]
- ❑ $P_{(//)}$ [fluctuations quasi // to the sampling direction]

Dasso et al., (2005): Ecliptic turbulence with Ulysses data

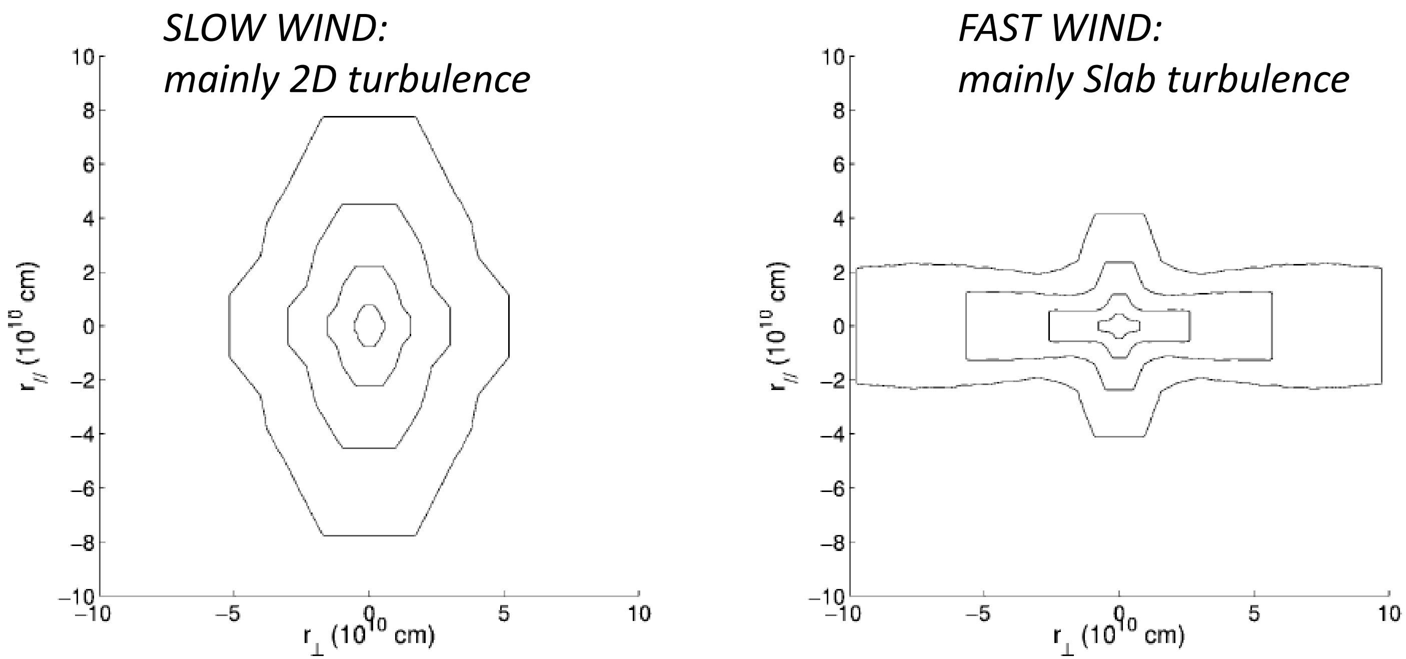

FIG. 1.—Level contours for $R_{bb}(r)$. *Left*, slow solar wind ($V_{sw} < 400$ km s^{-1}); *right*, fast solar wind ($V_{sw} > 500$ km s^{-1}). (See text.) Levels are at 1200, 1400, 1600, and 1800 km^2 s^{-2}.

TABLE 2
ESTIMATE OF $(\lambda_{\parallel}^{corr}/\lambda_{\perp}^{corr})^2$: SQUARED RATIO OF CORRELATION SCALES

Wind	R_{bb}	R_{vv}	R_{out}	R_{in}	R_{vb}
Slow	1.4	1.1	1.4	1.1	1.7
Fast	0.5	0.4	0.5	0.8	0.4

- Fluctuations decorrelate faster in the perpendicular direction in the slow wind while the opposite occurs in the fast wind

Which mechanism does generate turbulence in the ecliptic?

Different origin for Z^+ and Z^- modes in interplanetary space

Outside the Alfvén radius we need Z^- modes in order to have

$$\left(\vec{Z}^{\mp}\cdot\nabla\right)\vec{Z}^{\pm}\neq 0$$

Need for a mechanisms able to generate locally Z^- modes

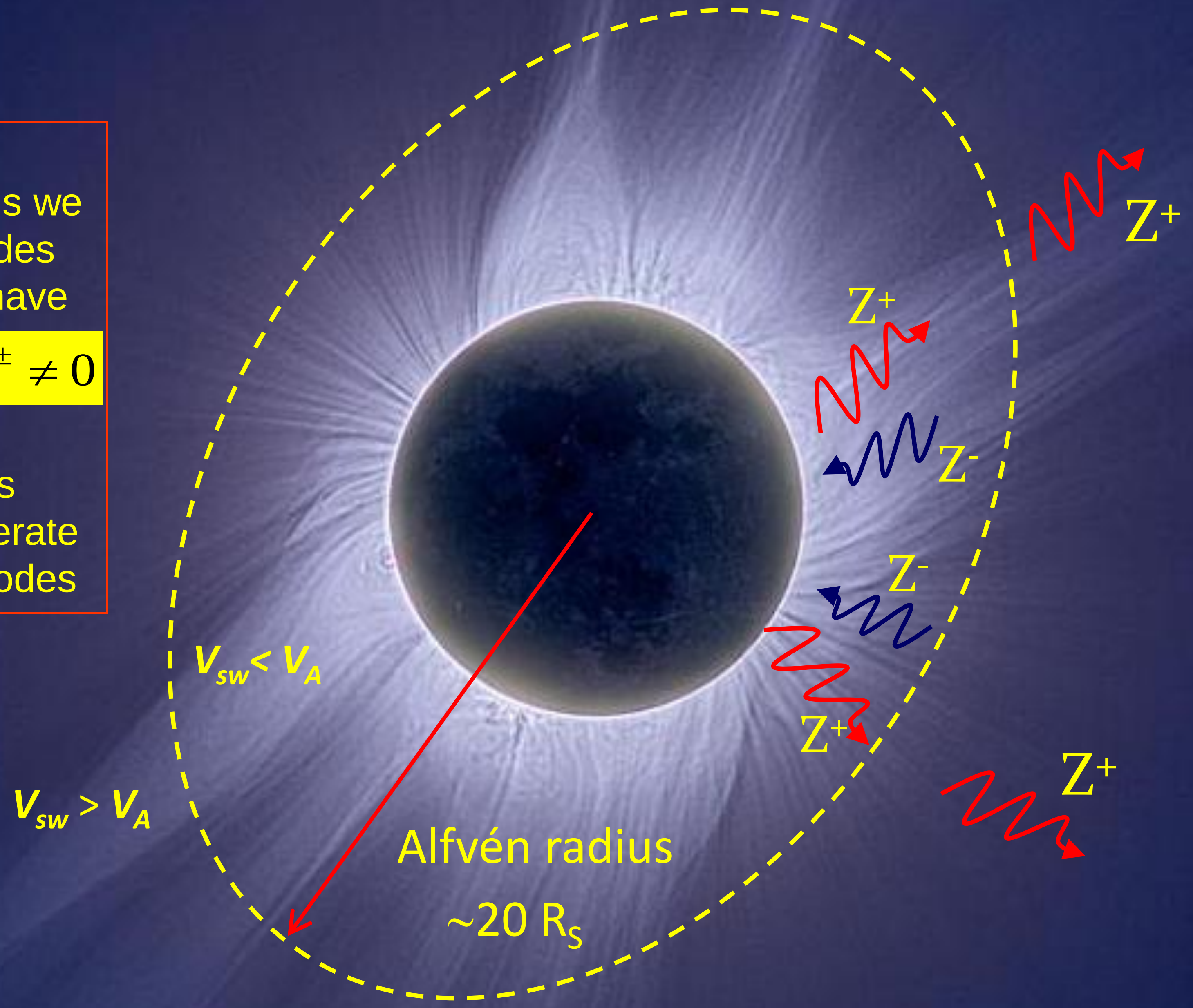

Radial evolution of σ_C in the ecliptic

Normalized cross-helicity

$$\sigma_c = \frac{e^+ - e^-}{e^+ + e^-}$$

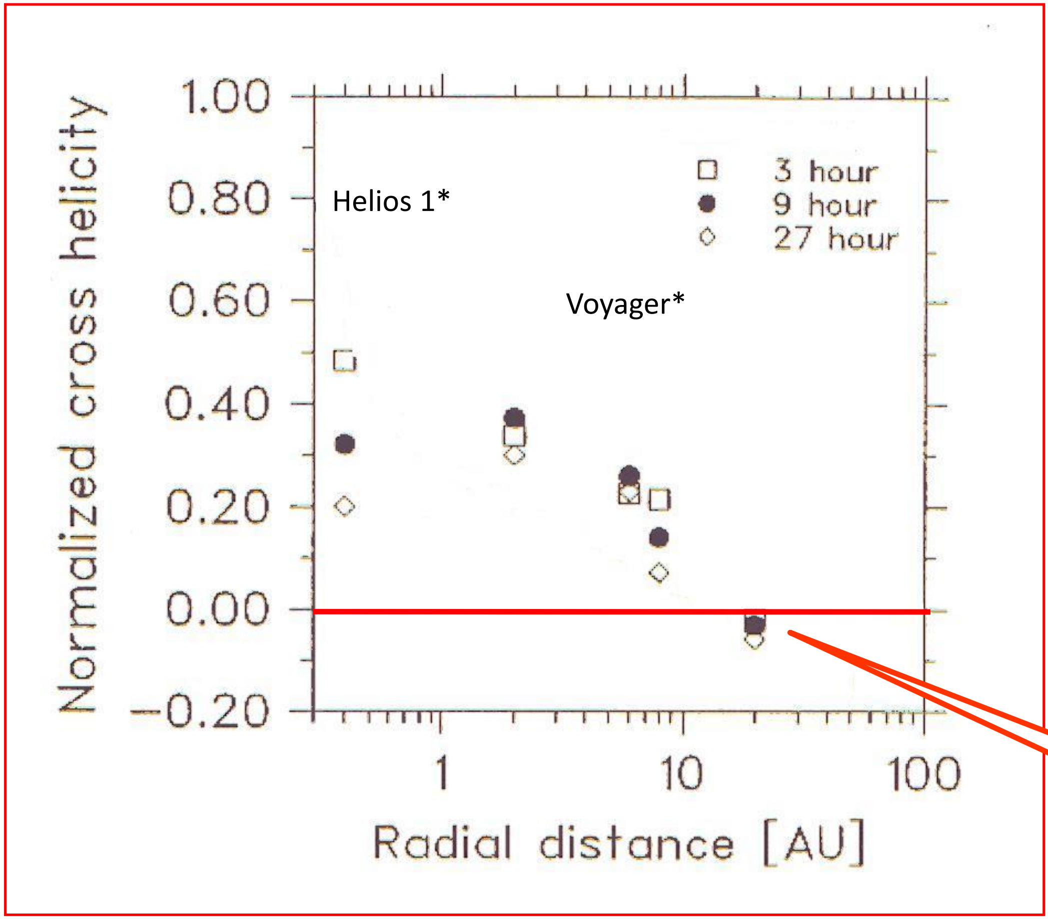

$\sigma_C \rightarrow 0$

[Adopted from Matthaeus et al., 2004]

*mixing fast and slow wind

Radial evolution of σ_C in the ecliptic

Normalized cross-helicity

$$\sigma_c = \frac{e^+ - e^-}{e^+ + e^-}$$

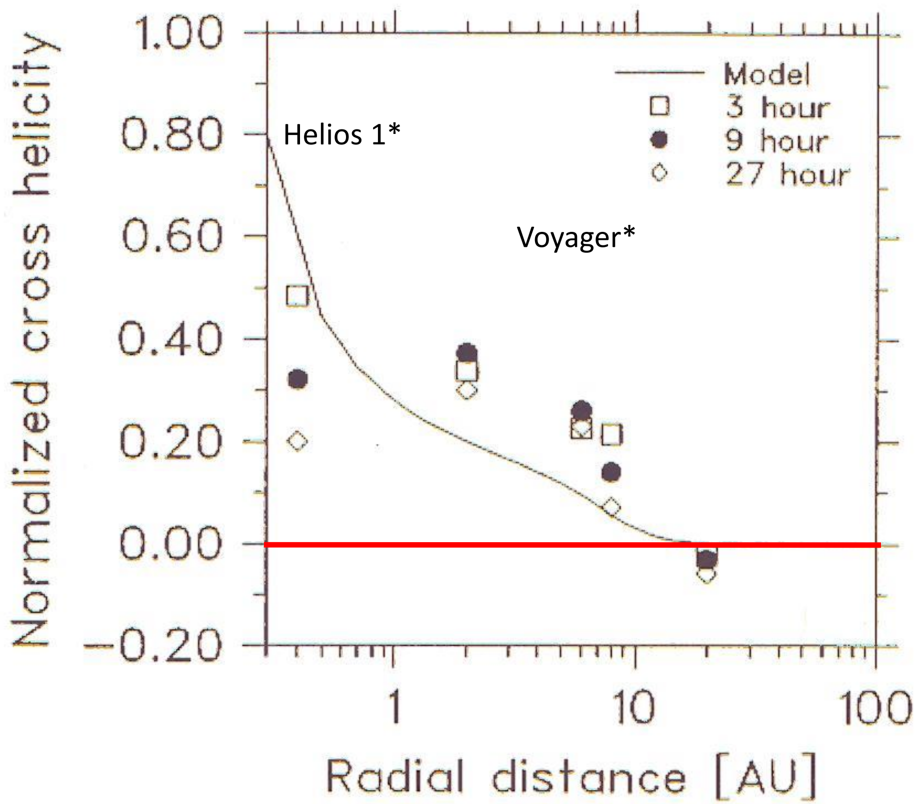

[Adopted from Matthaeus et al., 2004]

Combining dynamic alignment and velocity shear mechanism

Dynamic alignment $\Rightarrow |\sigma_C|$ increases
(Dobrowolny et al., 1980)

velocity shear $\Rightarrow |\sigma_C|$ decreases
(Coleman, 1968)

*mixing fast and slow wind

Dynamic alignment

(Dobrowolny et al., 1980)

This model was stimulated by apparently contradictory observations recorded close to the sun by Helios:

1. observation of $\boldsymbol{\sigma_c \sim 1}$ means correlations of only one type (δZ^{+})

→ absence of non-linear interactions

2. turbulent spectrum clearly observed

→ presence of non-linear interactions

?

Dynamic alignment

(Dobrowolny et al., 1980)

Interactions between Alfvénic fluctuations are local in **k**-space

We can define 2 different time-scales for these interactions

$$\boxed{t_i^{\pm} \sim \frac{\ell}{\delta Z_\ell^{\mp}}}$$

$$\boxed{t_a^{\pm} \sim \frac{\ell}{C_a}}$$

The Alfvén effect increases the non-linear interaction time

$$\boxed{T_\ell^{\pm} \sim t_i^{\pm}\,\frac{t_i^{\pm}}{t_A} \rightarrow \frac{\ell C_A}{(\delta Z_\ell^{\mp})^2}}$$

We can define an energy transfer rate

$$\boxed{\Pi_\ell^{\pm} \sim \frac{(\delta Z_\ell^{\pm})^2}{T_\ell^{\pm}} \sim \ell^{-1} C_A^{-1} (\delta Z_\ell^{\pm})^2 (\delta Z_\ell^{\mp})^2}$$

The energy transfer rate is the same for dZ^+ and dZ^-
An initial unbalance between dZ^+ and dZ^- , as observed close to the Sun, would end up in the disappearance of the minority modes dZ^- towards a total alignment between dB and dV as the wind expands

Radial evolution of σ_C in the ecliptic

Normalized cross-helicity

$$\sigma_c = \frac{e^+ - e^-}{e^+ + e^-}$$

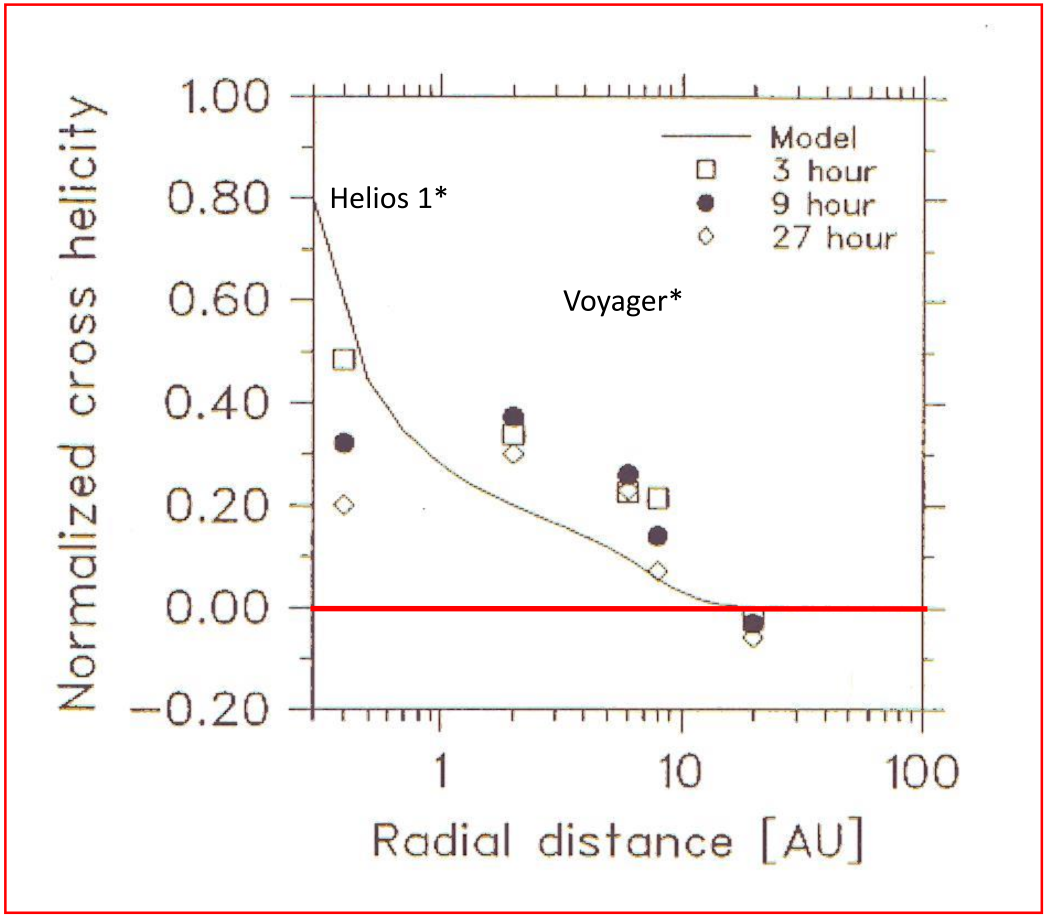

[Adopted from Matthaeus et al., 2004]

Combining dynamic alignment and velocity shear mechanism

Dynamic alignment $\Rightarrow |\sigma_C|$ increases
(Dobrowolny et al., 1980)

velocity shear $\Rightarrow |\sigma_C|$ decreases
(Coleman, 1968)

*mixing fast and slow wind

Typical velocity shear region

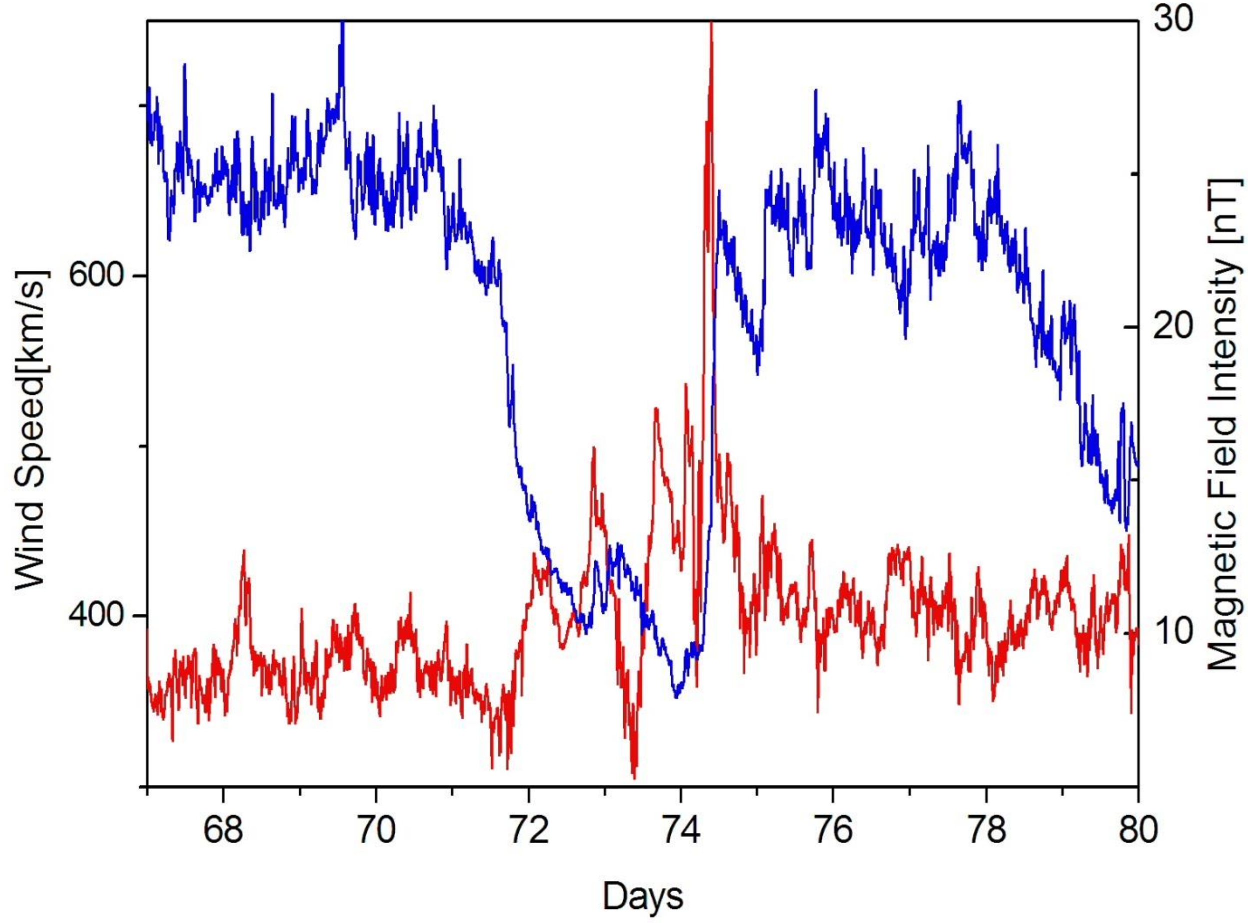

Turbulence generation in the ecliptic: velocity shear mechanism

(Coleman 1968)

•Solar wind turbulence may be locally generated by non-linear MHD processes at velocity-shear layers.
•Magnetic field reversals speed up the spectral evolution.

The z^+ spectrum evolves slowly

The 6 lowest Fourier modes of B and V define the shear profile

Alfvén modes added

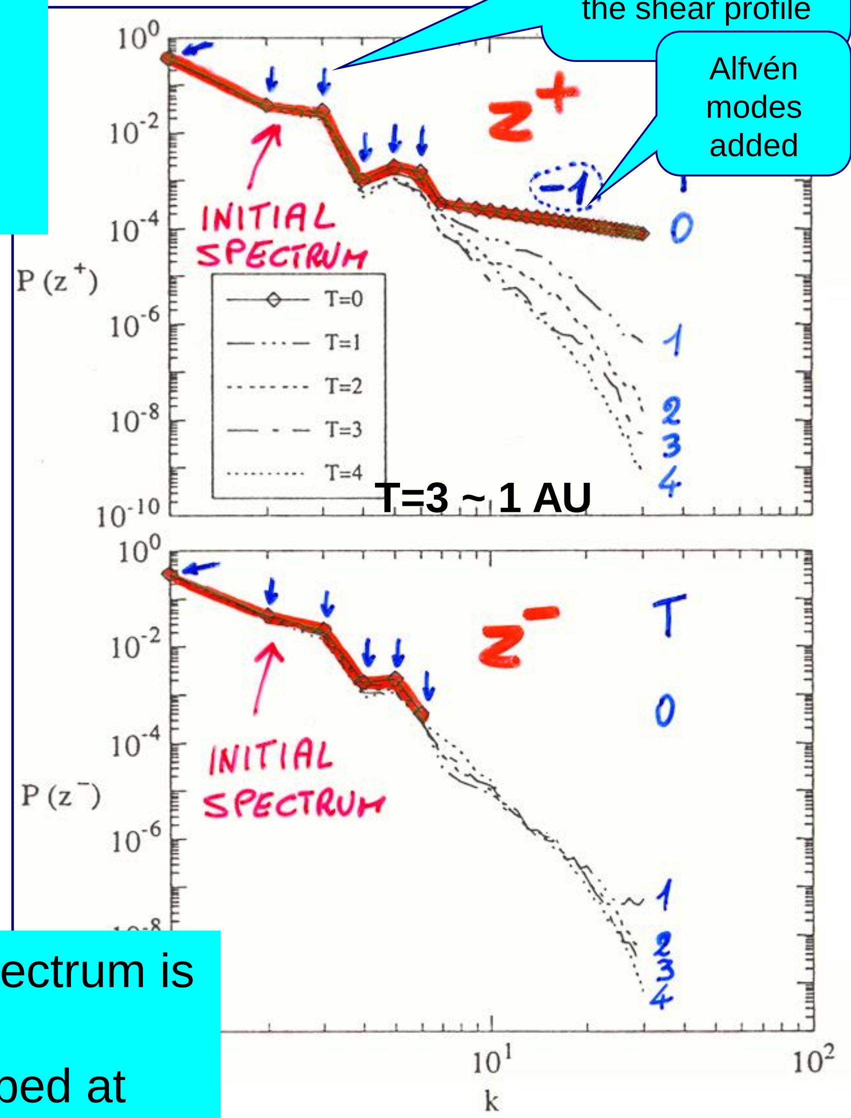

A z^- spectrum is quickly developed at high k

2D Incompressible simulations by Roberts et al., Phys. Rev. Lett., 67, 3741, 1991

This process might have a relevant role in driving turbulence evolution in low-latitude solar wind, where a fast-slow stream structure and reversals of magnetic polarity are common features.

In-situ observations at high latitude

Polar wind features

At **LOW** activity the polar wind fills a large fraction of the heliosphere.
In contrast, polar wind almost disappears at **HIGH** activity.

The polar wind, **a relatively homogeneous environment**, offers the opportunity of studying how the Alfvénic turbulence evolves under almost **undisturbed** conditions.

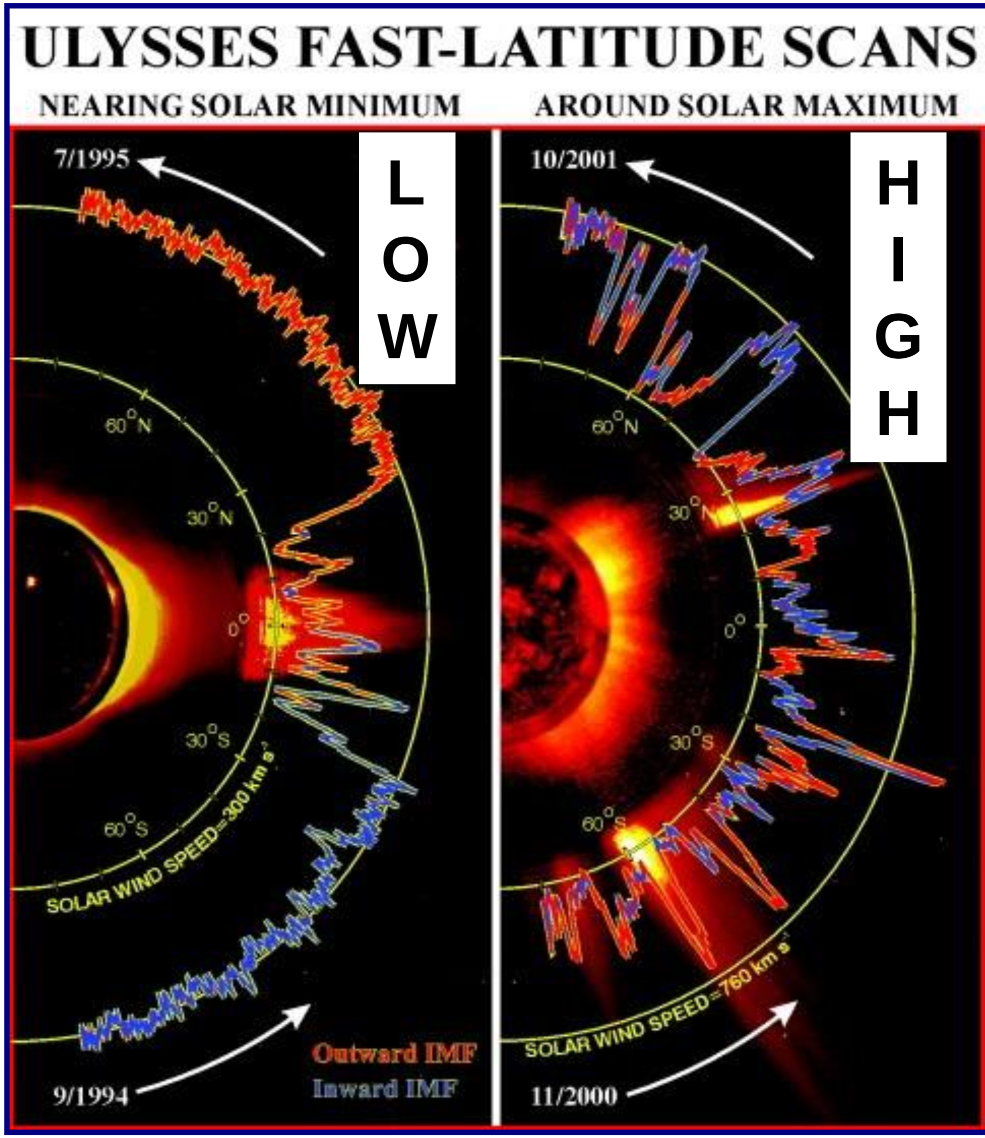

McComas et al., GRL, 29 (9), 2002

Polar wind: spectral evolution

Power spectra of z^+ and z^- at 2 and 4 AU in polar wind clearly indicate a spectral evolution qualitatively similar to that observed in ecliptic wind.

The development of a turbulent cascade with increasing distance moves the breakpoint between the f^{-1} and $f^{-5/3}$ regimes to larger scales.

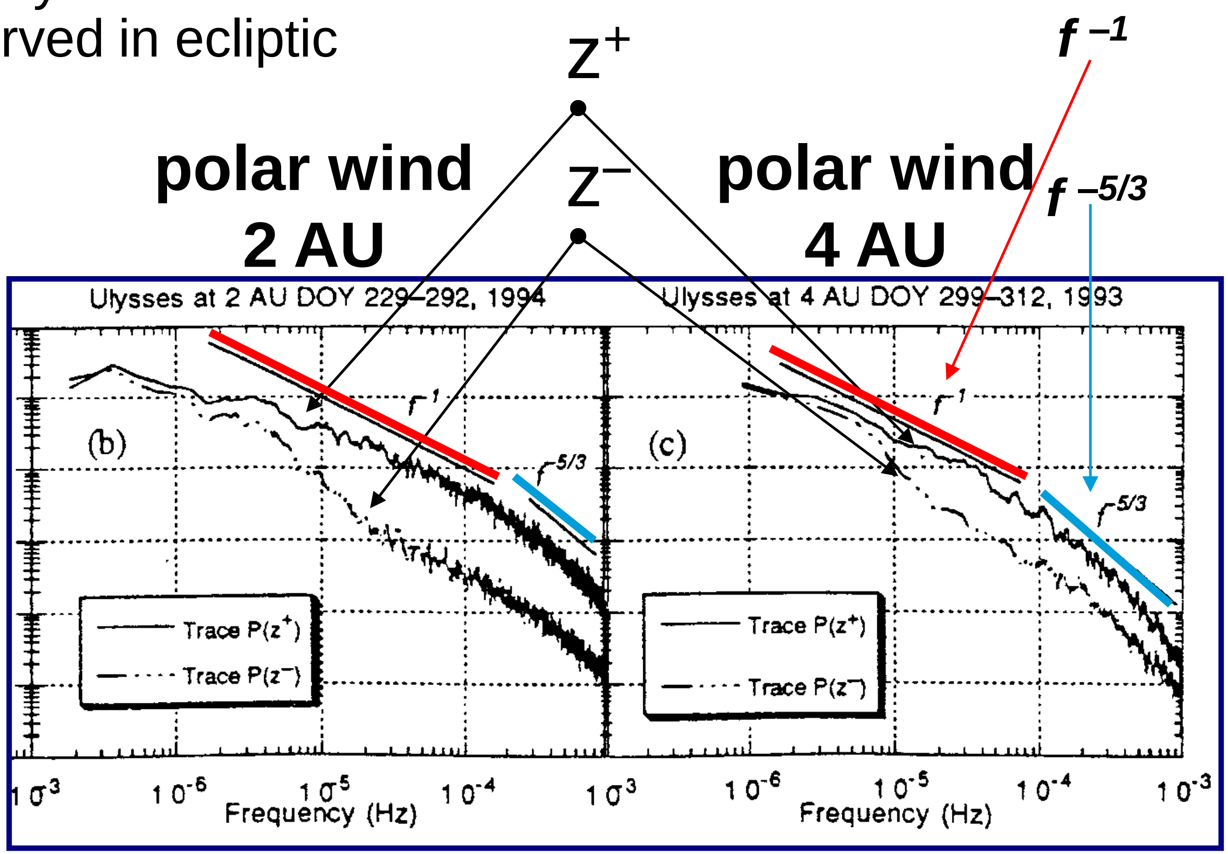

Goldstein et al., GRL, 22, 3393, 1995

Polar wind:
Spectral breakpoint, a comparison with ecliptic wind

polar wind

In the polar wind the breakpoint is at smaller scale than at similar distances in the ecliptic wind.
Thus, spectral evolution in the polar wind is slower than in the ecliptic wind.

(data from: Helios, IMP, Pioneer, Voyager, Ulysses)

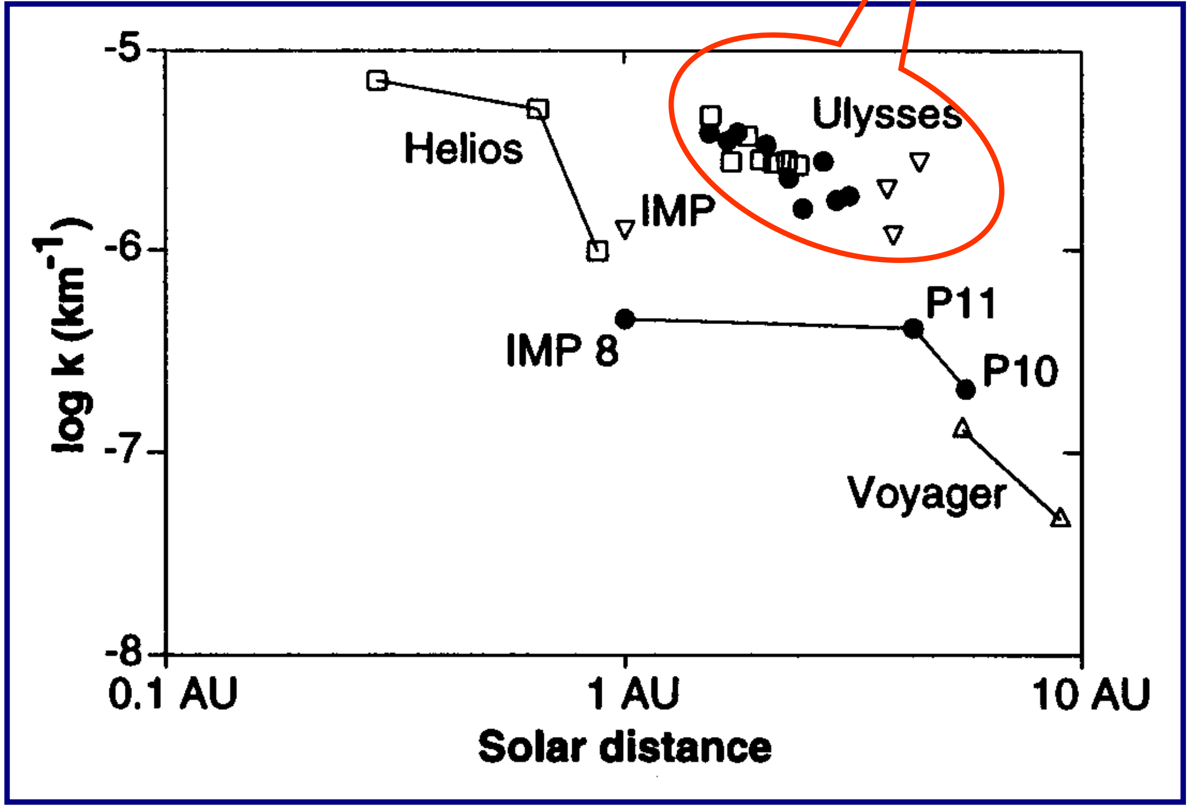

Horbury et al., Astron. Astrophys., 316, 333, 1996

Polar wind: radial dependence of e^+ and e^-

Ulysses polar wind observations show that e^+ exhibits the same radial gradient over all the investigated range of distances. In contrast, e^- shows a change of slope at ~2.5 AU.

Perhaps, e^- generated by some mechanism acting on e^+ which saturates for a given ratio of e^- / e^+

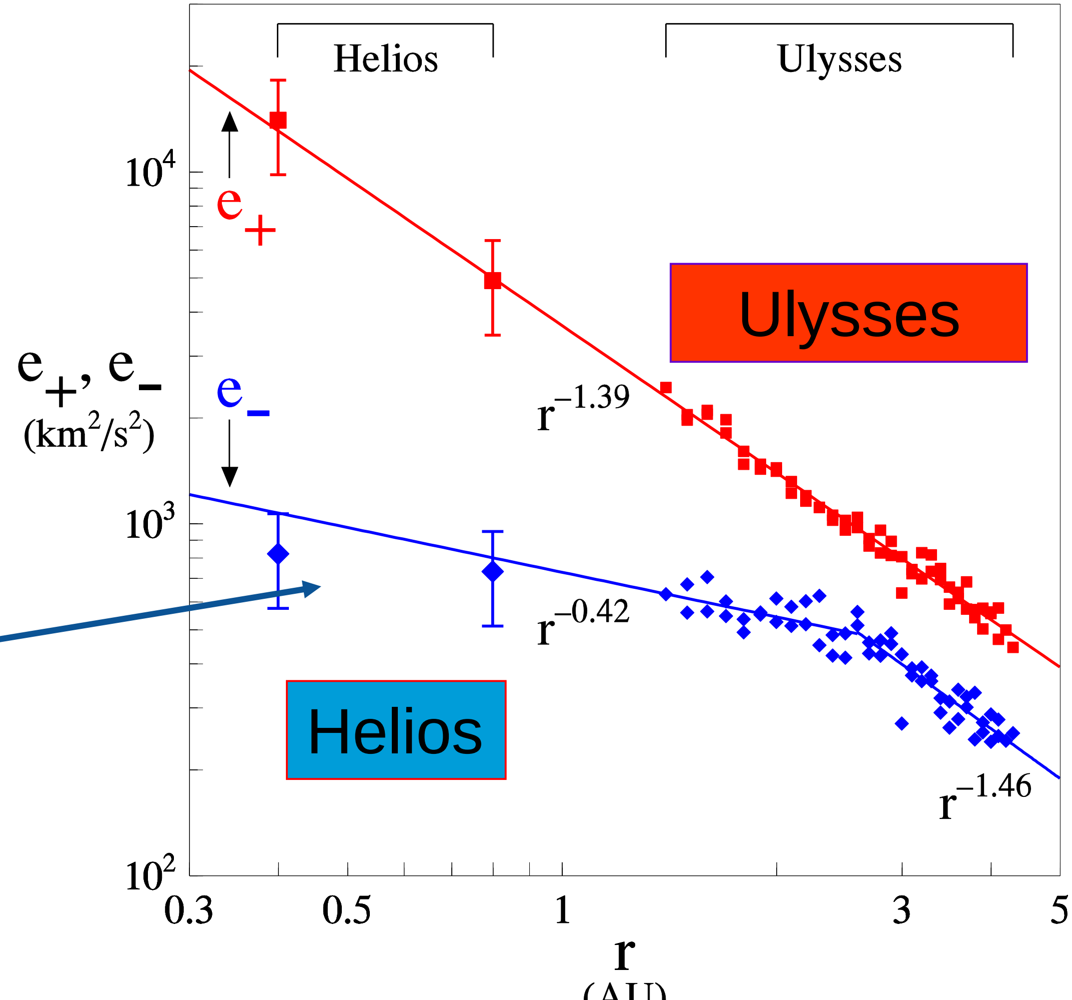

Bavassano et al., JGR, 105, 15959, 2000

Turbulence generation in the polar wind: <u>parametric decay</u>

The <u>absence of strong velocity shears</u> plays in favour of the parametric decay mechanism

This instability develops in a compressible plasma and, in its simplest form, involves the decay of a large amplitude Alfvén wave (called "pump wave", or "mother wave") in a magnetosonic fluctuation and a backscattered Alfvén wave.

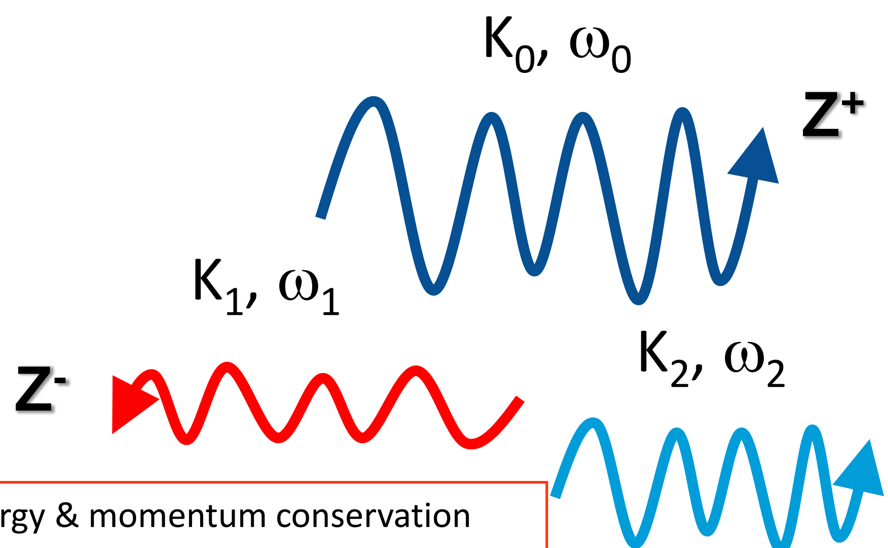

energy & momentum conservation

$\omega_0 = \omega_1 + \omega_2 \quad k_0 = k_1 + k_2$

Test for parametric instability for β~1

MHD compressible simulation by L. Primavera (2003)

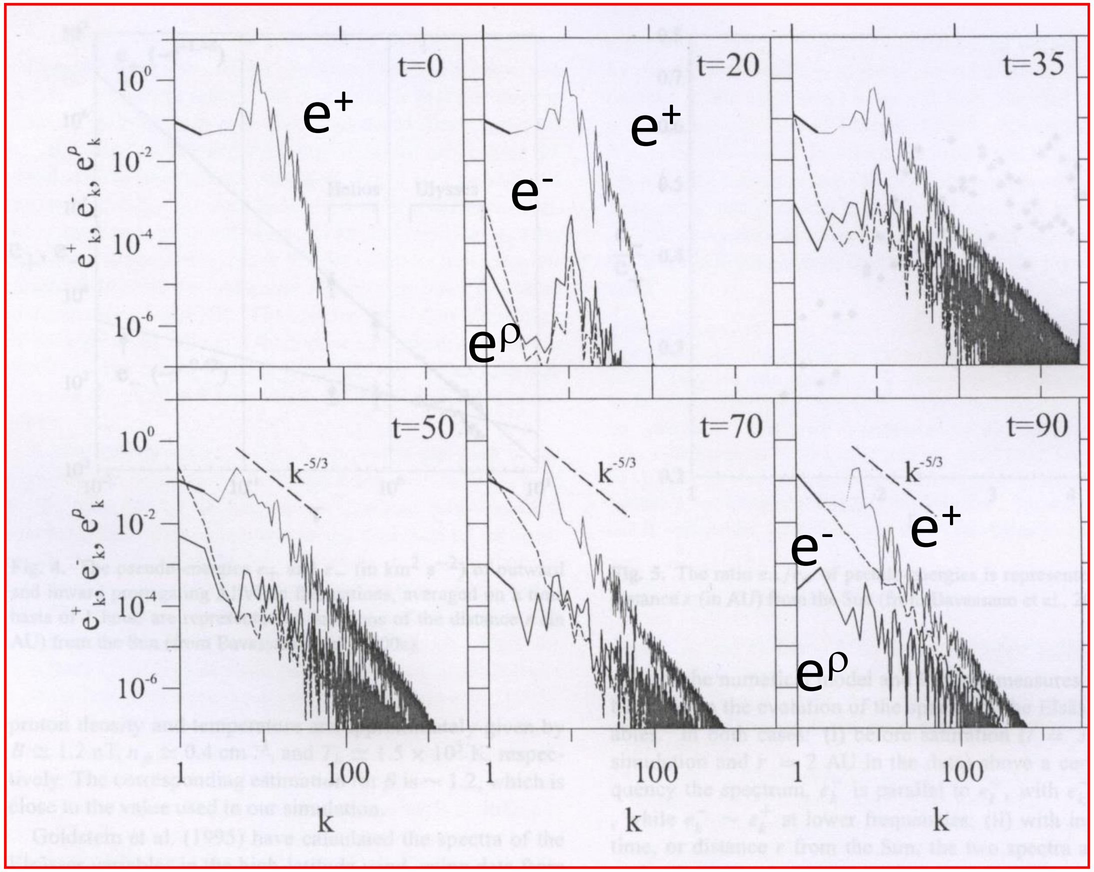

non-monochromatic, large amplitude Alfvén wave experiencing parametric instability creates backscattered fluctuations (e^-) and compressive modes (e^ρ).

(Malara et al., 2001 Nl.Proc in Geophys.)

(Simulation details in: Malara et al., JGR, 101, 21597, 1996, Malara et al., Phys. Plasmas, 7, 2866, 2000, Primavera et al. in Solar Wind 10, 2003)

The parametric instability for β~1

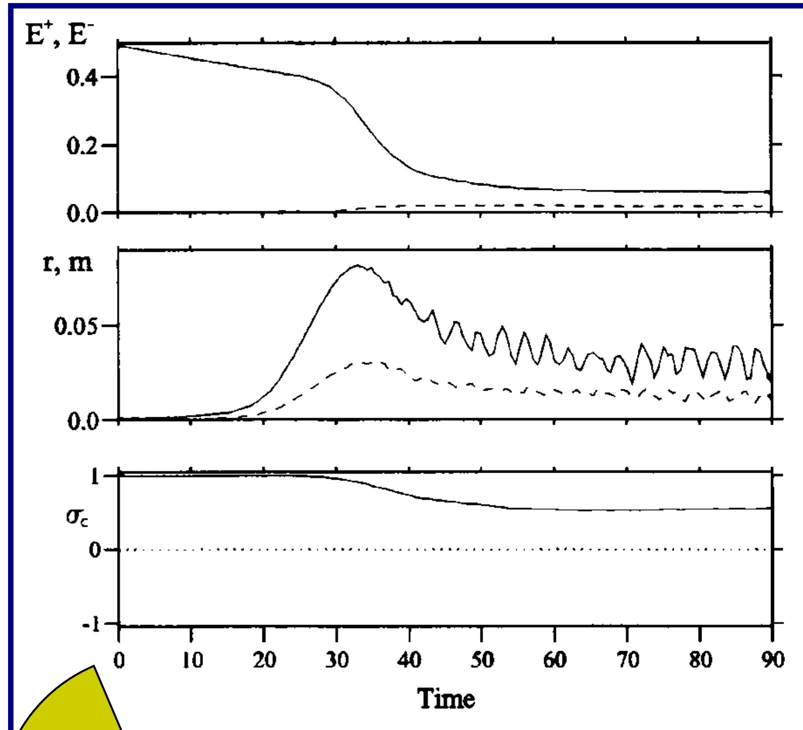

Malara et al., Phys. Plasmas, 7, 2866, 2000

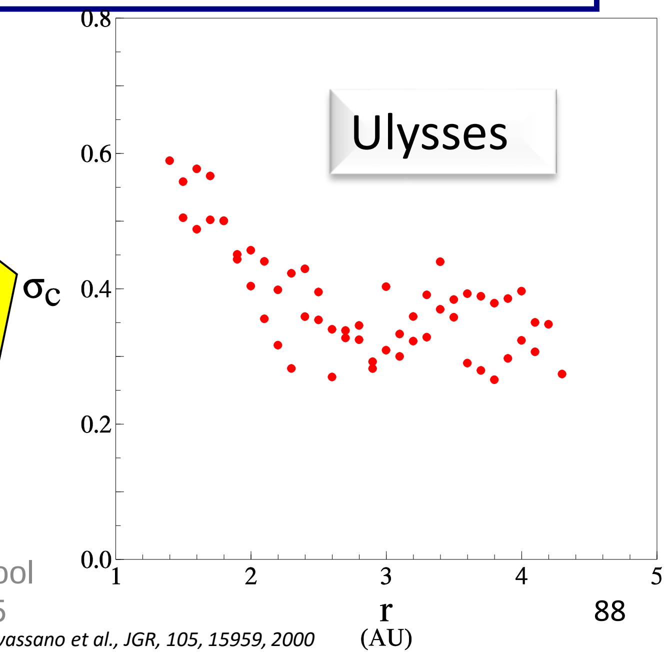

Bavassano et al., JGR, 105, 15959, 2000

- The decay ends in a state in which the initial Alfvénic correlation is partially preserved.
- The predicted cross-helicity behaviour <u>qualitatively</u> agrees with that observed by Ulysses.

Summary

- Solar wind is a turbulent medium (Re~10^5 @1AU)
- Fast wind: radially evolving Alfvénic turbulence (predominance of outward correlations)
- Slow wind: developed turbulence, no radial evolution (equal amount of outward and inward correlations)
- We have a comprehensive, phenomenological view of the Alfvénic turbulence evolution in the 3-D heliosphere.
- The dominant character of outward fluctuations in the polar wind extends to larger distances from the Sun compared to the ecliptic
- polar turbulence evolution is slower than ecliptic turbulence.
- ecliptic evolution driven by velocity shear;
- polar evolution driven by parametric decay

For those who want to know more about turbulence of the interplanetary medium see the following review:

Roberto Bruno and Vincenzo Carbone,
“The Solar Wind as a Turbulence Laboratory”,
Living Rev. Solar Phys. 10 (2013), 2

http://solarphysics.livingreviews.org/Articles/lrsp-2013-2/

Differences in the power associated to e^+ and e^-

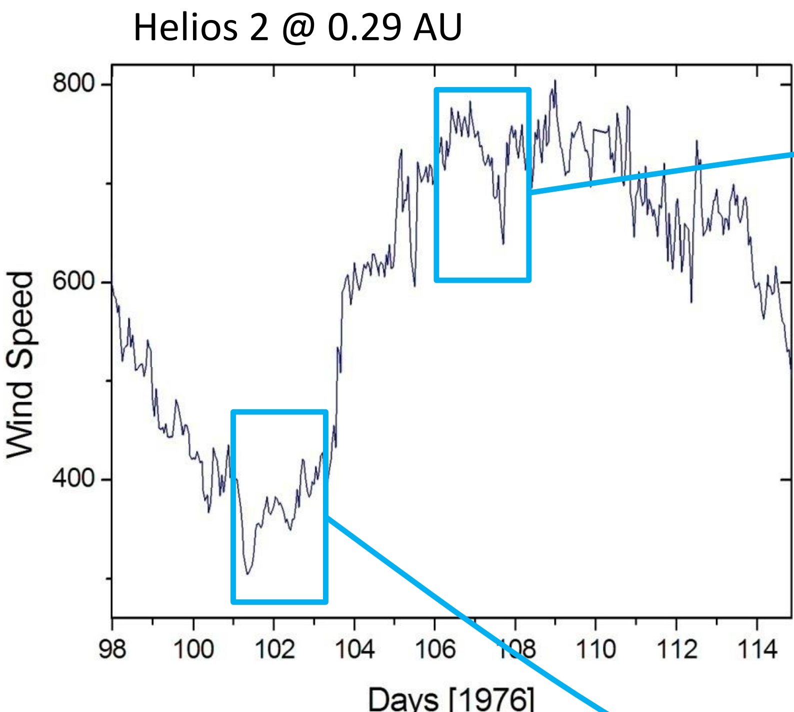

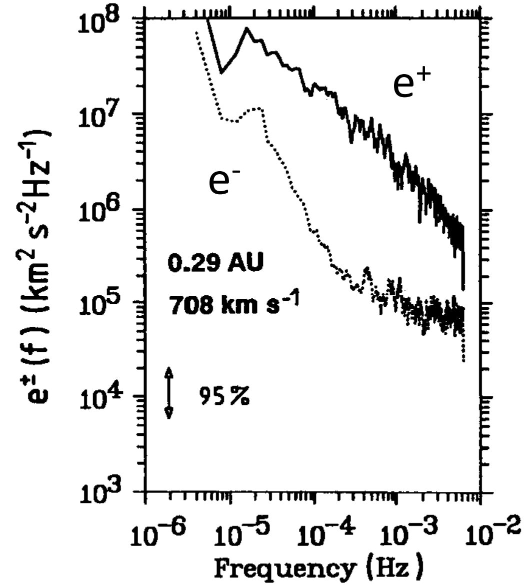

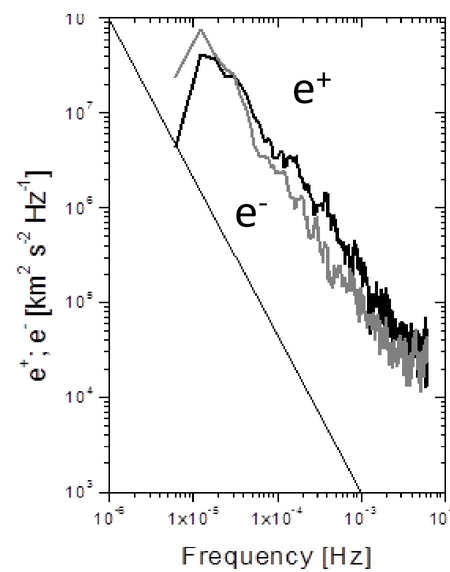

[Tu et al., 1990]

$$\vec{z}^{\pm} = \vec{u} \pm \vec{b} = \vec{u} \pm \vec{B} / \sqrt{4\pi\rho}$$

$$e_j^{\pm}(f_k) = \frac{2\Delta T}{n} \delta Z_{j,k}^{\pm} \left(\delta Z_{j,k}^{\pm}\right)^*$$

$$e^{\pm}(f_k) = \frac{1}{2} \sum_{j=x,y,z} e_j^{\pm}(f_k)$$